Universitat Autònoma de Barcelona

CReSA
Centre de Recerca en Sanitat Animal

Microarray-based gene expression analysis in natural and experimental cases of porcine circovirus type 2 infection

Tesis doctoral presentada por Lana Teixeira Fernandes para acceder al grado de Doctor en Veterinaria dentro del programa de *Doctorat en Medicina i Sanitat Animals* de la *Facultat de Veterinària* de la *Universitat Autònoma de Barcelona*, bajo la dirección del Dr. Joaquim Segalés Coma y la Dra. Anna Tomás Sangenís.

Bellaterra (Barcelona), 2015

FACULTAT DE VETERINÀRIA DE BARCELONA

JOAQUIM SEGALÉS I COMA, profesor titular del *Departament de Sanitat i d'Anatomia Animals* de la *Facultat de Veterinària* de la *Universitat Autònoma de Barcelona* e investigador del *Centre de Recerca en Sanitat Animal* (CReSA) y ANNA TOMÁS SANGENÍS, investigadora del Instituto de Investigación Sanitaria de Palma – IdISPa,

Certifican:

Que la memoria titulada "*Microarray-based gene expression analysis in natural and experimental cases of porcine circovirus type 2 infection*" presentada por Lana Teixeira Fernandes para la obtención del grado de Doctor en Veterinaria, se ha realizado bajo nuestra supervisión en la *Universitat Autònoma de Barcelona* y el *Centre de Recerca en Sanitat Animal*.

Para que conste a los efectos oportunos, firman el presente certificado en Bellaterra (Barcelona), a 22 de abril de 2015.

Dr. Joaquim Segalés Coma Dra. Anna Tomás Sangenís

Lana Teixeira Fernandes

PhD studies of Ms. Lana Teixeira Fernandes were funded by a CAPES grant (BEX2893/04-5) from the Ministry of Education of Brazil.

This work was funded by the projects No. 513928 from the Sixth Framework Programme of the European Commission, GEN2003-20658-C05-02 (Spanish Government) and Consolider Ingenio 2010-PORCIVIR (Spanish Government).

ABSTRACT/RESUMEN

ABSTRACT

Porcine circovirus type 2 (PCV2)-systemic disease (SD) is one of the most economically important pig diseases worldwide. It is a multifactorial condition that mainly affects nursery and growing pigs, which is characterized clinically by progressive weight loss and wasting, pallor of skin, respiratory distress and digestive alterations. PCV2 is the essential infectious agent of PCV2-SD. This virus is ubiquitous in the global pig population since it is present in both healthy and PCV2-SD affected farms. The most striking histological feature associated to this disease is lymphocyte depletion together with granulomatous inflammation of lymphoid tissues.

Although many aspects of the PCV2 infection have been elucidated by traditional techniques over the last two decades, a more global understanding about the mechanisms involved in the host-virus interaction has not yet been achieved. Microarray technology allows simultaneous measurement of the mRNA levels of thousands of genes and have been used during recent years to examine gene expression profiles of tissues or cell lines subjected to infection, helping to unravel host–pathogen interactions relevant to pathogenesis of a variety of diseases. Therefore, this Thesis aimed to characterize the molecular mechanisms underlying the PCV2 infection using the microarray technology. The ultimate purpose was to identify genes and biological processes implicated in the immune response of pigs subclinically infected by PCV2 and also of animals naturally affected by PCV2-SD.

In the study of this Thesis, an exploratory work was conducted to evaluate the technical feasibility of utilizing the Affymetrix Porcine GeneChip® platform to study the global transcriptional profile of caesarean-derived, colostrum-deprived (CDCD) Duroc piglets experimentally infected with PCV2. At seven days of age, two piglets were inoculated with $10^{5\cdot2}$ $TCID_{50}$/ml of the Burgos PCV2 isolate and other two were kept as uninfected controls. All animals were euthanized at 23 days post-inoculation (p.i.) and tissue samples were collected at necropsy. PCV2-inoculated piglets developed a subclinical infection, as confirmed by serology, *in situ* hybridization and quantitative PCR. Total RNA from mesenteric lymph nodes and lungs from the four animals was obtained by duplicate and was hybridized to the Affymetrix Porcine GeneChip®. To assess technical reproducibility, Pearson's correlation coefficients were calculated and MA-plots were drawn for all

possible combinations between arrays for each tissue (8 chips, ${}^{8}C_{2}$ = 28 combinations). A high correlation coefficient between biological and technical replicates of each tissue studied (ranging from 0.93 to 0.99) was observed, confirming the high reproducibility across arrays. The microarray analysis detected 25 and 33 significantly differentially expressed (DE) between control and PCV2 groups for mesenteric lymph node and lung, respectively. Most up-regulated genes in PCV2 group were closely related to the immune response, such as cytokines, MHC binding molecules, immunoglubulins and T cell activation. From a transcriptional point of view, PCV2-inoculated pigs were able to activate a cell-mediated response and develop PCV2-specific antibodies, which probably led to a subclinical infection. The results from this study also indicate that a microarray-based approach is a helpful tool to better understand the pathogenesis of PCV2 infection.

The second study was aimed to characterize the early and late molecular events underlying the immune response taking place during a subclinical PCV2 infection. Twenty-four, seven-day-old CDCD Landrace piglets were distributed into two groups: control (n = 8) and pigs inoculated with $10^{5\cdot2}$ $TCID_{50}$/ml of the Burgos PCV2 isolate (n = 16). One control and three inoculated pigs were necropsied on days 1, 2, 5, and 8 p.i.. The remaining pigs (four of each group) were sequentially bled on days 0, 7, 14, 21, and 29 p.i. (necropsy). Total RNA from the mediastinal lymph node (MLN) and lysed whole blood (LWB) samples were hybridized to microarrays. Forty-three probes DE detected in MLN samples were distributed into three clusters: globally down-regulated genes, and up-regulated genes at early (first week p.i.) and late (day 29 p.i.) stages of infection. In LWB samples, maximal differences were observed at day 7 p.i., with 54 probes DE between control and inoculated pigs. Down-regulated genes from MLN samples were mainly related to cell adhesion and migration, suggesting the participation of these genes in the inflammatory processes (granulomatous infiltration) observed in the PCV2 infection. Innate immunity developed within the first week p.i. and it was demonstrated by the up-regulation of several interferon-stimulated genes (ISGs) both in MLN and LWB samples from PCV2-infected pigs. An increased expression of genes related to lymphocyte activation was also detected during the first week p.i. in LWB samples of infected animals, indicating an early activation of adaptive responses. Similar results were obtained at late stages of infection by the up-regulation of genes coding for interferon (IFN)-γ from day 8 to 29 p.i. and the immunoglobulin (Ig)-G at 29 days p.i. in MLN samples.

The aim of the third study was to investigate the global transcriptional profile of MLNs from pigs naturally affected by PCV2-SD, as well as healthy counterparts. Twenty-five conventional 13–15-week-old pigs (12 diseased and 13 clinically healthy controls) were selected from three farms with historical records of PCV2-SD. All pigs were necropsied and samples of MLN were obtained for RNA extraction and hybridization to the Affymetrix Porcine GeneChip®. The microarray data analysis detected 366 transcripts with significant differential abundance in the PCV2-SD group of pigs relative to healthy animals. Results obtained from hierarchical clustering analyses indicate that the microarray technique would be able to discriminate stages of infection within natural cases of PCV2-SD. A persistent inflammation mediated by distinct mechanisms occurs in diseased pigs, as demonstrated by the increased mRNA levels of a large set of inflammatory mediators, acute phase proteins, transcriptional regulators, and genes related to stress response and tissue remodelling. The complement system was altered by PCV2-SD, especially by the lower levels of Cr1 mRNA, which might favour both complement deposition and secondary infections by impairing phagocytosis. Decreased mRNA abundance of several genes involved in lymphocyte activation/differentiation, and the high level of Vsig4 mRNA, which can compromise the activation of residing T-cells, pointed towards a defective adaptive immunity. Results from this study identified potential mechanisms (complement mediated damage and immunosuppression) underlying the inflammation and lymphocyte depletion in lymphoid tissues, which are key features of PCV2-SD.

RESUMEN

La enfermedad sistémica (ES) por circovirus porcino tipo 2 (PCV2) es una de las enfermedades porcinas más importantes económicamente a nivel mundial. La ES-PCV2 tiene carácter multifactorial, afecta principalmente a cerdos en las fases de transición y engorde y está clínicamente caracterizada por la pérdida progresiva de peso, adelgazamiento, palidez de la piel y alteraciones respiratorias y digestivas. PCV2 es el agente infeccioso esencial de la ES-PCV2. Este virus es ubicuo en la población porcina mundial, y se puede encontrar presente tanto en granjas afectadas por la ES-PCV2 como en granjas sin la enfermedad. Los hallazgos histopatológicos más notables asociados a la enfermedad son la depleción linfocitaria y la inflamación granulomatosa en los tejidos linfoides.

Aunque muchos aspectos de la infección por PCV2 han sido elucidados utilizando técnicas tradicionales en las últimas dos décadas, al inicio de esta tesis no se tenía una comprensión global de los mecanismos involucrados en la interacción huésped-virus. La tecnología de los microarrays permite la determinación simultánea de los niveles de ARNm de miles de genes y ha sido utilizada en los últimos años para investigar los perfiles de expresión génica de tejidos y líneas celulares, ayudando a descifrar las interacciones huésped-patógeno que son relevantes para la patogénesis de varias enfermedades. Es por ello que esta Tesis se orientó a la caracterización molecular de la infección causada por PCV2 utilizando la tecnología de los microarrays con el fin de identificar genes y procesos biológicos implicados en la respuesta inmune de cerdos subclinicamente infectados por el PCV2 y también de animales naturalmente afectados por la ES-PCV2.

La primera parte de esta Tesis consistió en un trabajo exploratorio dirigido a evaluar la utilidad de la plataforma Affymetrix Porcine GeneChip® para estudiar el perfil global del transcriptoma de lechones de la raza Duroc, derivados por cesárea y privados de calostro (DCPC), experimentalmente infectados por PCV2. A los siete días de vida, dos lechones fueron inoculados con $10^{5.2}$ $TCID_{50}$/ml de la cepa Burgos de PCV2 y dos animales más permanecieron sin infectar y fueron utilizados como controles. Todos los animales fueron sacrificados a los 23 días post-inoculación (p.i.) y se tomaron muestras de tejidos en la necropsia. Los lechones inoculados con PCV2 desarrollaron una infección subclínica que

fue confirmada por serología, hibridación *in situ* y PCR cuantitativa. Se extrajeron muestras de ARN total de linfonodos mesentéricos y pulmón de los cuatro animales por duplicado para la hibridación con el Affymetrix Porcine GeneChip®. Para investigar la reproductibilidad técnica, se calcularon los coeficientes de correlación de Pearson y se construyeron gráficos MA-plots para todas las posibles combinaciones entre chips para cada tejido (8 chips, $^{8}C_{2}$ = 28 combinaciones). Se observó un alto coeficiente de correlación entre réplicas biológicas y técnicas para cada tejido estudiado (entre 0,93 a 0,99), lo que confirmó la alta reproductibilidad entre los chips. A partir del análisis de los datos de los microarrays, se seleccionaron 25 y 33 genes que resultaron diferencialmente expresados (DE) entre los grupos control e inoculados con PCV2 en linfonodos mesentéricos y pulmones, respectivamente. La gran mayoría de los genes sobre-expresados en el grupo inoculado con PCV2 estaba relacionada a la respuesta inmune, como citoquinas, moléculas asociadas al complejo mayor de histocompatibilidad, inmunoglobulinas y la activación de las células T. Desde el punto de vista del transcriptoma, los animales inoculados con PCV2 fueron capaces de activar la respuesta mediada por células y desarrollar anticuerpos específicos para PCV2, hechos que se asocian a la generación de una infección subclínica. Los resultados de este trabajo indicaron que la técnica de los microarrays es una herramienta útil para el estudio de la patogénesis de la infección por el PCV2.

El segundo estudio fue dirigido a caracterizar los mecanismos moleculares de la respuesta inmune que tienen lugar en las fases temprana y tardía de la infección subclínica por PCV2. Veinticuatro lechones de la raza Landrace DCPC fueron separados en dos grupos a los siete días de edad: control (n= 8) y animales inoculados con $10^{5\cdot2}$ $TCID_{50}$/ml de la cepa Burgos de PCV2 (n= 16). Un animal del grupo control y tres inoculados con PCV2 fueron necropsiados a los días 1, 2, 5 y 8 p.i. Se tomaron muestras de sangre de los lechones restantes (4 de cada grupo) a los días 0, 7, 14, 21 y 29 p.i, cuando se realizó la necropsia y la toma de muestras. Se extrajeron muestras de ARN total de linfonodos mediastínicos (LM) y de sangre total (ST) para la hibridación con los microarrays. Las 43 sondas DE identificadas en las muestras de LM fueron distribuidas en tres *clusters*: genes globalmente sub-expresados, genes sobre-expresados en las fases temprana (primera semana p.i) y tardía (día 29 p.i) de la infección. En las muestras de ST, los cambios de expresión génica fueron observados principalmente al día 7 p.i, con 54 sondas DE entre los cerdos control e inoculados con PCV2. Los genes sub-expresados en las

muestras de LM se relacionaron principalmente a la adhesión celular y migración, lo que sugiere la participación de esos genes en los procesos inflamatorios (infiltración granulomatosa) observados en la infección por PCV2. La inmunidad innata se desarrolló en la primera semana p.i. y se demostró por la sobre-expresión de varios genes estimulados por interferón (ISGs) entre las muestras de LM y ST de los animales inoculados con PCV2. También se detectó un aumento en la expresión de genes relacionados con la activación linfocitaria en la primera semana p.i. en las muestras de LM de los cerdos infectados, lo que indica la activación temprana de la respuesta adaptativa. Se obtuvieron resultados similares en las fases tardías de la infección, dada la sobre-expresión de los genes que codifican para el interferón (IFN)-γ a partir del día 8 p.i. hasta el día 29 p.i. y para la inmunoglobulina (Ig)-G en el día 29 p.i en las muestras de LM.

El tercer estudio consistió en investigar los cambios globales en el transcriptoma de animales naturalmente afectados por ES-PCV2 y congéneres sanos. Se utilizaron un total de 25 animales (12 enfermos y 13 controles clínicamente sanos) de 13-15 semanas de edad y provenientes de tres explotaciones con histórico de ES-PCV2. Los animales fueron necropsiados y se tomaron muestras de LM para la extracción del ARN e hibridación con el Affymetrix Porcine GeneChip®. Tras los análisis de datos, se encontraron 366 tránscritos con significativa abundancia diferencial en el grupo de animales afectados por ES-PCV2 en relación al grupo control. Los resultados del análisis de agrupamientos jerárquicos indicaron que la técnica de microarrays es capaz de discriminar fases de la infección en casos naturales de ES-PCV2. Se observó que en animales enfermos se genera una inflamación persistente mediada por diferentes mecanismos, dado el aumento de los niveles de ARNm de un gran número de mediadores inflamatorios, proteínas de la fase aguda, reguladores de la transcripción, y genes relacionados a la respuesta al estrés y a la remodelación de tejidos. Se observó el aumento de la abundancia de ARNms codificados por un gran número de genes involucrados en la respuesta inflamatoria (citoquinas y proteínas de fase aguda) en los animales enfermos. El sistema de complemento se mostró alterado por la enfermedad, particularmente por los bajos niveles de ARNm del Cr1, el cual puede favorecer la deposición del complemento e infecciones secundarias por afectar la fagocitosis. La disminución de la abundancia de ARNm de una serie de genes involucrados en la activación/diferenciación de linfocitos y el alto nivel de ARNm del Vsig4, el cual puede comprometer la activación de células T residentes, sugiere una

inmunidad adaptativa defectiva. Los resultados de este estudio identificaron mecanismos (daño mediado por el complemento e inmunosupresión) potencialmente involucrados en la inflamación y depleción linfocitaria en tejidos linfoides, características histopatológicas claves de la ES-PCV2.

The results from the present Thesis have been published in international scientific peer-reviewed journals:

Fernandes, L.T., Tomas, A., Bensaid, A., Perez-Enciso, M., Sibila, M., Sanchez, A., Segales, J., 2009. Exploratory study on the transcriptional profile of pigs subclinically infected with porcine circovirus type 2. Anim Biotechnol 20, 96-109.

Tomas, A., Fernandes, L.T., Sanchez, A., Segales, J., 2010. Time course differential gene expression in response to porcine circovirus type 2 subclinical infection. Vet Res 41, 12.

Fernandes, L.T., Tomas, A., Bensaid, A., Sibila, M., Sanchez, A., Segales, J., 2012. Microarray analysis of mediastinal lymph node of pigs naturally affected by postweaning multisystemic wasting syndrome. Virus Res 165, 134-142.

TABLE OF CONTENTS

CHAPTER 1

INTRODUCTION

1.1. Porcine circovirus type 2 (PCV2)

1.1.1. History

Tischer and co-workers, in 1974, reported a picornavirus-like agent contaminating the porcine kidney cell line PK-15 (Tischer *et al.*, 1974). Later on, based on its circular, single-stranded DNA (ssDNA) genome, this virus was named porcine circovirus (PCV) (Tischer *et al.*, 1982). Although PCV antibodies were found to be widespread in the pig population, no disease was associated with this viral infection and, consequently, this infectious agent was considered as non-pathogenic (Tischer *et al.*, 1986; Allan *et al.*, 1995). In the late 1990s, a variant strain of PCV was isolated from tissues of pigs suffering from an emerging disease characterized by emaciated pigs in Europe and North America, which was later designated as postweaning multisystemic wasting syndrome (PCV2-SD) (Allan *et al.*, 1998a; Ellis *et al.*, 1998). Since the two types of PCV were different in terms of antigenicity and genome sequence (Allan *et al.*, 1998b; Meehan *et al.*, 1998), the non-pathogenic PK-15 cell culture contaminant virus was designated as PCV type 1 (PCV1), and the virus associated with PCV2-SD outbreaks as PCV type 2 (PCV2) (Hamel *et al.*, 1998; Meehan *et al.*, 1998). Although the association of PCV2 with PCV2-SD was only established in the late 1990s, retrospective studies have demonstrated that the virus was present in the swine population as early as 1962 in Europe (Jacobsen *et al*., 2009) and 1973 in North America (Ramírez-Mendoza *et al*., 2009). In 2012, in order to homogenize nomenclature, it was suggested to adopt the name PCV2-systemic disease (PCV2-SD) to designate PCV2-SD (Segalés, 2012). Therefore, this will be the terminology used in this thesis from now onwards.

Besides PCV2-SD, PCV2 has been associated with other disease complexes, such as porcine dermatitis and nephropathy syndrome (PDNS), PCV2-lung disease, PCV2-enteric disease, and PCV2-reproductive disease (Segalés, 2012). Collectively, in Europe, these diseases have been named porcine circovirus diseases (PCVD, Segalés *et al*., 2005), although, to date, only PCV2-SD and PCV2-reproductive disease have been experimentally demonstrated (Allan *et al*., 1999; Sanchez *et al*., 2001). In North America, the term porcine circovirus associated diseases (PCVAD, http://www.aasv.org/) is more frequently used to name diseases associated with PCV2 infection (Opriessnig *et al*., 2007). Moreover, the subclinical infection by PCV2 should also be considered within the

scope of PCVDs (Segalés, 2012). In 2009, a possible new syndrome related to PCV2, referred as acute pulmonary oedema (APE), was described in pigs from PCV2-vaccinated herds in the United States (Cino-Ozuna *et al*., 2011). This syndrome primarily affected nursery and younger finisher pigs and was clinically characterized by a rapid onset of respiratory distress followed rapidly by death. However, the real implication of PCV2 in APE needs further investigation, since this condition has only been described once.

1.1.2. Taxonomy

PCV2 belongs to the *Circoviridae* family, which includes small, non-enveloped ssDNA viruses that infect vertebrates (Lukert *et al*., 1995). Based on virion size and genomic organization, the family is divided into the genera *Circovirus* and G*yrovirus* according to the International Committee on Taxonomy of Viruses (ICTV, www.ictvonline.org). Besides PCV1 and PCV2, the genus *Circovirus* includes nine avian viruses: beak and feather disease virus (BFDV), pigeon circovirus (PiCV), canary circovirus (CaCV), goose cirvovirus (GoCV), duck circovirus (DuCV), finch circovirus (FiCV), starling circovirus (StCV), gull circovirus (GuCV) and swan circovirus (SwCV). The second genus, *Gyrovirus,* is represented by chicken anaemia virus (CAV) and a newly reported human gyrovirus (Sauvage *et al*., 2011). Recently, a new viral genus named *Cyclovirus,* which includes viruses with an ambisense DNA genome able to infect humans and chimpanzees, has been proposed as a new member of the *Circoviridae* family (Blinkova *et al*., 2010; Li *et al*., 2010). Most circoviruses and also CAV are associated with diseases affecting the immune system (Todd, 2004).

1.1.3. Morphological features and genomic organization

PCV2 is an icosahedric, non-enveloped virus of 17 nm in diameter (Figure 1A) and contains a covalently closed, circular ssDNA of approximately 1.76 kilobases (Hamel *et al*., 1998; Meehan *et al*., 1998; Crowther *et al*., 2003; Rodríguez-Cariño *et al*., 2009).

PCV2 replicates by a mechanism known as rolling-circle replication (Faurez *et al*., 2009; Cheung *et al*., 2012). Upon infection, host cell factors convert the viral ssDNA to an intermediate double-stranded DNA (dsDNA), also named as replicative form (RF). The RF has an ambisense organization, consisting of the viral and complementary strands,

with positive and negative senses, respectively. Two major open reading frames (ORFs), divergently oriented, are located in the opposite sides of the origin of replication, which is characterized by a putative stem-loop structure with a conserved nonanucleotide motif sequence (Figure 1B). The ORF1 or *rep* gene, located on the plus strand in a clockwise orientation, codes for the non-structural replicase proteins Rep and the spliced variant Rep'. Both proteins are essential for the replication of the viral genome (Cheung *et al*., 2003, Mankertz *et al*., 2004). ORF2 or *cap* gene encodes the major structural protein Cap and is located in the complementary strand, in an anti-clockwise orientation (Nawagitgul *et al*., 2000). Furthermore, a third ORF (ORF3) is found within the ORF1 complementary sequence, but in an anti-clockwise orientation. The ORF3 protein has been shown to induce apoptosis in PCV2 infected cells *in vitro* (Liu *et al*., 2005; Karuppannan *et al*., 2010) and to play a role in the pathogenesis of PCV2 infection in mouse models and SPF piglets (Liu *et al*., 2006; An *et al*., 2008; Karuppannan *et al*., 2009). However, other authors were not able to confirm the involvement of the ORF3 protein in the PCV2 pathogenesis in pigs, and its role is still controversial (Chaiyakul *et al*., 2010; Juhan *et al*., 2010). Very recently, a fourth ORF (ORF4) gene of PCV2 was identified overlapping the ORF3 and oriented in the same direction (Gao *et al*., 2013; He *et al*., 2013). ORF4 protein is not essential for PCV2 replication but may play a role in suppressing the caspase activity by restricting ORF3 transcription (Gao *et al*., 2014) and regulating $CD4^+$ and $CD8^+$ T lymphocytes during PCV2 infection (He *et al*., 2013).

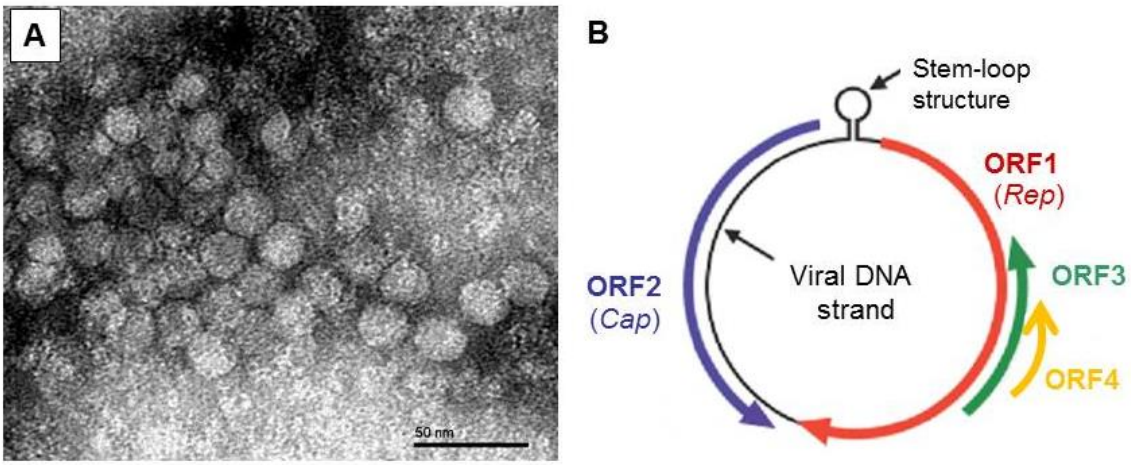

Figure 1. (A) Electron microscopy of PCV2 viral particles (kindly provided by Dr. Carolina Rodríguez Cariño). (B) Genomic organization of PCV2. The covalently closed, circular ssDNA contains a stem-loop structure (origin of replication). In the viral strand, the ORF1 (red) is located in a clockwise orientation. On the opposite direction, ORF2 (blue), ORF3 (green) and ORF4 (orange) are transcribed from the complementary strand. Figure adapted from Lefebvre, 2009a.

1.1.4. Genetic differences among PCV2 isolates and genotypes

PCV2 isolates share high level of nucleotide identity among their genomes (Meehan *et al*., 1998, Mankertz *et al*., 2000, Larochelle *et al*., 2002); however, some genetic diversity within PCV2 strains has been described. To date, four different PCV2 genotypes have been recognized (Segalés *et al*., 2013): PCV2a and PCV2b, which have been recovered from PCV2-SD cases worldwide (Gagnon *et al*., 2007, Olvera *et al*., 2007, Grau-Roma *et al*., 2008), PCV2c, identified from archived samples in Denmark during the 1980s, prior the PCV2-SD outbreaks (Dupont *et al*., 2008), and PCV2d, from strains isolated in China which carried an ORF2 mutation resulting in ORF2 genes of 705 bp in length (Guo *et al*., 2010). In Canada, 2008, a novel PCV2 genotype named PCV1/2a was proposed, whose genome was composed with the ORF1 of PCV1 and the ORF2 of PCV2a (Gagnon *et al*., 2010). In fact, this novel virus genotype highly resembled the inactivated virus that was contained in a former commercial vaccine used in North America. Therefore, it was speculated that this variant might be related with a non-sufficiently inactivated vaccine (Gagnon *et al*., 2010). Recently, Wang *et al*. (2009) compared 40 PCV2 genomes isolated in China between 2004 and 2008 and proposed the existence of two new PCV2 genotypes: PCV2d and PCV2e. However, other researchers concluded that, using the existing criteria

for PCV2 genotype definition (Grau-Roma *et al*., 2008; Segalés *et al*., 2008), those new proposed genotypes were not divergent enough to have the consideration of new genotypes (Cortey *et al*., 2011). In 2012, a variant PCV2 strain, called mutant PCV2b, with a 74 elongation of ORF2 by one amino acid (Lysine (K)), was also detected in several PCVAD cases in the United States (Xiao *et al*., 2012). This variant has been nowadays classified as PCV2d.

Recent studies have suggested that a genotype shift of PCV2 isolates over time has been linked with the epidemiological transition from sporadic to epidemic PCV2-SD under field conditions worldwide. PCV2a was predominant on pig farms with sporadic PCV2-SD and without notice of the disease in several countries prior 2000-02, while PCV2b has been significantly more prevalent in epidemic PCV2-SD outbreaks from 2002 onwards (Cheung *et al*., 2007; Dupont *et al*., 2008; Timmusk *et al*., 2008; Wiederkehr *et al*., 2009; Cortey *et al*., 2011; Ge *et al*., 2012). Clinical observations from field cases suggested that PCV2b could be a more adapted or potentially more pathogenic genotype than PCV2a. However, this concept is not completely supported since both PCV2 genotypes can reproduce PCV2-SD experimentally (Opriessnig *et al*., 2008a; Gauger *et al*., 2011) and, to date, there are no confirmed conclusions about which genotype is more pathogenic.

Firth *et al*. (2009) suggested that PCV2 emerged in pigs possibly as the result of a cross-species jump from birds into domestic pigs, most likely through intermediate contact with wild boars approximately a hundred years ago. It seems that PCV2a and PCV2b have followed independent evolutionary trajectories since that time, despite co-circulating in the same host species and geographic regions (Olvera *et al*., 2007). The high levels of swine trade due to the global pig market along with the high prevalence of asymptomatic PCV2 infections may have facilitated the rapid spread of the presumably more virulent PCV2b genotype around the world (Allan *et al*., 2012). The rate of nucleotide substitution was also estimated to be approximately 1.2×10^{-3} substitutions/site/year (s/s/y), the highest rate described for a single-stranded DNA virus and closer to those reported for most RNA viruses, which might facilitate the emergence of new PCV2 genotypes in the future (Firth *et al*., 2009). Similar results (3.12×10^{-3} to 6.57×10^{-3} s/s/y) were found in a recent study analyzing the genetic variability of PCV2 sequences from Cuba, comparing isolates from two different regions (Pérez *et al*., 2011). In comparison with PCV2, lower

evolutionary rates were estimated for PCV1 (1.15 x 10^{-5} nucleotide substitutions per site per year; Cortey and Segalés, 2012).

1.2. PCV2-systemic disease (PCV2-SD) and PCV2 infection

1.2.1. Epidemiology

Since the first description of PCV2-SD in Canada in the 90s (Clark, 1996), the disease has been reported in countries from all continents. PCV2 infection is considered endemic, causing major economic impact in most pig-producing countries around the world (Grau-Roma *et al.*, 2011). Retrospective studies detected PCV2 infection in archived pig tissues in 1962 and PCV2-SD-associated lesions together with PCV2 antigen were identified as early as 1985 (Jacobsen *et al*., 2009). The prevalence of PCV2-SD varies among farms, and when it is present, morbidity ranges from 4 to 30%. In these affected farms, mortality rates are 4-20% (Segalés and Domingo, 2002). PCV2 is considered ubiquitous, with almost all farms worldwide experiencing infection in some time point during the production cycle (Grau-Roma *et al*., 2011).

1.2.2. Clinical presentation and pathological findings

PCV2-SD mainly affects 2 to 4 month-old pigs, although infection with PCV2 can happen during their whole productive life (Carman *et al*., 2008; Grau-Roma *et al.*, 2009). Major clinical signs of this syndrome are growth retardation and progressive weight loss, but respiratory distress, digestive alterations or pallor of the skin are signs frequently observed in affected pigs (Baekbo *et al.*, 2012).

Most usual gross lesions include lymph node enlargement and non-collapsed lungs. Thymus atrophy, white-spotted kidneys and gastric ulceration can also be observed (Rosell *et al*., 1999). Histopathological findings in lymphoid tissues are the hallmark of PCV2-SD, although inflammatory infiltrates can be detected in a wide variety of organs. At early clinical stages, microscopic lesions consist of histiocytic infiltration and loss of lymphocytes from lymphoid follicles. Multinucleate giant cells can be observed in the lymphoid follicles and parafollicular areas. Frequently, basophilic inclusion bodies can be found in the cytoplasm of histiocytes or dendritic cells (DCs). Later on, the lymphocyte

depletion also affects the parafollicular areas. At terminal clinical stages, the lymphoid tissue is almost devoid of lymphocytes, with a prominent stromal tissue (Rosell *et al*., 1999; Segalés *et al*., 2005).

1.2.3. Diagnosis

The diagnosis of PCV2-SD is somehow complicated, because most clinical signs and gross lesions are relatively unspecific and variable, being common to a variety of other pig diseases. Moreover, most PCV2 infections are of subclinical nature and do not necessarily lead to PCV2-SD development. Therefore, the mere detection of PCV2 in pig tissues or blood is not sufficient to establish the diagnosis. Thus, to perform an individual diagnosis of PCV2-SD, three criteria should be accomplished (Segalés *et al*., 2005):

i) Clinical signs including growth retardation and wasting (Figure 2A); at necropsy, generalized enlargement of lymph nodes, lack of pulmonary collapse and/or white-spotted kidneys may help orienting the suspected diagnosis.
ii) Presence of moderate to severe histopathological lesions in lymphoid tissues, including lymphocyte depletion with granulomatous inflammation (Figure 2B).
iii) Detection of moderate to high amount of PCV2 within microscopic lymphoid lesions (Figure 2C).

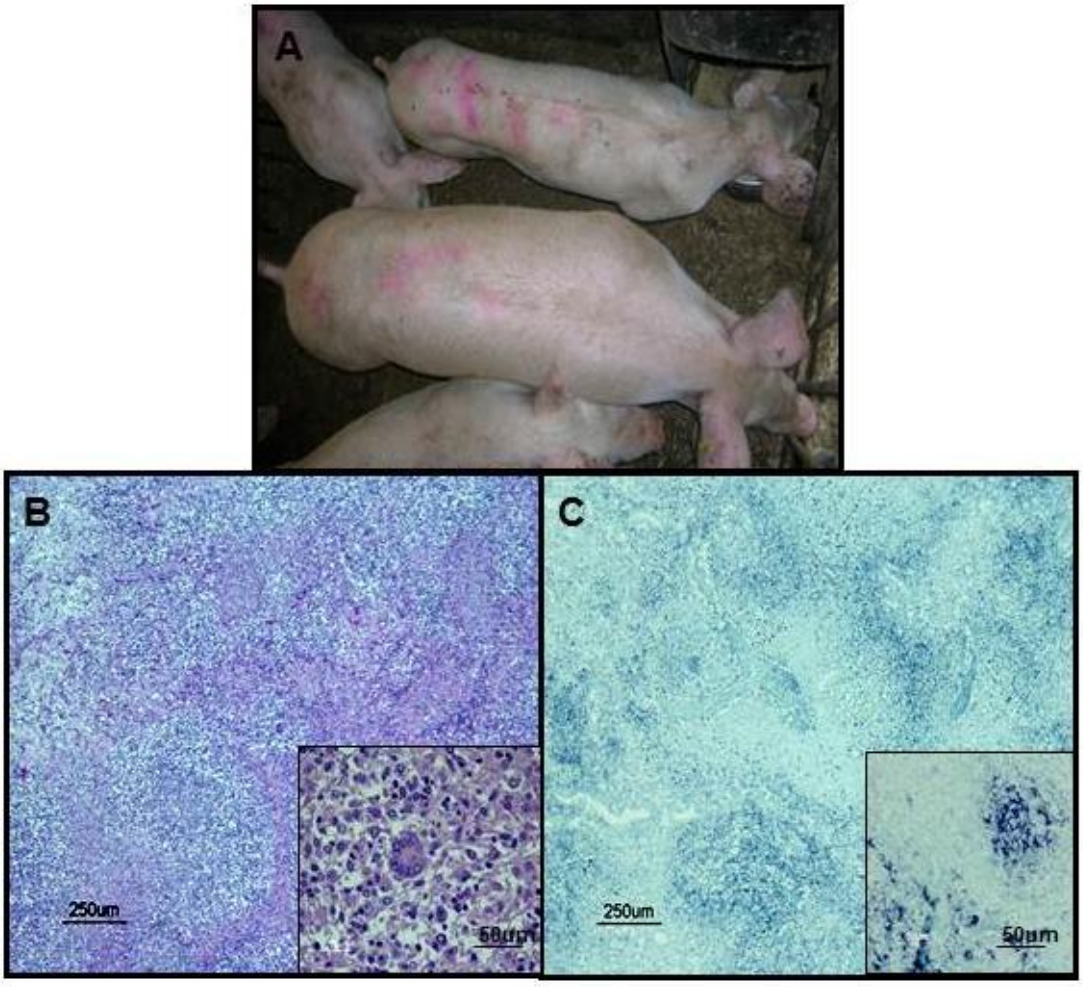

Figure 2. Criteria to establish an individual PCV2-SD diagnosis: (A) Clinical signs, mainly characterized by wasting; (B) Moderate to severe lymphocyte depletion and granulomatous infiltration in lymphoid tissues; multinucleate giant cell in the inset (Haematoxylin and eosin stain); (C) Moderate to high amount of PCV2 genome detected in lymphoid tissues by *in situ* hybridisation; high amount of viral genome in lymphoid follicles in the inset (ISH, fast green counterstain).

A diagnosis of PCV2 subclinical infection is established when the presence of low amounts of PCV2 is associated with no or mild lesions detected in lymphoid tissues from healthy pigs (Oppriessnig *et al*., 2007).

It is known that individual cases of PCV2-SD can occur in herds that otherwise show good production data and low overall mortality (Nielsen *et al*., 2008). Therefore, a formal establishment of a herd case definition for PCV2-SD was proposed by Grau-Roma *et al*. (2012). This proposal was based on overall clinical signs in terms of mortality and statistical calculations. Two criteria must be fulfilled:

i) Significant increase in postweaning mortality compared to the historical background in the herd associated to the presentation of clinical signs compatible to PCV2-SD.
ii) Individual diagnosis of PCV2-SD in at least one out of three to five necropsied pigs performed during the increase in mortality period previously mentioned. Moreover, relevant diagnostic procedures to exclude other potential causes of increase in mortality besides PCV2-SD should be implemented.

Another factor to consider within PCV2-SD is the severity of clinical signs, which vary widely between affected farms. In addition, pig production systems between countries differ; leading to different levels of mortality associated with PCV2-SD, which difficult the diagnosis of the disease at the herd level (Alarcon *et al*., 2011). A quantitative approach (principal component analysis – PCA) was developed very recently in the United Kingdom to measure severity of PCV2-SD at herd level by using information on morbidity, mortality and presence of PCV2 (by polymerase chain reaction, PCR) (Alarcon *et al*., 2011). This method may provide the basis for future risk factor studies, and it may also be used to assess the efficacy of vaccination and other interventions to reduce PCV2-SD severity.

1.2.4. Pathogenesis

Transmission of PCV2 mainly occurs through direct contact via oronasal, faecal and/or urinary routes (Segalés *et al*., 2005). Vertically, PCV2 can be transmitted via intrauterine and by the colostrum of infected sows (Madson and Opriessnig, 2011). PCV2 has been found in the semen of adult boars, but it appears that the risk of virus spread through insemination is negligible; however, when PCV2 spiked semen was used, transmission through semen can occur in a dose-dependent manner (Madson *et al*., 2008; 2009a). Moreover, PCV2 DNA can be detected early in the infectious process and persists for extended periods of time (Patterson and Opriessnig, 2010).

The mechanisms by which the virus crosses the body barriers and primary sites of replication in the pig are still not clear. In PCV2-infected pigs, viremia can be detected from 7 days post inoculation (dpi), and from this point onwards, the virus can be found

in a variety of lymphoid and non-lymphoid organs (Yu *et al*., 2007a). Maximum viral loads are detectable between 14 and 21 dpi (Rovira *et al*., 2002; Fort *et al*., 2009a).

Although the presence of PCV2 genome or antigen has been identified in several types of cells (e.g. monocyte/macrophage lineage cells, fibrocytes, lymphocytes, hepatocytes, epithelial and endothelial cells) by *in vivo* and *in vitro* studies, a unique primary target cell for viral replication has not been found (Gilpin *et al*., 2003; Hirai *et al*., 2006; Pérez-Martín *et al*., 2007; Yu *et al*., 2007b; Steiner *et al*., 2008; Rodríguez-Cariño *et al*., 2010). A high amount of PCV2 is found in the cytoplasm of monocyte/macrophages and also DCs, which accumulate virus by phagocytosis and/or endocytosis (Gilpin *et al*., 2003; Vincent *et al*., 2003). Although the virus can replicate at least in a certain proportion of macrophages (Pérez-Martín *et al*., 2007; Rodríguez-Cariño *et al*., 2010), PCV2 replication is apparently absent in DCs (Vincent *et al*., 2005), suggesting that the virus may employ these cells as vectors to spread within the body (Gilpin *et al*., 2003; Vincent *et al*., 2003, 2005). So far, the most consistent generic cell types supporting viral replication would be epithelial and endothelial cells but, apparently, the percentage of infected cells is low in a given individual at a given time point (Pérez-Martín *et al*., 2007).

To enter into the monocytic cell lines *in vitro*, PCV2 attaches to glycosaminoglycans receptors (heparan sulfate and chondroitin sulfate B) on the surface of the cells, and then virus particles are gradually internalized in a time dependent manner (Misinzo *et al*., 2005; 2006; Nauwynck *et al*., 2012). PCV2 internalization occurs via clathrin-mediated endocytosis and involves reorganization of the actin cytoskeleton. In epithelial cell lines, PCV2 may be internalized following two pathways: a clathrin-mediated one, which does not lead to a full infection, and a dynamin- and cholesterol-independent, but actin- and small GTPase-dependent one, which enables an efficient replication (Misinzo *et al*., 2009). After internalization, the acidification of the endosomal-lysosomal system is required to release virus into the cytoplasm of the monocytic cell lines, whereas the opposite was found for the epithelial cell lines, since blocking the pH drop increases PCV2 replication (Misinzo *et al*., 2005; 2008). It was shown that serine proteases are also involved in the disassembly of the virus in epithelial cells (Misinzo *et al*., 2008).

In PK-15 cells, the viral protein can be detected in the cytoplasm between 6 and 12 hours post-inoculation (p.i), and the replicase and capsid proteins are found in the nucleus from 12 to 24 hours p.i. Replication, virus assembly and release of viral progeny, probably by

nuclear disintegration and cell lysis, occur between 24 and 36 hours p.i (Cheung & Bolin, 2002; Meerts *et al*., 2005a; Rodríguez-Cariño *et al*., 2011).

Regarding specific immune responses, PCV2 antibodies and interferon-gamma (IFN-γ) are detected between 14 and 21 days p.i. (Pogranichnyy *et al*., 2000; Resendes *et al*., 2004a; Fort *et al*., 2007; Fort *et al*., 2009a). It has been suggested that the inability of a pig to mount an effective adaptive immune response is strongly correlated with the development of PCV2-SD. In pigs that do not develop PCV2-SD but remain subclinically infected by PCV2, the start of the decrease of viral titres usually coincides with the onset of antibodies against PCV2 (Meerts *et al*., 2005b; Fort *et al*., 2007; Opriessnig *et al*., 2008a). On the other hand, the delayed production of antibodies, and more specifically, the lack of PCV2-neutralizing antibodies is related with high viral replication and full clinical expression of the disease (Meerts *et al*., 2006; Fort *et al*., 2007).

1.2.4.1. Factors influencing the progression of PCV2 infection towards PCV2-SD

Despite advances in the general understanding of many aspects of PCV2-SD pathogenesis acquired during the last 15 years, key factors in the pathogenic mechanisms of the disease still remain largely unknown. PCV2-SD is considered to have a multifactorial basis, but common to all scenarios is the presence of PCV2. However, in the field, the majority of PCV2 infections are subclinical, which means that other intrinsic factors should be required to trigger the disease onset (Segalés *et al*., 2005). Indeed, the lack of a consistent model to reproduce PCV2-SD under experimental conditions illustrates the complexity of this disease (Tomás *et al*., 2008). A limited number of studies based on the inoculation of PCV2 alone have successfully reproduced PCV2-SD (Albina *et al*., 2001; Bolin *et al*., 2001; Okuda *et al*., 2003; Gauger *et al*., 2011), whereas other similar models only achieved subclinical infections (Balasch *et al*., 1999; Ellis *et al*., 1999; Pogranichnyy *et al*., 2000; Darwich *et al*., 2008). The most successful model to reproduce clinical disease is by activating the host immune system, either by dual infections with PCV2 and another swine pathogen, such as porcine parvovirus (PPV) (Allan *et al*., 1999; Krakowka *et al*., 2000; Hasslung *et al*., 2005), porcine reproductive and respiratory syndrome virus (PRRSV) (Harms *et al*., 2001; Rovira *et al*., 2002) or *Mycoplasma hyopneumoniae* (MHYO) (Opriessnig *et al*., 2004) or, alternatively, by injection of immunostimulant chemical products (Krakowka *et al*., 2001; Opriessnig *et al*., 2003; Grasland *et al*., 2005;

Krakowka *et al*., 2007; Wang *et al*., 2007). It has been postulated that the activation of the immune system increases PCV2 replication, and could be a key factor for triggering PCV2-SD. However, even in the presence of these factors, repeatable results are difficult to obtain (Allan *et al*., 2000; Ladekjaer-Mikkelsen *et al*., 2002; Resendes *et al*., 2004a; Loizel *et al*., 2005; Fernandes *et al*., 2007; Wei *et al*., 2010). Recently, it was reported that germ-free pigs inoculated 7 days apart with a dual heterologous PCV2a/2b isolates showed severe PCV2-SD-associated clinical illness and histopathological lesions (Harding *et al*., 2010). Such heterologous co-replication of most frequent genotypes has also been highlighted in retrospective natural occurring cases of PCV2-SD in pigs from Switzerland (Khaiseb *et al*., 2011).

1.2.4.1.1. Host-virus interaction

To date, little is known about the molecular basis underlying the pathogenesis of the infection, such as the mechanisms by which the virus interacts with its host and the events triggered by this interaction. Since PCV2 has a limited coding capacity due to its small genome size, host cell factors are necessary for the virus to complete its life cycle. Over the last years, a number of porcine proteins interacting with the viral proteins Rep, Cap and the ORF3 product were identified (table 1), either by a yeast or a bacteria-based two-hybrid assays (Timmusk *et al*., 2006, 2009; Liu *et al*., 2007; Finsterbusch *et al*., 2009). These host proteins can be associated with important aspects of viral replication, such as transcriptional regulation, intracellular transport and apoptosis-related processes. Furthermore, PCV2 has been shown to modify important cellular signalling pathways in cultured cells. These alterations include activation of the transcription factor NF-κB by IκBα degradation (Wei *et al*., 2008) or via reactive oxygen species (ROS) (Chen *et al*., 2012); the PI3K/Akt pathway (Wei *et al*., 2012), members of the MAPK cascades, such as ERK, JNK/SAPK and p38 MAPK pathways (Wei and Liu, 2009; Wei *et al*., 2009) and the ubiquitin-proteasome system (UPS) (Cheng *et al*., 20014).

Table 1. List of porcine proteins interacting with PCV2 proteins Rep, Cap and the ORF3 product (adapted from Finsterbusch & Mankertz, 2009).

Viral proteins	Cellular interacting proteins	Function of cellular proteins
Rep protein	Syncoilin	Transport processes
	c-myc	Transcriptional regulation
	ZNF265	Alternative splicing
	TDG	DNA repair, transcriptional regulation
	VG5Q	Angiogenesis
Cap protein	P-selectin	Cell adhesion molecule
	C1qB	Complement factor
	gC1qR	C1qb receptor, multifunctional
	MKRN1	E3 ubiquitin ligase
	Par-4	Apoptosis, cell mobility, transport
	NAP1	Transport, chaperonin
	HsP40	Chaperonin
	HsP70	Chaperonin
	NPM1	Ribosome biogenesis, transport
ORF3 protein	Membrane interacting protein RGS16	Cell signaling
	pPirh2	E3 ubiquitin ligase, p53-induced apoptosis

The host-PCV2 interaction has been analyzed by gene expression studies and would be discussed in the Chapter 6. Proteomics have been also used to identify potential host cellular processes involved in PCV2 infection. A number of different methods was used so far on PK-15 cells (Zhang *et al*., 2009; Fan *et al*., 2012; Liu *et al*., 2014), porcine alveolar macrophages (Cheng *et al*., 2012), pulmonary alveolar macrophages (Liu *et al*., 2013) and lymph nodes from caesarean-derived, colostrum-deprived (CDCD) piglets infected with PCV2 (Ramirez-Boo *et al*., 2011). Several differentially expressed proteins were identified related to molecular transport, signal transduction, cell adhesion, stress response and gene regulation.

1.2.4.1.2. Host-related factors

Farmer and veterinarian observations in the field suggested that certain pig breeds or genetic lines display different susceptibilities to PCV2-SD occurrence. Experimental studies have suggested that Landrace pigs are more susceptible to develop PCV2-SD and PCV2-associated lesions compared to Duroc, Large White and Piétrain breeds (Opriessnig *et al*., 2006; 2009a). In another study, the introduction of Piétrain boars onto PCV2-SD affected herds showed no improvement regarding the disease expression when comparing their offspring with that of other breeds (Rose *et al*., 2005). On the other hand, under field conditions, piglets with 100% Piétrain background had higher body weight at slaughter age and lower postweaning mortality compared with others with different genetic backgrounds (50% Piétrain x 50% Large White, and 75% Duroc x 25% Large White), suggesting that disease susceptibility/resistance might be more related to particular genetic lines rather than particular breeds (López-Soria *et al*., 2011).

An individual predisposition should also occur, since only a proportion of pigs within a particular susceptible genetic line develop the disease. To investigate this fact, Karlskov-Mortensen *et al*. (2008) carried out a case and control linkage study and found that the microsatellite KVL3525, located in the *MYRIP* gene, was related to the development of PCV2-SD. These authors sequenced this gene, identified single nucleotide polymorphisms (SNPs), and performed an association study; however, they did not find any significant result. This result was mainly attributed to the small number of animals used in this study. Very recently, a genome-wide association analysis (GWAS) was performed using different crossbred lines of pigs experimentally infected with PCV2b strain to analyse the host genetic variation of viral load, immune response and weight change (McKnite *et al*., 2014). The proportions of phenotypic variation explained by combined effects of 56,433 SNPs were 34.8–59.4% for viremia, 10.1–59.5% for antibody response and 5.6–14.9% for weight change. Animals that carried more favourable alleles across three SNPs on SSC9 (0.60 Mb) and SSC12 (6.8 and 18.2 Mb) had lower viral load, lower viremia at day 14, day 21 and day 28 and greater overall average daily gain during infection.

1.2.4.1.3. Virus-related factors

Over the last years, there has been an increased interest by various research groups in understanding how antigenic differences among PCV2 strains contribute to disease progression towards PCV2-SD. It has been shown that amino acid changes in the nucleocapsid protein sequence alter the potential virulence of PCV2 (Fenaux *et al*., 2004; Allemandou *et al*., 2011; Huang *et al*., 2011). Very recently, Krakowka *et al*. (2012) reported a linear nine nucleotide sequence difference in the ORF2 of PCV2 isolated from pig tissue samples collected in 1970-1971 when compared with current strains. The corresponding three amino acid changes (residues 133-135) alter the nucleocapsid conformation within the second immunogenic epitope from a hydrophobic (current PCV2 strains) to a hydrophilic (archival PCV2 strains) configuration. These authors suggested that genomic mutations in avirulent PCV2 strains, circulating in pig populations prior 1971, caused changes in the three-dimensional structure of the nucleocapsid protein, thus conferring a new putative "virulence factor" to these viruses, which may explain the emergence of PCV2-SD around the world.

It has been described that multiple PCV2 genotypes can be found in pig herds co-infecting the same animal (Grau-Roma *et al*., 2008; Hesse *et al*., 2008; Huang *et al*., 2013) and recombination events have been demonstrated to occur among PCV2 genotypes (Ma *et al*., 2007; Olvera *et al*., 2007; Hesse *et al*., 2008; Kim *et al*., 2009; Lefebvre *et al*., 2009b; Huang *et al*., 2013). These observations suggest that PCV2-SD might be induced when both PCV2a and PCV2b infect a pig simultaneously. Under this assumption, Harding *et al*. (2010) reported that germ-free piglets experimentally inoculated with PCV2b that have been infected with PCV2a 7 days before developed PCV2-SD. Interestingly, a study using pig tissue samples collected pre- and during PCV2-SD outbreaks in Switzerland showed that PCV2 *in vivo* replication was exclusive to cells with both PCV2a and 2b genotypes (Khaiseb *et al*., 2011). According to the authors, the cooperation among PCV2 genotype group members for an efficient co-replication could explain the heightened recombination ability of these viruses, which may lead to a rapid change on the PCV2 genome pool in pigs. Ultimately, this mechanism might allow the PCV2 to adapt and continually challenge the host immune system.

Besides intrinsic factors as host-virus interaction, pig genetics and virus strains, other extrinsic factors such as management practices, nutrition and vaccination schedules

(environmental-related factors) are thought to influence the course of the disease (Rose *et al*., 2009; Grau-Roma *et al*., 2011).

Finally, when all available information is taken together, the exact reason why certain animals remain subclinically infected and others develop PCV2-SD is not really known. However, it becomes evident that the balance between the host immune defences responding to the presence of the virus and the ability of the virus to interfere with the immune response development are two of the critical points in understanding the pathogenesis of PCV2 infection.

1.2.5. Interplay between PCV2 and the host immune response

1.2.5.1. Immunosupression in PCV2-SD

The most consistent histological feature associated to PCV2-SD is lymphocyte depletion affecting T- and B-lymphocyte populations combined with granulomatous inflammation of lymphoid tissues (Clark, 1997; Rosell *et al.*, 1999). The nature of these lesions, which cause extensive damage of lymphoid architecture, strongly suggests a severe suppression of immune responses. At the end-stages of the disease, a reduction or even a complete loss of B cells in follicular areas can be observed, as well as loss and/or redistribution of interfollicular DCs (Chianini *et al*., 2003). Depletion of the T cell population was found to affect mainly $CD4^+$ cells subset and, to a lesser extent, $CD8^+$ cells (Sarli *et al*., 2001).

Several mechanisms have been implicated in PCV2 infection-associated lymphocyte depletion, but the actual mechanism remains unsettled. It has been shown that B and T lymphocytes are indeed susceptible to PCV2 infection and replication (Pérez-Martín *et al*., 2007; Yu *et al*., 2007a,b; Lefebvre *et al*., 2008; Lin *et al*., 2008). Some works have demonstrated that concanavalin A (Con A) is an important enhancer of PCV2 *in vitro* replication in peripheral blood mononuclear cells (PBMCs) (Lefebvre *et al*., 2008). Also, Rodríguez-Cariño *et al*. (2011) showed that PCV2 replicates in a lymphoblastoid cell line and that viral infection could result in lysis of infected cells. At present, however, it still remains unclear whether the loss of lymphocytes is primarily caused by damage induced by viral replication, destruction of lymphocyte precursors in bone marrow and/or thymus, reduced cellular proliferation in secondary lymphoid tissues or apoptosis.

The implication of apoptosis in the mechanism of PCV2-mediated immunosupression is considered controversial (Shibahara *et al*., 2000; Kiupel *et al*., 2001; Mandrioli *et al.* 2004; Resendes *et al.* 2004b; Lv *et al*., 2012). It has been suggested that the ORF3 protein might be a candidate for virus-induced apoptosis through the activation of caspase 3 and 8 pathways (Liu *et al*., 2005, 2006). The PCV2 ORF3 product competes with a porcine ubiquitin E3 ligase, pPirh2 (porcine p53-induced RING-H2), for binding p53. This interaction promotes the alteration of the cellular localization of pPirh2 and its destabilization, leading to an increase of p53 expression and subsequent apoptosis of the infected cells (Liu *et al*., 2007; Karuppannan *et al*., 2010). It was also observed that the apoptotic activity of the PCV2 ORF3 protein favours the spread of the virus in PCV2-infected mice by recruiting macrophages to phagocytise the infected apoptotic cells (Karuppannan *et al*., 2011). Recently, Lin *et al*. (2011a) have shown that the PCV2 ORF3 protein is capable of triggering an apoptotic response in porcine PBMC and this apoptotic activity is correlated with the nuclear localization of the ORF3 protein. However, the role of this protein in apoptosis is debatable. Chaiyakul *et al*. (2010) characterized the properties of PCV1 and PCV2 regarding the induction of apoptosis. The PCV1 ORF3 protein induced more apoptotic cell death than the PCV2 ORF3 product and the mechanism responsible for PCV1 ORF3 cell death was caspase related. Moreover, truncation of PCV1 and elongation of PCV2 ORF3 proteins revealed that the first 104 amino acids contain a domain capable of inducing cell death, whereas the C terminus of PCV1 ORF3 displays a domain possibly responsible for enhancing cell death. Amazingly, however, PCV2 is considered pathogenic for swine, while PCV1 not. Another research group compared the pathogenicity of an ORF3-null mutant PCV2 infectious DNA clone and a wildtype PCV2 infectious DNA clone in pigs. No significant differences in lymphocyte depletion in secondary lymphoid organs or histiocytic replacement in lymph nodes among groups were observed (Juhan *et al*., 2010). These authors speculated that although the PCV2 ORF3 protein might be involved in immunosupression, induction of apoptosis may not be the pivotal mechanism.

Furthermore, using a tissue microarray technique to evaluate immunopathological changes in lymphoid follicles of PCV2-SD-affected pigs, Lin *et al*. (2011b) demonstrated that apoptosis was an apparent feature in association with lymphoid depletion. A high apoptotic rate associated with high PCV2 load were observed in the germinal centres, whereas a high apoptotic rate but low PCV2 load were present in the interfollicular region.

These findings, suggested that PCV2 may inflict direct injury to B lymphocytes and indirect apoptotic death of activated T cells. Very recently, it was shown that the ORF2 protein of PCV2 activates the autophagic pathway in PK-15 cells to enhance its replication (Zhu *et al*., 2012). Another study demonstrated that PCV2 induces lymphocyte apoptosis and calcium homeostasis modulation *in vitro* (Lv *et al*., 2012). Taking all these data together, it becomes clear that discrepancies regarding the role of apoptosis in PCV2-SD-associated lymphoid lesion development still exist, and deserves further elucidation.

1.2.5.2. PCV2 and the innate immune response

Nowadays, it is commonly agreed that interaction of PCV2 with the immune system is a key determinant of the outcome of the viral infection. Indeed, *in vitro* observations have shown that monocytes/macrophages and DCs are major targets for PCV2 infection, and accumulate infectious virus, allowing its persistence (Gilpin *et al*., 2003; Vincent *et al*., 2003; Pérez-Martín *et al*., 2007).

PCV2 induces *in vitro* changes in alveolar macrophages (AMs), including a decrease in the production of reactive oxygen species, a decrease in phagocytosis capabilities and reduction of microbial killing capacity (Chang *et al*., 2006). Modulation of cytokines/chemokines in macrophages includes an increase in the secretion of TNF-α and IL-8 and up-regulation of mRNA levels of AM-derived neutrophil chemotactic factor-II (AMCF-II), granulocyte colony-stimulating factor (G-CSF), and monocyte chemotactic protein-1 (MCP-1) (Chang *et al*., 2006). Moreover, it has been noted that AMs of piglets experimentally infected with PCV2 show impairment in the processing and presentation of endogenous antigens, displaying a decreased mRNA expression of *LMP7* and up-regulation of *UBP*, calreticulin, *HSP90*, β2-microglobulin and *GRP94* mRNA levels (Li *et al*., 2012). AMs are important target cells of PCV2, and thereby may be involved in PCV2-induced immunosupression, favouring secondary pulmonary infections.

The activity of monocytic cells is also modulated by PCV2. In a recent *in vitro* viral infection study (Tsai *et al*., 2010), proliferation and survival of monocyte-derived macrophages (MDM) and/or blood monocytes (Mo) were associated to multinucleate giant cells (MGC) formation and expression of chemokines (*MCP-1* and *MIP-1*). Such results were obtained by using PCV2 alone, without the involvement of other stimulating

factors. In the same work, PCV2-inoculated MDM displayed an enhanced chemotactic effect on the directional migration of blood Mo. These observations point to the impact that blood Mo recruitment and macrophage proliferation modulated by PCV2 may have on the development of granulomatous inflammation in PCV2-SD-affected pigs.

DCs play a central role in the initiation of immune defences, hence, they are ideal targets for virus evasion from the immune response. It has been shown that PCV2 can persist in monocyte-derived DCs (MoDCs) in absence of replication or cell death induction (Vincent *et al*., 2003). Myeloid DCs (mDCs) maturation is not affected by the presence of PCV2, neither their ability to express cell surface molecules or to process and present antigen to T lymphocytes (Vincent *et al*., 2003; 2005). However, PCV2 DNA, particularly the dsDNA RF, exerts an immunomodulatory effect in plasmocitoid DC (pDC), also known as natural interferon producing cells (NIPC). The virus inhibits the production of interferon (IFN)-α and tumor necrosis factor (TNF)-α by NIPC in response to oligodeoxynucleotides (ODNs) containing CpG motifs (CpG-ODN). In consequence, PCV2 impairs indirectly mDCs maturation, thereby affecting recognition of danger signals (Vincent e*t al*., 2005; 2007). Very recently, Baumann *et al*. (2013) used a panel of cytokines known to enhance IFN-α responses to CpG by pDC to examine their capacity to reverse the inhibitory effect mediated by PCV2. The study showed that the level of inhibition was significantly reduced in enriched pDC cultured in presence of IFN-γ in comparison with pDC cultures treated with CpG and PCV2 in the absence of cytokine. Also in the same work, a dose-response analysis of the PCV2 in the presence of IFN-γ indicated that inhibitory effects were most prominent at higher multiplicity of infection (MOIs) and the encapsulated ssDNA form of the PCV2 genome was apparently responsible for inducing IFN-α. Moreover, it has been speculated that PCV2 infection of DCs and macrophages could indirectly lead to lymphocyte depletion in tissues observed in diseased pigs. In accordance with this assumption, Hansen *et al*. (2010) showed that virus interaction with follicular DCs seems to interfere with maturation, survival and depletion of B cells.

1.2.5.3. PCV2 and the adaptive immune responses

1.2.5.3.1. The humoral immune response

Since the majority of sows under field conditions are seropositive against PCV2, most pigs are generally protected by passively acquired immunity during the first weeks of age, and active seroconversion to PCV2 mainly occurs between 7 and 15 weeks of age (Rodriguez-Arrioja *et al*., 2002). However, it has been shown that the sow PCV2 infection status and antibody levels around farrowing have a significant effect in disease occurrence on the offspring. Indeed, viremic sows or sows with low antibody titres against PCV2 around farrowing had a higher percentage of offspring affected by PCV2-SD (Calsamiglia *et al*., 2007). Moreover, maternal antibodies confer protection against PCV2 in a titre dependent manner; high PCV2 antibody titres are generally protective while low ones usually do not confer protection (McKeown *et al*., 2005; Ostanello *et al*., 2005; Opriessnig *et al*., 2008b).

In experimental infections with PCV2, seroconversion measured as total and neutralizing antibodies (NA) occurs between 10-28 days post-infection, regardless of the presence of clinical disease (Pogranichnyy *et al*., 2000; Bolin *et al*., 2001; Rovira *et al*., 2002; Okuda *et al*., 2003; Meerts *et al*., 2006, 2005; Fort *et al*., 2007). The predominant immunoglobulin isotypes (IgG1, IgG2 and IgA) generally follow the evolution of total antibody titres (Meerts *et al*., 2006). In subclinically infected animals, development of anti-PCV2 IgGs occurs between 14-21 dpi and titres increase at least until 69 dpi (Fort *et al*., 2007). IgMs develop between 7 and 14 dpi and peak around 21 dpi. In addition, Meerts *et al*. (2006) reported that two PCV2-SD affected pigs had increased IgM titres at 10 dpi and decreased titres at 21 dpi when compared with subclinically infected animals. Thus, the presence of IgM was subsequently proposed as an indicator of PCV2 viremia. By means of isotype specific ELISAs and virus neutralization assays, it has been reported that IgG rather than IgM seems to be the primary antibody isotype responsible for virus neutralization (Fort *et al*., 2007). The appearance of NA correlates with the reduction of PCV2 serum viral load. However, the level of NA is significantly decreased or non-existent in PCV2-SD affected pigs (Meerts *et al*., 2005, 2006; Fort *et al*., 2007).

It has been shown that the humoral immunity during the course of PCV2 infection is directed to neutralizing as well as to non-neutralizing epitopes. A linear epitope specific to the PCV2 ORF1 protein was recently mapped by Meng *et al*. (2010) and several immunoreactive regions within the capsid protein (CP), the major immunogenic protein of PCV2, have been identified by a number of studies (Mahé *et al*., 2000; Lekcharoensuk *et al*., 2004; Shang *et al*., 2009; Trible *et al*., 2011; Truong *et al*., 2001).

In summary, subclinically PCV2 infected pigs and PCV2-SD affected animals show differences on dynamics of the humoral immune response. High levels of total antibodies against PCV2 are insufficient to prevent infection, since asymptomatic pigs may remain viremic (Larochelle *et al*., 2003; Grau-Roma *et al*., 2008). The inefficient NA response observed in clinically diseased animals could lead to an uncontrolled virus replication, allowing the development of subsequent immunosuppression and, eventually, concurrent bacterial and viral infections.

1.2.5.3.2. Cell-mediated immune response

Clearance of PCV2 likely occurs by a combination of NA and cell-mediated responses, where interferon (IFN)-γ secreting cells (SC) seem to play a relevant role (Fort *et al*., 2009a; 2009b; Steiner *et al*., 2009). In CDCD piglets infected with PCV2 alone or in combination with lipopolysaccharide (LPS), specific IFN-γ SC were observed between 21 and 29 dpi (Fort *et al*., 2009a). Conventional pigs experimentally infected with PCV2 developed detectable IFN-γ SC 14 days after PCV2 infection (Fort *et al*., 2009b). Finally, co-infection of specific pathogen free (SPF) pigs with PCV2 and PPV led to the production of IFN-γ SC at 7 dpi, whereas in the PCV2 single-infected group it just occurred at 21 dpi (Steiner *et al*., 2009). In the same study, treatment with anti-CD4+ or CD8+ antibodies significantly reduced the number of IFN-γ SC, suggesting that both types of T-cells may be involved in the cellular immune response against PCV2. Insufficient production of IFN-γ correlated with low levels of NA and high PCV2 load, which was associated with PCV2-SD development (Meerts *et al*., 2005b).

Analysis of cytokine patterns in lymphoid tissues, PBMC or serum from PCV2-SD affected pigs revealed that high levels of IL-10 expression is a usual finding (Darwich *et al*., 2003a,b; Sipos *et al*., 2004; Stevenson *et al*., 2006; Crisci *et al*., 2010; Doster *et al*.,

2010). Noteworthy, some of these studies reported that IL-10 was highly expressed in bystander cells such as T-cells and non-infected macrophages, but rarely in PCV2-infected cells, suggesting that PCV2 may exert a paracrine effect on the IL-10 production (Crisci *et al*., 2010; Doster *et al*., 2010). In subclinically PCV2-infected pigs, a transient IL-10 response develops during the viremic phase of the infection (Darwich *et al*., 2008). In addition, PCV2 seems to be able to strongly inhibit IL-12, IFN-α, IFN-γ and IL-2 recall responses of PBMCs after *in vitro* pseudorabies virus (PRV) infection, and the PCV2-induced IL-10 secretion by monocytic cells may participate in this mechanism (Kekarainen *et al*., 2008). Thus, IL-10-mediated immunosuppression may play an important role in the pathogenesis and maintenance of naturally occurring PCV2 infection. Apart from IL-10, PCV2 has the ability to alter the production or the mRNA expression profiles of several cytokines in a variety of conditions (Darwich *et al*., 2003a; 2003b; Fort et al., 2009a; Zhang *et al*., 2011). Therefore, increased levels of pro-inflammatory cytokines, such as IL-8, IL-1α and IL-1β, and reduced levels of IL-2 and IL-4 are usually observed.

In summary, the immune deregulation promoted by PCV2 infection is complex. The underlying mechanisms by which the vast majority of pigs effectively overcome the infection while some animals are unable to counteract the immunological imbalance induced by PCV2 remain to be elucidated.

1.2.6. PCVD control strategies

Initially, control of PCV2-SD was primarily focused on minimizing risk factors that could trigger PCV2 infection to progress into disease. To achieve this, a 20-point plan that gave practical recommendations regarding housing and herd management was proposed (Madec *et al*., 2001). Essentially, the major goals of this plan included minimizing mixing of pigs from different sources or age groups, reduction of stress, improvement of cleaning and disinfection procedures and appropriate nutrition. The implementation of this strategy significantly reduced production losses in PCV2-SD affected farms (Madec *et al*., 2008). Additionally, it has been shown that changes in the pig genetic background and the control of concurrent infections have a significant impact on the occurrence and/or severity of the disease (López-Soria *et al*., 2011; Opriessnig and Halbur, 2012).

Nowadays, besides these indirect control measures, prevention of PCV2-SD has been successfully achieved by means of PCV2 vaccination. To date, several commercial vaccines are currently available; all of them are based on PCV2a strains (Beach and Meng, 2012). The first vaccine on the market (Circovac®, Merial), based on inactivated and oil-adjuvanted PCV2, is administered either in 3 week-old piglets or breeding sows and gilts. Vaccination of gilts and sows protects the offspring through increased levels of maternally derived antibodies. The other vaccines were designed for its application, as single or dual doses, in piglets older than 2 to 4 weeks of age. Ingelvac CircoFLEX® (Boehringer Ingelheim), Porcilis PCV® and Circumvent® (MSD) are subunit vaccines based on the ORF2 capsid protein expressed in a baculovirus system. Fostera™ PCV in North-America and Suvaxyn® PCV2 in Europe (from Zoetis) are based on an inactivated chimeric virus containing the immunogenic ORF2 capsid gene into the genomic backbone of the PCV1. Furthermore, DS Circo Pigvac (DAE SUNG Microbiological Labs. Co., Ltd.) is an inactivated vaccine commercially available in Southeast Asia. Nowadays, an increasing number of vaccines against PCV2 are becoming available worldwide (Beach and Meng, 2012).

Despite differences in the source and concentration of the antigen, adjuvant formulation, and dose of administration, all commercial vaccines have shown outstanding efficacy against PCV2-SD as demonstrated by field and experimental studies (Kristensen *et al*., 2011; Beach and Meng, 2012). PCV2 vaccination improves pig performance, decreases overall mortality rate and reduces co-infections and medication costs (Kixmöller *et al*., 2008; Segalés *et al*., 2009; Lyoo *et al*., 2011). Moreover, the severity of PCV2-SD-lymphoid lesions, systemic viral loads and shedding are also reduced in vaccinated pigs (Fachinger *et al*., 2008; Fort *et al*., 2008; 2009b; Opriessnig *et al*., 2008b). Finally, they are able to induce IFN-γ secreting cells as well as strong total and neutralizing antibody responses (Fort *et al*., 2008; 2009b; Opriessnig *et al*., 2008b; Ferrari *et al*., 2014). It is worthy to comment that benefits of the vaccination have highlighted the importance of the PCV2 subclinical infection in the field. Even farms with no diagnosis of the disease and farms without PCV2-SD clinical signs seem to have been able to significantly increase their overall productivity since PCV2 vaccination (Young *et al*., 2011; Fraile *et al*., 2012).

The effect of vaccination against PCV2 on vertical transmission has been also assessed. Sow vaccination seems to be effective in reducing systemic viral loads, although it does not prevent intrauterine infection nor eliminate viral shedding in the colostrum (Madson *et al*., 2009b; Gerber *et al*., 2011). Besides, shedding of PCV2 in semen and viremia can be reduced by vaccination of boars naturally and experimentally exposed to the virus (Alberti *et al*., 2011; Opriessnig *et al*., 2011).

Remarkably, a clear cross-protection of PCV2a vaccines against the PCV2b genotype has been observed (Fort *et al*., 2008; Takahagi *et al*., 2010). However, it has been suggested that in order to be more effective in protecting against PCV2-SD, the next generation of vaccines should be based on PCV2b genotype, since nowadays it is the dominant subtype circulating worldwide (Opriessnig *et al*., 2013a). Furthermore, as already observed by Xiao *et al*. (2012), the vaccination pressure against PCV2 might result on selection of viral variants that may not be as sensitive to vaccines. To support this hypothesis, a perceived vaccine failure was found in two farms in the United States in 2012, in which a mutant PCV2b strain was identified in PCV2-vaccinated pigs (Opriessnig *et al*., 2013b). However, a recent experimental study challenged vaccinated pigs with this putative new strain and cross-protection was achieved similarly to what happen when pigs are challenged with PCVb strains (Opriessnig et al., 2014).

Different strategies have been employed to design vaccine prototypes over the years, including RNA-based vaccines (Yoon *et al*., 2010), DNA-based vaccines (Shen *et al*., 2009), viral-vectored systems (Fan *et al*., 2008) and modified live-attenuated (MLV) PCV2 vaccines (Beach *et al*., 2011). It has been suggested that the use of these technologies to develop effective PCV2b-based vaccines would reduce the impact of PCVDs by improving the immune response as well as reducing the cost of vaccination programs.

Finally, taking into account the high effectiveness of all vaccines available in controlling PCV2-SD, Feng *et al*. (2014) investigated the feasibility to eradicate PCV2 infection by an extensive vaccination program in a conventional farm. All sows, gilts, boars and piglets were vaccinated in a 12 month period. Although PCV2 infectious pressure was significantly reduced, reaching undetectable levels by the end of the year, evidence of PCV2 infection was detected again when the vaccination program stopped. This result

indicated that mass vaccination, as a potential method to eradicate PCV2 infection, should be extended over a longer period, similarly as other pathogen eradication programs.

1.3. Microarray Technology

1.3.1. History

A DNA microarray can be broadly defined as a tool for multiple paralleled hybridization assays where nucleic acids fragments are placed at high density in a defined pattern on a solid support for recognizing target molecules (Schena *et al*., 1998). This technology has evolved from the basic concept that labeled nucleic acids can hybridize to complementary DNA molecules attached to nitrocellulose membranes (Gillespie & Spiegelman, 1965). The DNA microarrays ancestors were "blotting" methods developed in the late 1970s (Kafatos *et al*., 1979; Southern, 1975). This concept was later expanded with the development of methods for spatial synthesis of nucleic acids (Fodor *et al*., 1991; Schena *et al*., 1995; Wallace *et al*., 1979), the introduction of automation (Lennon & Lehrach, 1991; Southern *et al*., 1992) and the use of non-porous solid supports (Maskos and Southern, 1993a, b), which facilitated parallelization, miniaturization and fluorescence-based detection, and provided the foundation for DNA microarray technology. Finally, the first miniaturized microarray for gene expression profiling was published in 1995 (Schena *et al*., 1995). Since then, microarray-based methods have evolved steadily over the last two decades from the typical in-house made complementary DNA (cDNA) arrays to robust commercial platforms that offer chips with increasing density and improving analytical methodologies. Therefore, vast amounts of information with few experiments can be generated. Nowadays, besides large-scale gene expression analysis, this technology has been successfully adapted for a variety of applications such as comparative genomic hybridization (Pollack *et al*., 1999), genome-wide association studies (Rioux *et al*., 2007), chromatin immunoprecipitation (Nègre *et al*., 2006), microRNA expression profiling (Yin *et al*., 2008) and microorganism identification (Wang *et al*., 2002).

1.3.2. Gene expression microarrays

In practice, the application of microarrays in gene expression profiling consists in the immobilization of DNA sequences (named probes), which are complementary to the DNA sequence of a particular gene of interest, to a surface in pre-defined locations called spots or features. The single-stranded mRNA (named target), which is isolated from a biological sample, is fluorescently labeled. Details of this process may vary with the technology platform. Once in contact with the surface of the array, the labeled targets will hybridize to their complementary probe sequences, whereas the non-hybridized ones are washed off the chip. After hybridization, laser light is used to excite the fluorescent dye. The hybridization intensity at each feature is measured by the amount of fluorescent emission, which gives an estimate of the abundance for each of the transcripts represented on the array (Deyholos and Galbraith, 2001). The idea behind this procedure is that changes in the abundance of mRNA are a reflection of the activity level of genes in the biological sample.

Microarray platforms for gene expression profiling can be classified into three main categories based on the nature of the probes and the method of placing these probes onto the array surface: printed microarrays (Schena *et al*., 1995), *in situ*-synthesized arrays (Lockhart *et al*., 1996) and high-density bead arrays (Michael *et al*., 1998).

In printed microarrays (also called two-color arrays), pre-synthesized probes (cDNAs, shorter PCR amplified gene specific tags or single-stranded oligonucleotides) are printed (spotted) on a solid surface, usually a glass microscope slide, by robotic pin-based dispensers or ink-jet printers. The mRNA extracted separately from two biological samples is reversely transcribed, fluorescently labeled with different dyes (usually the cyanine dyes Cy3 and Cy5) and simultaneously hybridized to the same array. After hybridization, a scanner is used to obtain images, where each fluorescent emission is measured separately, and subsequently merged to produce a composed picture. An image analysis software is used to determine the two signal intensities for each spotted feature on the array, and the resulting values are used to calculate the expression ratio (i.e. test/reference samples) for each probe.

High-density bead arrays, rather than attaching probes onto a microarray at known locations, are based on randomly assembled arrays of thousands of 3-µm silica beads in either a fiber-optic bundle or a silica slide surface (Michael *et al*., 1998). Each bead is coated with many thousand copies of the same oligonucleotide probe and a shorter address sequence is used for bead identification. Following random assembly, the location and identity of each bead is determined by a sequential decoding process (Gunderson *et al*., 2004).

In *in situ*-synthesized microarrays, oligonucleotide probes are chemically synthesized at specific locations directly onto the array surface. Three main techniques can be used for this purpose: photolithographic masking techniques (Fodor *et al*., 1991; Singh-Gasson *et al*., 1999), ink-jet spotting process (Hughes *et al*., 2001) and addressable electrodes to cause deprotection of the previously deposited nucleotides via electrochemical methods (Maurer *et al*., 2006). These technologies allow the synthesis of oligonucleotide probes with 25-60 nucleotides in length. Specifically, the present thesis focuses on the high-density oligonucleotide microarray technology developed by Affymetrix GeneChip® in the mid 90's, which is the most widely known *in situ*-synthesis technique (Lockhart *et al*., 1996). Details about this technology and the main steps to perform a microarray experiment using Affymetrix GeneChips® for gene expression profiling (Figure 3) are provided in the following sections.

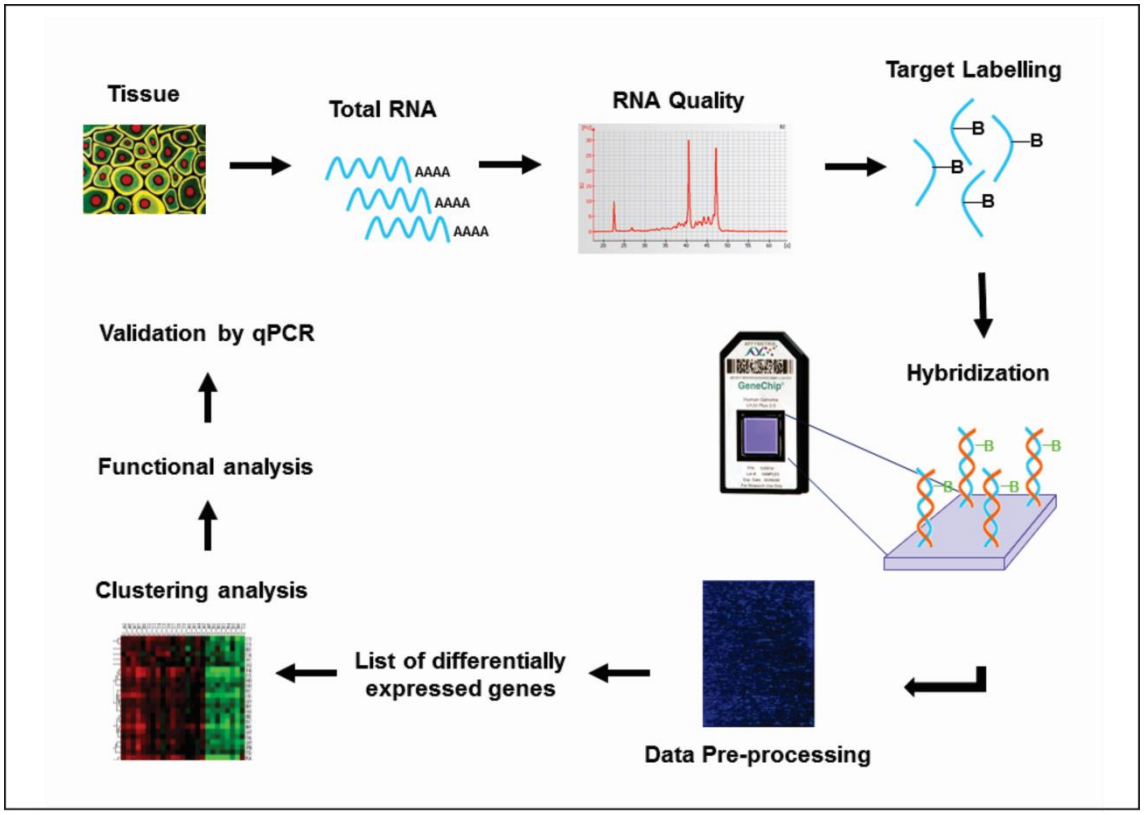

Figure 3. Schematic summary of the main steps to perform a microarray study using Affymetrix GeneChips® for gene expression profiling. qPCR: real time quantitative PCR.

1.3.3. *In situ*-synthesized oligonucleotide microarrays

1.3.3.1. Array Manufacturing

The Affymetrix GeneChip® technology is based on photolithographic masking techniques used in semiconductor industry to synthesize oligonucleotide probes directly on the surface of 1.25 cm^2 quartz wafers (Fodor *et al.*, 1991; Lockhart *et al.*, 1996). Briefly, synthetic linker molecules with light-sensitive protecting groups are attached on the array surface. Photolithographic masks are designed to determine the probe position on the chip and each mask has a pattern of windows that either block or transmit ultraviolet light (UV). Then, UV light is directed through a photolithographic mask deprotecting linker molecule in exposed areas, thereby activating them for nucleotide coupling. Linkers in unexposed regions of the array remain protected and inactive. A solution containing a single nucleotide type with a protection group is flushed over the wafer surface and a nucleotide attaches to the activated linkers, initiating the synthesis

process. A new mask is then applied and the same process is repeated. After several rounds, the desired set of probes with 25-mer becomes fully constructed. Figure 4 shows the synthesis process.

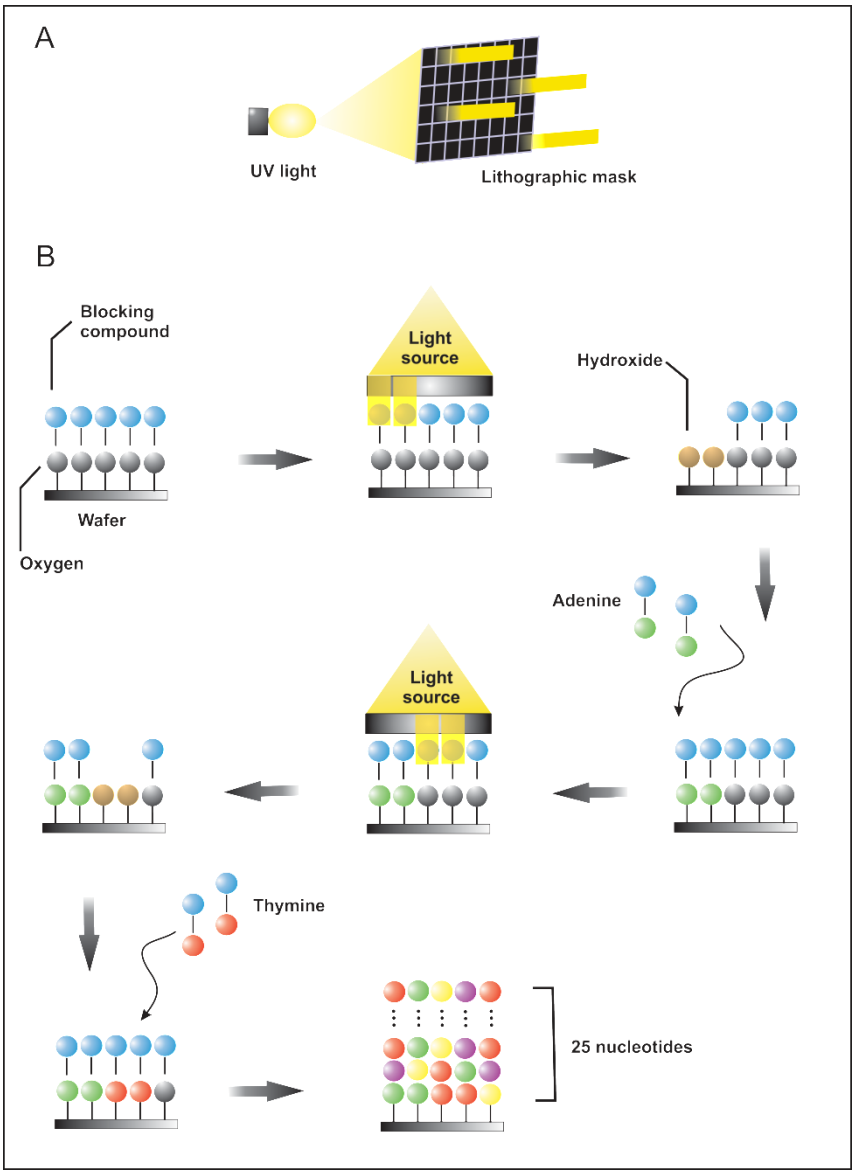

Figure 4. Photolithographic masking technique. A) Schematic representation of the lithographic mask. B) The synthesis cycle. A series of masks are used to deprotect different locations and base by base oligonucleotides with 25-mer are built in parallel. Adapted from Miller and Tang (2009) with permission of the publisher (ASM Journals).

1.3.3.2. Array design

The surface of the GeneChip® Porcine Genome Array used in the present thesis is divided by 11x11 µm squares, called features or probe cells. Each feature contains millions of probe molecules with a unique sequence of 25-mer. Every transcript sequence is represented by 11 probe pairs and this group of probes is referred as a probeset. A probe pair is composed by a probe that perfectly matches (PM) its target sequence, and another one containing a single mismatch (MM) located at the 13th position of the 25-mer probe sequence. Mismatch probes are assumed to measure non-specific hybridization, allowing the detection and subtraction of background and cross-hybridization signals (Lipshutz *et al*., 1999). Additionally, this array contains a number of different control probes used for quality control assays.

Probe sequences are selected from the transcribed regions of a gene and near to the 3' end of the gene sequence. Public databases including UniGene GenBank® mRNAs, GenBank porcine mitochondrial and rRNA sequences were the references for the gene sequence. The assignment of the probesets to genes (annotation) provided by Affymetrix (retrieved from the NetAffx service on the Affymetrix homepage) *is* considered poorly annotated, which difficults the biological interpretation of data. Therefore, attempts have been made to achieve a more precise and accurate annotation of the probes present on the array (Tsai *et al*., 2006a; http://www4.ncsu.edu/~stsai2/annotation/; Naraballobh *et al*., 2010). In summary, the Porcine GeneChip® array contains 23,937 probesets that interrogate approximately 23,256 transcripts from 20,201 *Sus scrofa* genes (http://media.affymetrix.com/support/*technical*/datasheets/ porcine_datasheet.pdf).

1.3.3.3. RNA quality assessment

As with most RNA-based assays, the output from microarray data critically depends on the integrity of the starting RNA. Quality assessment of total RNA can be determined by conventional methods, such as the visualization of 28S and 18S ribosomal RNA bands on ethidium bromide gels, where a 28S:18S ratio of 2.0 is an indicator of high quality RNA (Sambrook and Russel, 2001). However, these methods are sample-consuming and not sensitive enough to detect slight RNA degradation. Nowadays, microfluidic capillary electrophoresis (Agilent 2100 bioanalyzer, Agilent Technologies, USA) has become

widely used. It requires very small amounts of RNA samples which are electrophoretically separated by their molecular weight on a microfabricated chip and subsequently detected via laser-induced fluorescence detection. The result is visualized as an electropherogram or translated to gel-like images, where the amount of measured fluorescence correlates with the amount of RNA of a given size. The ratio 28S:18S is also used as a measure for RNA quality assessment. The gradual degradation of RNA is reflected by a continuous shift towards shorter fragment sizes and consequently, by a decrease in 28S:18S ratios. In addition, a software algorithm that describes RNA integrity can be used (Schroeder *et al*., 2006). The RNA Integrity Number (RIN) is a tool based on a neural network which allows the classification of total RNA on a numbering system from 1 to 10, with 1 being the most degraded and 10 the most preserved RNA. The Microarray Quality Control Consortium considers a RIN > 8.0 and 28S:18S ratio > 0.9 as quality criteria.

1.3.3.4. Target labeling and hybridization

Labeling efficiency of target molecules is an important factor to ensure a high quality microarray data (Dumur *et al*., 2004). Affymetrix standardized protocol (GeneChip® Expression Analysis Technical Manual, http://www.affymetrix.com) uses the linear amplification based on *in vitro* transcription (IVT) (Van Gelder *et al*., 1990) and biotin labeling strategies. Briefly, total RNA (1 to 15 μg) is reversely transcribed in the presence of a T7-Oligo (dT) promoter primer for the first-strand cDNA synthesis. When the second-strand cDNA is completed, the double-stranded cDNA originated is purified and used as a template for IVT reaction. The IVT reaction is performed using a T7 RNA polymerase and a biotinylated nucleotide for complementary RNA (cRNA) amplification and biotin labeling. The biotin-labelled cRNA target is subsequently cleaned, fragmented to reduce cross-hybridization and hybridized to a GeneChip expression array. Affymetrix chips are single-channel arrays, i.e., only a single sample can be hybridized to each chip. Therefore, the comparison between different samples is done by using several chips. For smaller amounts of the starting material (10 to 100 ng), a variation of this technique (called one-cycle assay) can be done by performing two cycles of cDNA synthesis and IVT amplification (two cycle-assay). After the hybridization, biotinylated cRNA target molecules are stained with a fluorescent streptavidin–phycoerythrin (SAPE) conjugate. Afterwards, biotinylated anti-streptavidin antibodies are bound to the stained molecules

and then a second round of staining with SAPE is performed, enabling subsequent detection by a laser scanner. These protocols are used by the standard Affymetrix hybridization and fluidics station, which are controlled by the GeneChip® Operating Software (GCOS).

1.3.3.5. Scanning

In this step, also controlled by the GCOS, a high resolution confocal scanner that uses a laser to excite fluorophores bound to hybridized nucleic acids is used to measure the amount of hybridized target at each probe. Photomultiplier tubes (PMT) are used to detect and record the emitted fluorescence signals, which are stored as *.TIFF images for further analysis. Three main output files are generated by each sample hybridized to a chip:

- Image Data File (*.DAT): This file contains the raw image (*.TIFF) of the scanned array, where the fluorescence intensities are represented by pixel intensity values,
- Cell Intensity File (*.CEL): This file is generated from the primary image in *.DAT file and contains an intensity value for each probe cell on the array (probe-level data). All of the analyses in this thesis began with data read from these files,
- Chip Description File (*.CDF file): Describes the location of probe pair sets on the array and determine the identity of the probes into the probesets.

1.3.3.6. Data analyses

1.3.3.6.1. Software for data analysis

Over the years, an increasing number of bioinformatics tools have been developed to handle the huge amount of data generated from microarray experiments. Several commercial softwares are available for management and analysis of Affymetrix gene expression data, including the Affymetrix software suite GCOS (http://www.affymetrix.com), Spotfire® DecisionSite (http://www.spotfire.com) and Rosetta Resolver (http://www.rosettabio.com/products/resolve). In addition, open source software have become widely used, providing freely available alternatives for gene expression analysis, such as dChip (Zhong *et al*., 2003), BRB-Array tools

(http://linus.nci.nih.gov/BRB-ArrayTools.html) and the Bioconductor project (http://bioconductor.org), which was used in this thesis.

The Bioconductor is an open-development software project that provides a broad variety of statistical and graphical tools for high-throughput genomic data analysis (Gentleman *et al*., 2004) and it is considered nowadays the "gold standard" for analysis of dual color microarrays and Affymetrix chips. This software is mainly based on the R programming language (http://cran.r-project.org/) and consists on a series of packages or library files. Each package usually comprises a vignette, which is a document that provides codes to use within the R environment and a description of the package's functionality. A number of specific tools and modeling approaches are available for Affymetrix gene expression data sets, including data pre-processing, normalization as well as advanced statistical algorithms for differential gene expression and downstream analyses as gene ontology. The Bioconductor platform offers a number of advantages including the diversity of analysis options that are not often available into commercial software, the reproducibility of data analysis, and the flexibility of the R language, which allows researchers to modify the codes according to their needs.

1.3.3.6.2. Quality control assessment

The quality of RNA samples and slide hybridizations are paramount for gene expression studies. Therefore, a number of quality control (QC) measures should be implemented prior to downstream analyses to ensure that arrays have hybridized correctly and the sample quality is acceptable. The packages "*affy*" (Gautier *et al*., 2012) and "*affyPLM*" (Bolstad, 2012) implemented in the Bioconductor software offer tools for computing diagnostic plots and statistics that can be used as a starting point for quality assessment of microarrays. These include image plots for detection of spatial effects, boxplots and histograms which summarize the distribution of probe intensities, the degree of RNA degradation between chips, the distribution of the log expression levels of each probeset on the array relative to the median expression of this probeset across all arrays of the experiment (RLE), and the normalized standard error estimates (NUSE) of probesets. Moreover, the "*simpleaffy*" package (Wilson and Miller, 2005) provides a QC report which comprises several functions:

- Average background: this value should be similar across all arrays and variations can indicate different amounts of cRNA or differences in hybridization efficiency that can produce a brighter chip. The background values between arrays should be within a range of 20 units,
- Percentage (%) of probes called present: a probeset is considered present when the PM values for that probeset are significantly higher than their MM counterparts. Thus, this value represents the percentage of probesets called present on a chip and should be within a range of 10% across the arrays,
- The scaling factor: this function represents the amount of scaling necessary to equalize the mean intensities for all arrays, so, each array will have the same mean. Therefore, the amount of scaling applied provides a measure of the overall expression level for an array, which reflects the amount of labeled RNA that has been hybridized to the chip. Affymetrix recommends that the scaling factors should be within 3-fold of one array to another,
- 3'/5' ratios for *beta-actin* and *glyceraldehyde 3-phosphate dehydrogenase* (*GAPDH*): these housekeeping genes are used in this function as controls for the RNA quality. Each control gene is represented on the array by three probesets, one from the 5' end, one from the middle and the last one from the 3' end of their transcripts. The ratio of the intensity value from the 3' probeset to either the mid or 5' probesets gives an indication of the quality of the RNA hybridized to the chip. To consider an array of good quality, the 3'/5' ratio should not exceed 3 for *beta-actin* and 1.25 for *GAPDH*. High ratios may indicate the presence of truncated transcripts.

1.3.3.6.3. Data pre-processing

Pre-processing data from GeneChip arrays is a crucial step required to allow measurements from different arrays to be compared and usually involves three basic steps (Clarke and Zhu, 2006; Gautier *et al*., 2004):

- Background adjustment, which removes unspecific signal intensities caused by optical noise and non-specific binding

- Normalization, which removes non-biological or systematic variation among samples due to technical factors to give accurate measurements of specific hybridizations
- Summarization, which converts the signal intensities from all probes of a particular probeset into a single expression value representing the transcript level of a given gene

Different methods have been developed for each of the above mentioned steps, allowing a great variety of analyses to be performed (Irizarry *et al*., 2006). The most popular algorithms for pre-processing Affymetrix data (Table 2) include the MicroArray Suite (MAS 5.0, Affymetrix, 2002), the Variance Stabilization and Normalization (VSN, Huber *et al*., 2002), the Robust Multi-array Average (RMA, Irizarry *et al*., 2003a,b), GCRMA (Wu *et al*., 2004), dChip (Li and Wong, 2011; Zhong *et al*., 2003), and Probe Logarithmic Intensity Error (PLIER, Affymetrix, 2005). Most of them are integrated into the Bioconductor project.

Table 2. Methods for pre-processing Affymetrix Genechip data.

Method	**Background adjustment**	**Normalization**	**Summarization**
MAS 5.0	Subtraction of the spatial effect and MM intensities	Scale factor	A robust average (Tukey Biweight)
VSN	Only uses PM intensities	Scale factor	A robust linear model (Median polish)
RMA	Convolution model Only uses PM intensities	Quantile	A robust linear model (Median polish)
GCRMA	Uses MM and probe sequence information (GC content)	Quantile	A robust linear model (Median polish)
dChip	Multiple choices: PM-MM, PM only, etc.	Spline fitted to rank invariant set	Model assuming multiplicative probe effect and additive error
PLIER	Multiple choices: PM-MM, PM only, etc.	Quantile	Multiplicative model is fitted

The RMA method (Irizarry *et al*., 2003a,b) was applied for pre-processing microarray data generated in this thesis. This is a widely used algorithm implemented in the "*affy*" and "*affyPLM*" libraries within Bioconductor to apply background correction, to normalize the data between arrays, and to compute the expression measurements. The background adjustment is based on a convolution model, which assumes that observed PM intensities are a composition of normally distributed noise and exponentially distributed signal. Therefore, this algorithm does not take into account intensities of MM probes due to the high proportion of MM probes with higher intensities than the corresponding PM probes (Naef *et al*., 2002; Millenaar *et al*., 2006). The PM values are corrected on an array-by-array basis and the noise distribution is truncated at zero to avoid

negative values. For the normalization step, RMA uses the quantile normalization algorithm in which the background-corrected PM probe intensities are adjusted to produce identical distributions across arrays (Bolstad *et al*., 2003). Then, the normalized PM intensity values are log2-transformed and a robust multi-array model using the median polish algorithm is fitted for each probeset to estimate the expression value for the corresponding gene. This method allows combining information across chips and protects against outlier probes (Irizarry *et al*., 2003b). Finally, an expression matrix containing numerical information about the expression values for each transcript (rows) in each array (columns) of the data set is obtained. Although the choice of the most appropriate pre-processing procedure is not a trivial process and there is no standard method (Irizarry *et al*., 2006; Karakach *et al*., 2010), it has been shown that the RMA algorithm is robust and reproducible, providing consistent estimates of fold change and good correlation coefficients with quantitative real-time PCR (qPCR) (Irizarry *et al*., 2003b; Millenaar *et al*., 2006).

1.3.3.6.4. Differential gene expression

One of the main goals of microarray studies is to identify genes whose expression levels are significantly different between two or more conditions under investigation. Several statistical tests have been applied for this purpose (Barrera *et al*., 2004; Sohn *et al*., 2008; Tuscher *et al*., 2001; Troyanskaya *et al*., 2001) and, in the present thesis, the moderated t-statistic method based on an empirical Bayes approach (Smyth, 2004) was used for detection of differentially expressed genes (DE). This method is implemented in the "*limma*" package of Bioconductor (Smyth *et al*., 2012) and it is one of the most widely used for Affymetrix gene expression analyses. The general idea behind this approach is to fit a linear model to the expression data (log-intensity values) for each transcript. The model is specified by a design matrix, where each row corresponds to an array and each column corresponds to a coefficient that represents the treatments of the experiment. This step is performed to estimate the variability of the data. Then, a contrast matrix is designed using the fitted coefficients to make the comparisons of interest between treatments. To assess differential expression for each transcript and each contrast, a moderated t-statistic is calculated based on an empirical Bayesian model, which shrinks individual estimates of variance towards a common value. A number of summary statistics are provided for each transcript and for the selected contrast, including the $\log_2$-fold change between the

experimental conditions (M-value), the moderated t-statistic and correspondent *p*-value, and the B-statistic, which is the log-odds that a given transcript is DE. Moreover, an adjustment of the calculated *p*-values to control the false discovery rate (FDR) can be performed to account for multiple hypothesis testing problem. This algorithm was developed by Benjamini and Hochberg (1995) and represents the expected proportion of false positives among the transcripts declared as significantly different.

1.3.3.6.5. Cluster analysis

Once a list of DE genes has been achieved, correlations and patterns among gene expression values can be explored. The most frequently methods used to reveal the natural data structures and gain some initial insights regarding data distribution are the unsupervised clustering algorithms, which assign genes to groups of similar expression patterns without any a *priori* knowledge about the biological functions of the genes on the arrays (Eisen *et al*., 1998; Raychaudhuri *et al*., 2001). There are several softwares available to perform and visualize cluster analyses, such as the freeware Cluster 3.0 (http://bonsai.hgc.jp/~mdehoon/software/cluster/software.htm#ctv) and the Java Tree-View (http://jtreeview.sourceforge.net/), which were used in this thesis.

Commonly unsupervised clustering methods include the k-means (MacQueen, 1967), self-organizing map (SOM, Kohonen, 1997) and the hierarchical analyses (Eisen *et al*., 1998). The k-means and SOM analyses are partition-based clustering methods, which attempt to directly decompose the data set into a group of disjoint clusters. The number of clusters to be generated by these methods is predetermined by the user.

The hierarchical clustering, which was applied in the present thesis, generates groups of nested clusters based on a statistical determination of similarity (distance) between data. A wide range of distance metrics is available to measure the similarity between two expression patterns (e.g. Euclidian distance, Pearson correlation, Spearman's rank or Kendall's tau). Initially, each transcript is considered as a separate cluster, then, at every stage of the clustering process, the two nearest clusters are merged into a new one. The most commonly used methods to determine when two clusters are sufficiently similar to be linked together include the complete linkage, average linkage and single linkage, which use maximum, average, and minimum distances between the members of two

clusters, respectively. Finally, the clustering process is repeated until the whole data set is agglomerated into one single cluster.

The result of the hierarchical clustering analysis can be graphically represented by a tree-like diagram (also called as dendrogram) combined with a heat map, in which normalized levels of expression are mapped on a color scale (Figure 5). Each node (cluster) in the tree is the union of subclusters, and the root of the tree is the final cluster containing all the objects. Similarity between transcripts or transcript groups is represented by the distance to their closest branch point. Transcripts belonging to common sub-branches have the most similar expression pattern, while others connected at the highest level of branching are the most dissimilar.

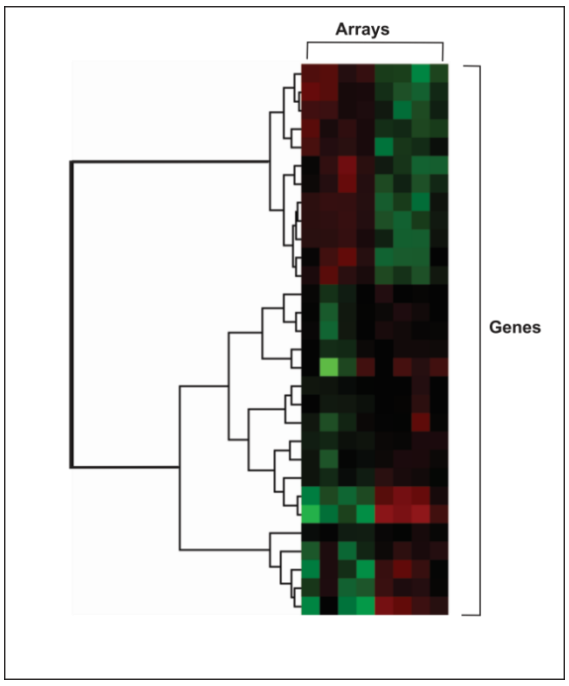

Figure 5. Hierarchical clustering analysis. This figure combines a heat map, which is the part of the figure containing colors, and the dendrogram, which is the tree-like structure displayed to the left of the heat map. Rows represent genes and the arrays are represented by columns. The color means the expression level of the transcripts. Red represents high expression level, while green represents low expression level.

1.3.3.6.6. Functional analysis of DE genes

The ultimate goal of gene expression microarray studies, after obtaining a list of DE genes, is the extraction of biological information from the generated data, aiming to improve the understanding of the underlying mechanisms of diseases. Therefore, a wide variety of computational tools has been developed over the last years to help the biological interpretation of microarray results.

A widely used approach to translate a given list of DE genes into functional categories is based on the biological knowledge accumulated in public databases such as the Gene Ontology (GO, Ashburner *et al*., 2000) coupled with an enrichment analysis. The GO project (http://www.geneontology.org/) is a collaborative effort created to provide a collection of controlled vocabularies (ontologies) describing the biology of a gene product in any organism. There are three organizing principles or categories of GO:

- the biological process, which refers to a biological function that a gene product participates
- the molecular function, which represents its biochemical activity
- the cellular component, representing its placement in the cell

The enrichment analysis is a method to systematically map a set of genes to their associated biological annotations and then to statistically determine the most over-represented (enriched) annotation out of the terms associated with the genes of interest. This approach compares the number of DE genes found in each GO category of interest with the number of genes expected to be found in the same category by random chance. A large number of high-throughput enrichment tools are currently available (Huang *et al*., 2009a; Khatri and Draghici, 2005; Van den Berg *et al*., 2009; http://www.geneontology.org/GO.tools.shtml). For the results of GO enrichment shown later in this thesis, the open source software DAVID (Database for Annotation, Visualization and Integrated Discovery, Huang *et al*., 2009b) was used. DAVID integrates annotation terms from over 30 sources besides GO, adopts the Fisher Exact test (referred as EASE score, Hosack *et al*., 2003) to measure the significance of the gene-term enrichment, and globally correct enrichment *p*-values to control the FDR.

Another way to acquire deeper biological understanding of molecular and cellular mechanisms derived from a microarray study is to identify biological pathways and molecular networks that are most significantly associated with the dataset of interest. This can be accomplished through pathway analyses which are performed by commercial software such as MetaCore™ (GeneGo, Inc., St. Joseph, http://www.genego.com/metacore.php) and IPA (Ingenuity Pathway Analysis, Ingenuity Systems, Mountain View, CA, http://www.ingenuity.com/), or by open source platforms including the Cytoscape (http://www.cytoscape.org/what_is_cytoscape.html). Several pathway analysis tools rely on pre-compiled databases of pathways derived from large-scale literature analyses such as the Kyoto Encyclopedia of Genes and Genomes (KEGG, http://www.genome.jp/kegg/).

In the current thesis, pathway analyses were performed by MetaCore™, which is a commercial software for functional analysis of high-throughput techniques such as microarrays (http://www.genego.com/metacore.php). This application is based on a manually curated database of mammalian biology and medicinal chemistry and enables the identification of biological mechanisms, pathways, networks and cellular functions most relevant to the experimental data sets or genes of interest. The software constructs molecular networks centered on the significant genes identified in the study and calculates the probabilistic fit between each network and the observed expression data from the array, assigning a chance probability score to each network. Users can create custom pathways or perform searches for particular targets, disease areas, or biological functions.

1.3.3. Public databases

To address the need of comparing data from microarray experiments conducted by different laboratories and performed by a vast variety of different platforms and methodologies, the Minimum Information About a Microarray Experiment (MIAME, Brazma *et al.*, 2001) was created by the Microarray Gene Expression Database group (MGED; http://www.mged.org). The MIAME is a document that describes the reporting standards required to interpret the microarray data and to ensure that the results can be independently verified. Public repositories to store data sets from microarray experiments have been developed based on MIAME guidelines. The most popular databases include the ArrayExpress (Brazma *et al.*, 2003) and the Gene Expression Omnibus (GEO, Edgar

et al., 2002). Nowadays, during the process of publication of a microarray study, the submission of data to public repositories is a step often required by scientific journals.

1.3.4. Technical validation of microarray measurements

The maturation of the microarray technique over the past several years led this technology to be considered nowadays as robust, sensitive and accurate to detect differential gene expression. There is an increasing consensus among the scientific community that microarrays are capable of generating reproducible measurements across different platforms as well as within and across different laboratories when appropriate analysis procedures are applied (Shi *et al*., 2006; Yauk and Berndt, 2007). Moreover, Affymetrix Genechips show high specificity, reproducibility, show low levels of variance and high correlation among replicates, when compared with other microarray platforms (Irizarry *et al*., 2005).

However, as any high-throughput technology, microarray studies are complex and prone to errors due to the several experimental steps needed to perform the analyses. Therefore, it is of paramount importance that microarray data is experimentally validated by an independent method to confirm that changes observed on the mRNA levels of a group of genes detected by microarray can be reproducible in a large number of samples by other techniques (Canales *et al*., 2006; Dallas *et al*., 2005; Rockett and Hellmann, 2004). Among the different methods that have been applied to validate the expression results from microarrays, including the northern blot, ribonuclease protection assay and *in situ* hybridization, the quantitative PCR (qPCR, SYBR® Green PCR and TaqMan assays) is the most common technique used nowadays (Aikawa *et al*., 2008; Canales *et al*., 2006). The qPCR is a widely used approach because of the ease in designing the assays, high sensitivity, relatively low cost and generally generates strong correlation with microarray data (Aikawa *et al*., 2008; Dallas *et al*., 2005; VanGuilder *et al*., 2008).

In the present thesis, the validation of microarray results was performed by the SYBR® Green PCR method, which consists in using an intercalating dye that fluoresces upon binding to double-stranded DNA. Changes in mRNA levels of a target gene across multiple samples are compared to an endogenous reference gene. The number of mRNA targets in a sample is quantified based on a comparison with a cycle threshold (Ct),

defined as the cycle at which the fluorescence signal can be detected above background fluorescence in the exponential phase. The Ct is inversely proportional to the log of the starting number of transcript molecules. Relative standard curves should be performed in order to compare the amplification efficiencies of the target and control primer pairs. Then, gene expression levels are calculated by the ratio between the amount of target gene and the control gene using the $2^{-\Delta\Delta Ct}$ method (Livak and Schmittgen, 2001). Firstly, the ΔCt between the target gene and the reference gene is calculated for each sample, and subsequently the difference between the ΔCt of each sample and the ΔCt of a calibrator sample is obtained, resulting in the ΔΔCt value. In order to transform the results into fold variation, the formula $2^{-\Delta\Delta Ct}$ may be applied. A positive result would indicate an increase in the expression of the gene of interest in a given condition, whereas a negative result would indicate a decreased expression.

Despite the advances on the microarray field, until today no standard definition of validation exists, nor reporting requirements for publication. The most widely used methodology is to select a few candidate genes that show changes in their expression and are involved in a particular biological process of interest to the researcher. The selection of genes also depends on the availability of the material, time and the expense involved. Another point to consider is that the correlation between the results from the microarrays and qPCR can be affected by the sequence selected for designing probes and primers. The presence of inaccuracies on the probe sequence annotation, unknown single nucleotide polymorphisms (SNPs) and splice variants should be taken into account (Aikawa *et al*., 2008; Dallas *et al*., 2005).

CHAPTER 2

HYPOTHESIS AND OBJECTIVES

One of the major challenges in understanding the infection with PCV2 and its progression towards PCV2-SD was (and still is) the overall lack of knowledge about the biological processes and molecular mechanisms involved in the host-pathogen interaction. The role of PCV2 in the pathogenesis of PCV2-SD and its implications on the pig immune system has been a subject of many studies using traditional approaches during the last two decades. However, at the beginning of this Thesis, the analysis of the PCV2 infection from a transcriptional point of view was reported only by few studies using qPCR techniques to characterize the mRNA levels of cytokines in lymphoid organs and cells of pigs naturally affected by PCV2-SD. Microarray technology allows simultaneous measurement of the mRNA levels of thousands of genes and have been used during recent years to examine gene expression profiles of tissues or cell lines subjected to infection, helping to unravel host–pathogen interactions relevant to the pathogenesis of a variety of diseases.

Therefore, the general objective this Thesis was to use the microarray technique to study the global transcriptional profile of pigs subclinically infected by PCV2 and also in natural cases of PCV2-SD. The ultimate objective was to apply this technology to gain a more comprehensive picture of the PCV2 pathogenesis. The specific objectives were as follows:

- To evaluate the utility of the Affymetrix Porcine Genechip® platform to study the host transcriptional response against PCV2 infection and to investigate the molecular events taking place in response to a subclinical infection in a single time-point experiment.
- To characterize the early and late molecular mechanisms underlying the immune response of piglets subclinically infected with PCV2 in a time-course experiment.
- To characterize the global transcriptional profile of pigs naturally affected by PCV2-SD.

CHAPTER 3

STUDY I

Exploratory Study on the Transcriptional Profile of Pigs Subclinically Infected with Porcine Circovirus Type 2

3.1. Introduction

Most of the pigs become infected by PCV2 sometime during their life, but only some of them develop the disease. The explanation of this fact still remains unclear, suggesting that all factors playing a role in disease development are not yet known. Besides management (Madec *et al*., 2000), concurrent viral and bacterial infections (Allan *et al*., 1999; Opriessnig *et al*., 2004) and PCV2 genotype involvement (Gagnon *et al*., 2007; Grau-Roma *et al*., 2008), other predisposing factors might be involved in PCV2-SD triggering, such as the genetic background of the immune response that counteracts PCV2.

The role of PCV2 in the pathogenesis of PCV2-SD and its implications on the host immune system has been a subject of many studies during the last decade (Krakowka *et al*., 2001; Darwich *et al*., 2003b; Meerts *et al*., 2005a; 2005b; 2005c). However, to this date, no attempt has been made to determine the genetic transcriptional profile of pigs infected with PCV2. In this context, a more detailed genetic understanding of the PCV2–host interaction is needed.. Therefore, in the present study, an exploratory work on microarray analysis was carried out as a screening tool to identify changes in expression of potential genes associated with the immune response against PCV2 in CDCD Duroc piglets.

3.2. Materials and methods

3.2.1. Experimental Infection

Six CDCD Duroc piglets were obtained from two PCV2-seropositive sows. The animals were raised in experimental isolation facilities at the biosecurity level 3 laboratory of the Centre de Recerca en Sanitat Animal (CReSA) (Fernandes *et al*., 2007).

At 7 days of age, piglets were randomly divided into two experimental groups: one group (n=4) was challenged with 2 mL (1 mL by intranasal and 1 mL by oral routes) of $10^{5.2}$ 50% tissue culture infectious dose ($TCID_{50}$/ml) of PCV2 inoculum. The inoculum was prepared from the ninth cell passage from a Spanish PCV2 isolate (Burgos) recovered from lymphoid tissues of a PCV2-SD affected pig (Fernandes *et al*., 2007). The second

group of pigs (n=2) was kept as uninfected control and was inoculated with sterile cell culture medium (MEM) by the same route and dose. Experimental groups were kept in separate isolation rooms.

Clinical signs, rectal temperatures and body weight were recorded daily. During the first 11 days of the experiment, two PCV2-inoculated piglets died due to bacterial systemic infection (non-haemolytic *Escherichia coli* were isolated from faecal samples and thoracic and peritoneal swabs from both animals); thus, only four piglets (2 controls and 2 PCV2-inoculated pigs) remained alive to the end of the experiment. These unexpected deaths led to the situation that piglets of the infected and control groups had opposite sex (both controls were males and both PCV2 inoculated females), and all of them from the same sow.

A Western-blot analysis was performed in order to evaluate the serological profiles against *E. coli* of the remaining piglets. The *E. coli* isolated from the peritoneum of those pigs that died was grown in 4 mL LB broth up to a density of 0.6 uod/mL. The suspension was pelleted at 16000g for 5 minutes and resuspended in SDS x 4 urea 8M (30 µL for each mL of culture). Eighty-five µL of this suspension were runned in a NuPAGE® Novex 12% Bis-Tris precasted Gel 2D well (Invitrogen, Carlsbad, CA) for 1 hour at 180 v. The electrophoresis was transferred to a Hybond ECL™ nitrocellulose membrane (GE Helathcare, Buckinghamshire, UK). Sera (1:2000) from four animals at 3 time-points (7, 14 and 23 days p.i) were assayed using 5 mm strips and presence of IgG against *E. coli* protein detected with a Goat anti-Porcine IgG HRP (Serotec, Eching, Germany) and the ECL Advance Western Blotting Detection kit (GE Helathcare, Buckinghamshire, UK).

Piglets were bled on days 0, 7, 14 and 21 p.i. and serum samples were used for the detection of PCV2 antibodies by using an immunoperoxidase monolayer assay (IPMA) technique (Rodriguez-Arrioja *et al*., 2000) and for PCV2 DNA quantification by TaqMan-PCR (Olvera *et al*., 2004). At 23 days p.i., piglets were euthanized by an overdose of intravenous sodium thiobarbital. Animal care and procedures were in accordance with the guidelines of the Good Experimental Practices (GEP), under the supervision of the Ethical and Animal Welfare Committee of the Autonomous University of Barcelona.

At necropsy, samples of lymph nodes (including inguinal superficial, mesenteric, mediastinal, submandibular, and sternal lymph nodes), thymus, tonsil, trachea, lung, myocardium, spleen, ileum, liver, kidney, brain, nasal turbinate, and bone marrow were collected and divided for histopathological (fixed by immersion in 10% neutral buffered formalin) and microarray (immersed in RNAlater™ (Ambion, Austin, USA) and stored at -80ºC) studies. Fixed tissue sections were dehydrated and embedded in paraffin wax, sectioned at 4 mm, and stained with haematoxylin and eosin (HE) for morphologic evaluation. Moreover, to detect PCV2 nucleic acid on tissue sections, a previously described *in situ* hybridization (ISH) technique (Rosell *et al*., 1999) was performed.

3.2.2. Microarray Studies

3.2.2.1. RNA preparation

The gene expression study was performed in mesenteric lymph node and lung tissues. These tissues were selected because they had PCV2-SD-like microscopic lesions (mild lymphocyte depletion with granulomatous inflammation in the lymph node and mild interstitial pneumonia in the lung) and were positive by the PCV2 ISH technique. Total RNA from 100 mg of lungs and mesenteric lymph nodes from available piglets was extracted using the RiboPure™ kit (Ambion, Austin, USA) according to the manufacturer's protocol. The concentration of total RNA was determined using the NanoDrop ND-1000 spectrophotometer (NanoDrop Technologies, Wilmington, USA) and the RNA integrity number (RIN) was assessed by Agilent Bioanalyzer 2100 and RNA Nano 6000 Labchip kit (Agilent Technologies, Palo Alto, USA). The RIN values ranges from 1 to 10: a RIN of 1 is returned for a completely degraded RNA samples whereas a RIN of 10 is achieved for an intact RNA sample. All samples used for microarray analyses had RIN above 8, except one, which had RIN of 7.1. Two technical replicates, representing 2 independent RNA extractions, were generated for each sample. Therefore, a total of 16 samples corresponding to 4 individuals x 2 tissues x 2 replicates were used for microarray analysis.

3.2.2.2. Gene profiling

Transcript analysis was conducted using Affymetrix GeneChip® Porcine Genome Array (Affymetrix, Santa Clara, CA), which contains 24,123 probesets, interrogating 20,201 *Sus scrofa* genes.

Briefly, biotin-labelled cRNA was produced from 5 μg of total RNA using an Affymetrix "one-way" labelling kit (Affymetrix, Expression Analysis Technical Manual). Labelled cRNA was fractioned and hybridised with the GeneChip® Porcine Genome Array following the manufacturer's instructions. Subsequently, the arrays were stained with a GeneChip Fluidics Station 450 using the standard fluidics protocol and were scanned with an Affymetrix GeneChip Scanner 3000 (Affymetrix) by using the GeneChip Operating Software (GCOS) to produce a *.CEL file for further data processing. Microarrays were hybridised and scanned at the *Institut de Recerca Hospital Universitari Vall d'Hebron*, Barcelona, Spain.

Microarray data was analysed with the Bioconductor software (Gentleman *et al*., 2004). The first step of the analysis was the assessment of quality of the raw data by means of QC function (*simpleaffy* package). This function generates metrics including average background, average signal, and 3'/5' expression ratios for spike-in controls, β-actin, and GAPDH. Arrays that were within the limits of those parameters were considered of good quality and were included in the analysis. Array normalization was assessed using the Robust Multichip Average (RMA) methodology (Irizarry *et al*., 2003a). This methodology consists of three steps: convolution background correction, quantile normalization, and a summarization of probe intensity values based on a multiarray model using the median polish algorithm. Standard pairwise Pearson´s correlation was calculated for biological and technical replicates to compare technical reproducibility. The empirical Bayes moderated t-statistic implemented in *limma* package (Gentleman *et al*., 2004; Smyth, 2004) was used to identify differentially expressed (DE) genes between control and inoculated pigs for each tissue. The effect of technical replicates was included in the model to account for the within-replicates correlation. Significance threshold was set to $\alpha = 0.1$ after correction for multiple tests, following the Benjamini and Hochberg method (Benjamini and Hochberg, 1995).

Heat maps of the DE genes were generated using Cluster 3.0 and Java TreeView 1.1 software. The clustering method used was an uncentered correlation with the complete

linkage option. The DAVID platform (http://david.abcc.ncifcrf.gov/) was used for functional annotation of significant probesets.

3.2.3. Quantitative real-time polymerase chain reaction (qPCR)

Based on the results from the microarray experiment, qPCR was used to confirm differential expression of the *IGHG* (immunoglobulin G heavy chain) between groups using the same RNA samples that were assayed by microarray. One microgram of total RNA from each of the 16 samples were reverse transcribed using the High Capacity cDNA Transcription Kit (Applied Biosystems, Inc., Foster City, CA) according to the manufacturer's instructions. *Sus scrofa* hypoxanthine phosphoribosyltransferase 1 (*HPRT1*) (GenBank accession number DQ136030) was used as endogenous control. Primers were designed using the Primer Express 2.0 software (Applied Biosystems Inc., Foster City, CA). Primers for *IGHG* were designed on conserved regions based on sequences with GenBank accession numbers U03778 to U03782. Nucleotide sequences for *IGHG* primers were: 5'-CACGCTTGTCCACCTTGGT-3', and 5'-CAAGAGCTACACCTGCAATGTCA-3' for the sense and antisense primers, respectively, which yielded a 59 base pairs (bp) fragment. For *HPRT1* primers, the sense was: 5'-TCATTATGCCGAGGATTTGGA-3', and the antisense was: 5'-CTCTTTCATCACATCTCGAGCAA-3' (91 bp). The PCR reaction was performed in a 20 μl final volume containing 1X Power SYBR Green PCR Master Mix (Applied Biosystems, Warrington, UK), 300 nM of each forward and reverse primers for both tested genes, and 4 μl of 20-fold diluted cDNA. Samples were amplified in triplicate on an ABI 7000 (Applied Biosystems, Warrington, UK) for 10 min at 95 ºC and 40 cycles at 94 ºC for 15 s followed by fluorescence capture at 60ºC for 1 min. Relative standard curves for the target and endogenous control primer pairs were performed to verify that both PCR efficiencies were comparable and, therefore, the comparative $2^{-\Delta\Delta Ct}$ method (Livak and Schmittgen, 2001) was applied. A dissociation curve was also performed to ensure single amplicons. The control sample with the lowest expression level was used as a calibrator. Resulting Q-PCR data were analyzed by analysis of variance (ANOVA) using the SAS system (Statistics, V 9.1; SAS Institute, Inc., Cary, NC). A value of $p<0.05$ was considered statistically significant.

3.3. Results

3.3.1. Experimental infection

Piglets inoculated with PCV2 became viremic, although none of them developed PCV2-SD. The viral genome was detected as early as 7 days p.i. ($3.88 \times 10^8 \pm 7.06 \times 10^7$) and remained at detectable levels until the end of the study ($8.37 \times 10^8 \pm 1.14 \times 10^8$). The peak of viremia was observed at 14 days p.i. ($1.42 \times 10^9 \pm 4.71 \times 10^9$). Both animals seroconverted by 14 days p.i. (1:320), reaching maximum antibody titres at the end of the experiment (1:5120 and 1:20,480).

No gross lesions were observed in any organ or tissue of the 4 studied pigs. Histopathological studies were only observed in the two PCV2 inoculated animals, which had mild PCV2-SD-like lesions in lymphoid tissues, consisting of lymphocyte depletion with histiocytic infiltration and mild interstitial pneumonia in lung was also seen. Low amounts of viral nucleic acids were detected by ISH in lungs and in several lymph nodes (mediastinal, submandibular, inguinal superficial and mesenteric lymph nodes), mainly in lymphoid follicles of both infected animals. The two control piglets remained PCV2 negative by TaqMan PCR and serology during the whole experiment and were also negative by ISH at necropsy.

Considering that two PCV2-inoculated piglets died during the experiment due to bacterial systemic infection, a Western-blot analysis was performed to evaluate the serological profiles (IgG) of the remaining pigs from both groups (n=4) against a whole protein extract from the non-haemolytic *Escherichia coli* strain isolated from died animals. No apparent differences on the humoral response profile to *E. coli* were observed between control and inoculated groups (data not shown). This technique was performed to exclude a possible interference in the microarray technique due to different levels of *E. coli* infection between control and PCV2-infected animals.

3.3.2. Gene expression analysis

The concentration of RNA samples ranged from 0.65 to 2.45 µg/µL. All RNA samples were considered of high quality based on RIN values (ranging from 8.0 to 9.2, but one

(7.1)). All arrays were found to be of good quality based on low background levels as well as expected 3'/5' expression ratios for the spike-in controls, *β-actin*, and *GAPDH*. To assess technical reproducibility, Pearson's correlation coefficients were calculated and MA-plots were drawn for all possible combinations between arrays for each tissue (8 chips, $^{8}C_{2}$ = 28 combinations, Figure 5). The MA-plot for each comparison was constructed by plotting the differences in $\log_2$ intensities between two arrays against their average $\log_2$ intensity.

The highest correlation coefficients were found between technical replicates for mesenteric lymph node samples (0.99), although comparisons obtained from biological replicates also revealed high correlations, ranging from 0.97 to 0.99 (Figure 5A). These results indicate an agreement across the hybridizations and are illustrated on the MA-plots, in which the same general structure of data, roughly symmetrical around the x-axis with similar distributions of variability (y-axis), was observed.

Analysis of the lung samples showed more variable results than the mesenteric lymph node arrays (Figure 5B). Comparison of technical replicates gave a coefficient of correlation ranging from 0.95 to 0.97, while correlations between biological replicates ranged from 0.93 to 0.98. Variability between these arrays was observed by a higher spread of data from the y-axis on the MA-Plots.

A total of 25 probesets showed differential expression between PCV2-inoculated and control pigs for the mesenteric lymph node (FDR < 0.1 and Fold Change > 2.0). Of these, 17 probesets were up-regulated and 8 were down-regulated in PCV2-inoculated pigs. In lung tissue, among the 33 probe sets DE between groups, 21 were over-expressed in PCV2-inoculated animals, whereas 12 were down-regulated. The list of all DE genes for each tissue is presented in Table 3.

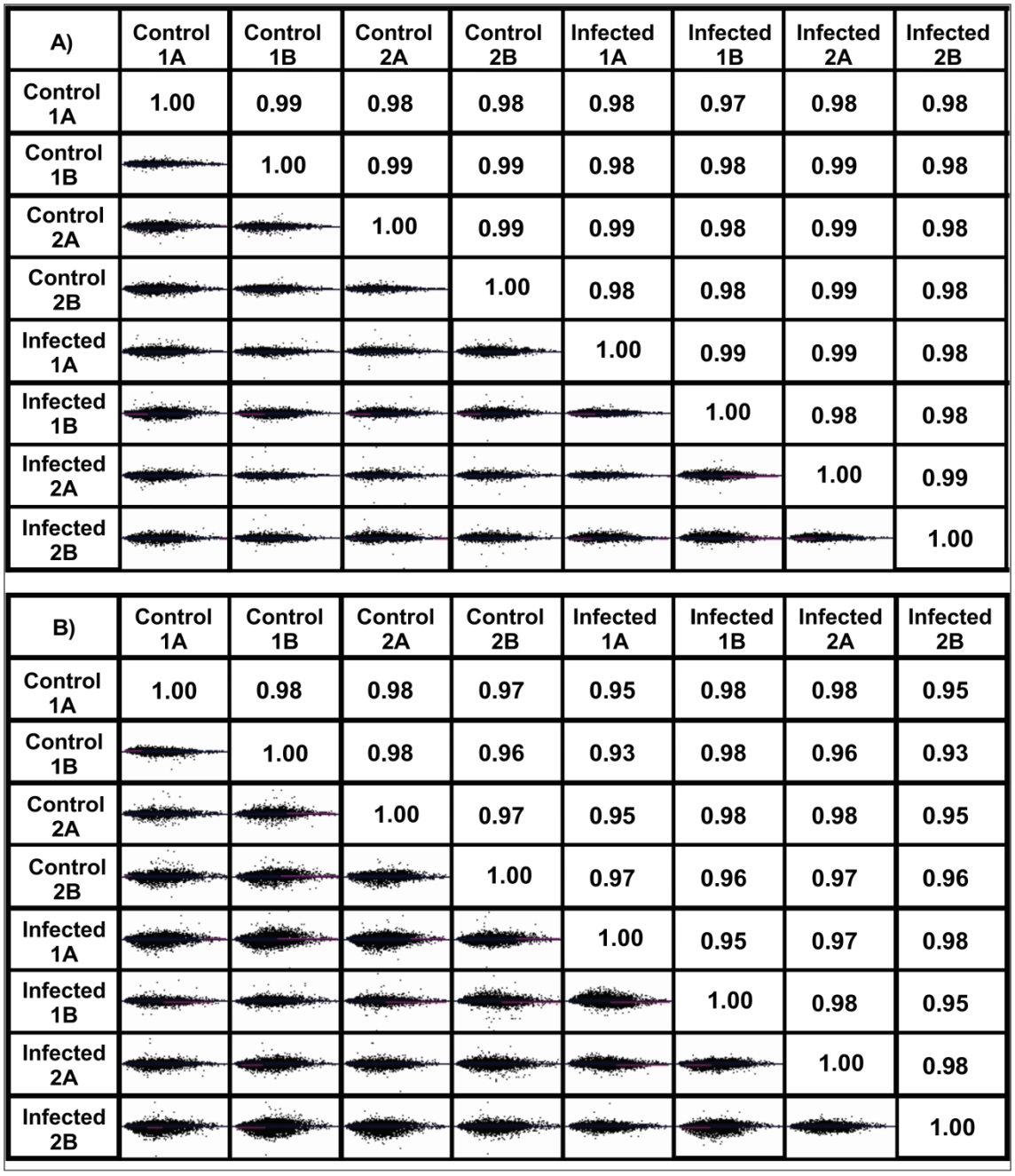

Figure 5. Reproducibility of technical and biological replicates of microarrays from A) mesenteric lymph node and B) lung samples. Above diagonal: average Pearson correlation coefficients across all comparisons. Below diagonal: pairwise MA plots.

Given that piglets from control and infected groups were males and females, respectively, a number of DE genes could be more influenced by sex differences rather than by the effect of infection with PCV2. The existence of sex-specific gene expression has been previously described in mice (Yang *et al*., 2006) and pigs (Ferraz *et al*., 2008). Based on

these studies, thirteen sex-related genes were found DE in the mesenteric lymph nodes and/or lung tissues (Table 3), and were, therefore, discarded for further evaluations on the effect of PCV2 infection.

Table 3. Differentially expressed genes in lung and mesenteric lymph node. Sex related genes are indicated by (*****).

Gene Symbol	Gene Name	Probe	Tissue	Fold Change	FDR
TCRA (V)	T-cell receptor alpha chain V region	Ssc.428.10.S1_s_at	Lung	8.6	0.026
TCRA (C)	T-cell receptor alpha chain C region	Ssc.428.5.S1_at		2.6	0.070
CXCL11	Small inducible cytokine B11 precursor	Ssc.30027.1.A1_at	Lung	6.5	0.005
CYP3A4	Cytochrome P450 3A4	Ssc.26326.1.S1_at	Lung	3.2	0.062
UBD	Ubiquitin D	Ssc.21582.1.S1_at	Lung	3.0	0.062
CD8A	T-cell surface CD8 alpha chain precursor	Ssc.23489.1.S1_at	Lung	3.0	0.070
AP1S3	Adapter-related protein complex 1 sigma 1C subunit	Ssc.25862.1.S1_at	Lung	2.6	0.006
LCK	T cell-specific protein-tyrosine kinase	Ssc.19619.1.S1_at	Lung	2.6	0.063
GBP2	Interferon-induced guanylate-binding protein 2	Ssc.883.1.S1_a_at	Lung	2.3	0.010
GRIK2	Glutamate receptor, ionotropic kainate 2 precursor	Ssc.19883.1.S1_at	Lung	2.1	0.059
PLAU	Urokinase-type plasminogen activator precursor	Ssc.11194.1.S1_at	Lung	2.1	0.059
APLN	Apelin precursor	Ssc.3436.1.A1_at	Lung	2.0	0.097
CXCL9	Small inducible cytokine B9 precursor	Ssc.26146.1.S1_at	Lung	8.0	0.002
			Mes LN	2.6	0.075
TACC1	Transforming acidic coiled-coil-containing protein 1	Ssc.7712.1.A1_at	Lung	3.5	0.006
			Mes LN	3.2	0.007
KLRK1	NKG2-D type II integral membrane	Ssc.15871.1.S1_a_at	Lung	3.2	0.045
			Mes LN	2.5	0.002
RASSF2	Ras association domain family 2.	Ssc.11258.1.A1_at	Lung	2.5	0.061
			Mes LN	2.6	0.015
IGHG		Ssc.11070.1.S1_at	Lung	13.0	0.058

	Immunoglobulin heavy constant gamma		Mes LN	3.0	4.2E-05
IGHG	Immunoglobulin heavy constant gamma	Ssc.13778.1.S1_at	Mes LN	7.5	0.039
CLYBL	citrate lyase beta like	Ssc.1137.1.S1_at	Mes LN	3.2	0.011
FNDC1	fibronectin type III domain containing 1	Ssc.6656.1.A1_at	Mes LN	2.5	0.023
Q96GV6	Hypothetical protein	Ssc.25100.1.S1_at	Mes LN	2.3	0.076
CCL4L	chemokine (C-C motif) ligand 4-like precursor	Ssc.23797.1.S1_at	Mes LN	2.1	0.009
OLFML2A	olfactomedin-like 2A	Ssc.17387.1.A1_at	Mes LN	2.1	0.023
Z-protein	Z-protein	Ssc.12863.2.A1_at	Lung	-2.5	0.059
Q93073	Hypothetical protein	Ssc.31079.1.A1_at	Lung	-2.5	0.059
COL24A1	collagen, type XXIV, alpha 1	Ssc.30042.1.A1_at	Lung	-2.3	0.059
AK7	Putative adenylate kinase 7	Ssc.12884.1.A1_at	Lung	-2.3	0.096
C13orf6	Similar to Chromosome 13 open reading frame 6	Ssc.22158.1.S1_at	Lung	-2.1	0.059
C10orf79	Similar to Chromosome 10 open reading frame 79	Ssc.30383.1.A1_at	Lung	-2.1	0.069
PPAP2A	phosphatidic acid phosphatase type 2A	Ssc.17899.1.A1_at	Mes LN	-2.3	0.076
PTPRM*	Receptor-type protein-tyrosine phosphatase mu precursor	Ssc.31029.1.A1_at	Lung	55.7	7.2E-05
			Mes LN	97.0	1.2E-09
MYCPBP*	c-myc promoter binding protein	Ssc.13426.1.A1_at	Lung	21.1	2.5E-03
			Mes LN	34.3	7.5E-05
LPHN2*	Latrophilin 2 precursor	Ssc.21512.1.A1_at	Lung	13.9	6.2E-02
			Mes LN	19.7	6.9E-06
FAM5C*	DBCCR1-like	Ssc.6667.1.A1_at	Lung	26.0	7.5E-02
			Mes LN	36.6	2.2E-06
CLOCK*	Circadian locomoter output cycles kaput protein	Ssc.4897.1.A1_at	Mes LN	26.0	1.2E-05
HIPK2*	Homeodomain-interacting protein kinase 2	Ssc.2434.1.A1_at	Mes LN	9.8	2.8E-04
DDX3Y*	DEAD-box protein 3. Y-linked	Ssc.7473.1.A1_at	Lung	-84.4	4.1E-06
			Mes LN	-11.4	5.9E-10
EIF1AY*	Eukaryotic translation initiation factor 1A. Y-linked	Ssc.26799.1.S1_at	Lung	-59.7	1.5E-07
			Mes LN	-52.0	5.9E-10
EIF2S3*		Ssc.16426.1.S1_at	Lung	-84.4	7.3E-07

	Eukaryotic translation initiation factor 2 subunit 3		Mes LN	-128.0	3.1E-09
JARID1C*	Jumonji/ARID domain-containing protein 1C	Ssc.21814.1.S1_at	Lung	-4.3	4.5E-02
			Mes LN	-9.8	4.5E-08
TMSB4X*	thymosin-like 1	Ssc.27304.1.S1_at	Lung	-64.0	2.9E-07
			Mes LN	-68.6	2.6E-08
UTY*	Ubiquitously transcribed tetratricopeptide repeat. Y-linked	Ssc.27236.1.S1_at	Lung	-5.7	0.059
			Mes LN	-11.3	4.5E-08
UTX*	Ubiquitously transcribed tetratricopeptide repeat. X chromosome	Ssc.15821.1.S1_at	Mes LN	-6.1	2.9E-05

A hierarchical clustering was performed to determine similar expression patterns among the DE genes between PCV2-inoculated and control pigs. Heat-maps were constructed using the DE genes from each tissue (Figure 6). Two differentiated clusters were observed in both tissues, one for the up-regulated and another for the down-regulated DE genes. Most up-regulated genes were closely related to the immune system, including chemokines (*CXCL9, CXCL11, CCL4L*), immunoglobulins (*IGHG*) and related with regulation of T cell activation (*LCK*), NK cell activation (*KLRK1*), interferon-inducible GTP binding (*GBP2*), MHC I antigen presentation (*CD8α, TCRα*), and transporter activity (*GRIK2*). Down-regulated genes were mainly involved in transferase and kinase activity (*AK7*), cell adhesion (*COL24A1*) and signal transduction (*PPA2PA*).

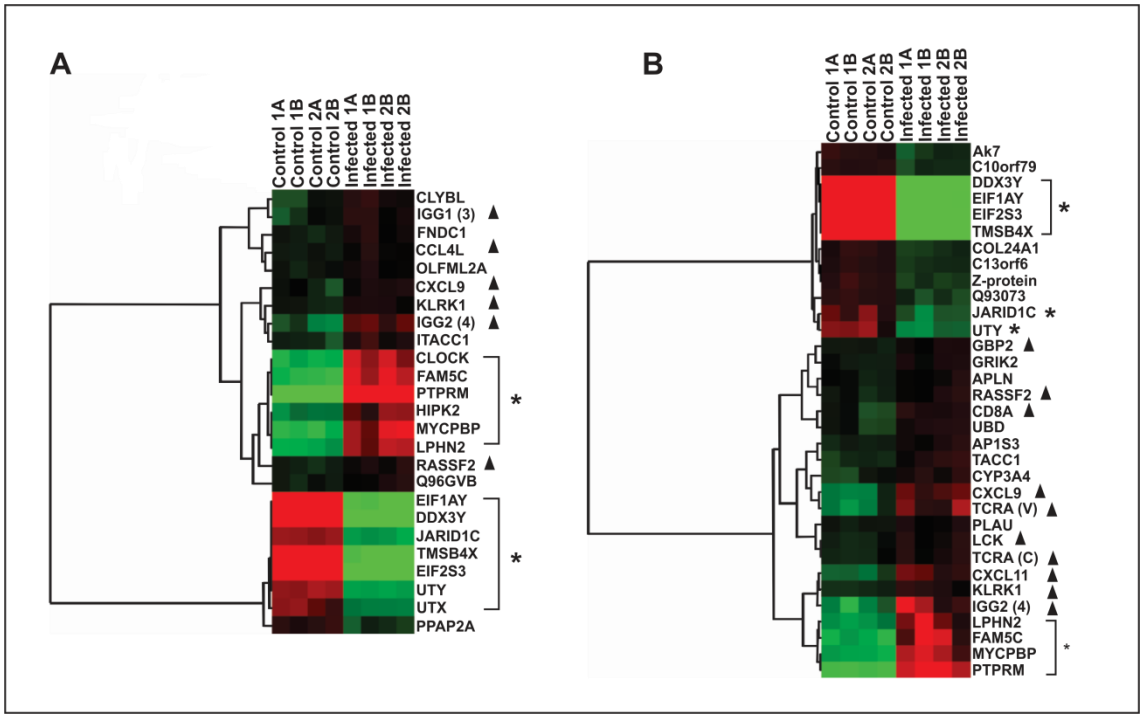

Figure 6. Hierarchical clustering analysis of declared differentially expressed genes after infection with PCV2 in A) mesenteric lymph node, and B) lung samples. Red represents up-regulation and green shows down-regulation for differentially expressed genes (FDR < 0.1, Fold Change > 2.0). Genes related to the immune system are represented by (▲) and sex related genes are indicated by (*****).

3.3.3. qPCR

To confirm the differences in gene expression observed in the microarray experiments, quantitative real-time PCR was performed on IGHG gene, which was selected due to its highest fold change values on both tissues. The qPCR results agreed with the microarray data with similar fold changes (3.65 $\pm$ 1.26 for mesenteric lymph node and 12.54 $\pm$ 1.77 for lungs, $p < 0.05$).

3.4. Discussion

Transcriptional profiling using microarray technology has been used over the last years as a tool for studying the molecular mechanisms underlying the host response against pathogenic microorganisms in pigs (Tuggle *et al.*, 2007). The present exploratory study

aimed to identify genes involved in the immune response against PCV2 in experimentally infected CDCD pigs. The use of CDCD pigs as a model for infection with PCV2 has been widely extended (Okuda *et al*., 2003; Fernandes *et al*., 2007) and their usefulness stems from the fact that they have not acquired the maternal immunity through colostrum intake. Therefore, the immune response activated in this type of pigs after infection with any pathogen should be considered caused by the inoculated pathogen. Although no PCV2-SD was reproduced, both PCV2 inoculated pigs that reached the end of the study were subclinically infected. Inoculated pigs developed viremia levels similar to animals showing mild PCV2-SD-like lesions (Olvera *et al*., 2004).

This study explored, for the first time, the technical feasibility of utilizing the microarray platform to analyze genes expressed in PCV2-infected piglets. Among the platforms currently available, the Affymetrix Porcine array has been considered the most sensitive and reproducible microarray for swine genomic studies (Tsai *et al*., 2006b). The present data showed a high correlation coefficient between biological and technical replicates of each tissue (ranging from 0.93 to 0.99), confirming the high reproducibility across arrays. However, some intrinsic variability between biological replicates from lung was found in this study. Although tissue samples were taken from the same lung lobule in all animals, a different proportion of cell populations between samples might be obtained.

Furthermore, important technical aspects of hybridizing pig RNA to this microarray platform were evaluated, such as the purity of RNA to avoid contamination with DNA that can confound the results on the microarray. The integrity of the RNA was also a crucial factor to obtain a full representation of the expressed genes in the sample. Finally, an adequate amount of RNA was necessary to obtain fully representative hybridization of the large number of genes on the Affymetrix microarray.

As shown in the present report, many of the DE genes found in mesenteric lymph node and lungs of PCV2 infected pigs were genes encoding immune system key molecules such as immunoglobulins, cytokines, antigen presenting molecules and GTPases.

An increase of the expression of different *IGHG* genes (code for IgG subclasses) was observed in both tissues of PCV2-inoculated pigs. These pigs seroconverted by day 14 p.i. and reached a peak of IPMA titre at 21 days p.i. As previously reported, the pattern

of seroconversion in PCV2-infected gnotobiotic piglets as well as in PCV2 asymptomatic pigs occurs between 14-21 days p.i., with the specific anti-PCV2 antibody IgG and subclasses IgG1 and IgG2 generally following the course of the IPMA antibody titres (Meerts *et al*., 2005a; Darwich *et al*., 2008; Fort *et al*., 2008). The prompt up-regulation of the expression of genes encoding for these antibodies in subclinically infected pigs could be a key event for protection against the development of disease since pigs suffering from PCV2-SD apparently have impairment of the humoral immune response (Okuda *et al*., 2003; Meerts *et al*., 2005a). However, it must be stated that disease was not reproduced in the present study and, therefore, comparison between clinically and subclinically infected pigs was not feasible.

PCV2-SD affected pigs suffer from a deep alteration of the immune system characterized by depletion of B lymphocytes, all T lymphocyte sub-populations and NK cells, as well as an impairment of the pattern of cytokine responses (Nielsen *et al*., 2003; Darwich *et al*., 2003b). Subclinical PCV2-infections apparently do not produce significant depletion of lymphocyte subsets, but the development of a transient IL-10 PCV2-specific response during the viremic phase of infection can be observed (Darwich *et al*., 2008). The data of the present study suggest the activation of a cell-mediated response in lung tissue as evidenced by the significantly up-regulated expression of *TCRα, CD8α, LCK, GBP2*, and a member of the Ras family, *RASSF2*, which was also over-expressed in lymph node tissue. Those genes play an important role on TCR signal transduction and activation of important signaling pathways, including the activation of Ras-mediated signaling pathways, which ultimately result in differentiation, proliferation, or activation of developing mature T cells (Kane *et al*., 2000). Only a variable TCRα chain showed over expression, what could indicate an epitope-driven selection of limited T-cell clones in lung of PCV2 infected pigs.

It has been shown that pigs have large numbers of lymphocytes, for example NK cells, with a significant innate cytotoxic activity (Denyer *et al*., 2006). We found an up-regulation of the expression of the *KLRK1* gene, which encodes the NKG2D-activating chain of the MIC receptor present in NK cells, both in lung and in lymph node tissues. The recognition of MIC proteins by NK cells triggers a range of effector mechanisms, including cellular cytotoxicity, cytokine secretion, and cellular proliferation (Vivier *et al*., 2002).

Although gamma interferon (IFN-γ) was not significantly over-expressed in the present study, PCV2-infected pigs had an increased transcription of *GBP2, CCL4L, CXCL9* and *CXCL11* genes, which are known to be induced or regulated by IFN-γ. *GBP2* is member of the GTPases protein family and play important roles in the resistance to intracellular pathogens, participating in the regulation of proliferation and invasion of endothelial cells in response to IFN-y (32). The *CCL4L*, *CXCL9* and *CXCL11* chemokines precursors are known as IFN-γ-induced chemokines by dendritic cells and macrophages in response to viral stimulation (Huang *et al*., 2001). *CCL4L* can also attract and activate natural killer (NK) cells.

IFN-γ is a Th1-specific cytokine produced by macrophages, NK cells, and other cell types during the onset of an infection. In the course of a virus infection, an early release of IFN-γ could lead to the activation of genes related to the Th1-mediated immune response with a specific-neutralizing antibody response and could be correlated with the development of a strong cell-mediated immunity, thus, leading to an effective clearance of virus (Takaoka and Yanai, 2006). This is in agreement to previous observations in PCV2-SD-affected animals and gnotobiotic PCV2-inoculated piglets for which the levels of IFN-γ were notably higher (Meerts *et al*., 2005c; 2006).

This is the first study to evaluate the gene expression profile of PCV2-infected piglets. Results obtained suggest, from a transcriptional point of view, that PCV2-inoculated pigs activated a cell-mediated immunity and developed PCV2-specific antibodies resulting in a subclinical infection. One may argue that the main weakness of this work is the small number of animals. However, this is a study of an exploratory nature that aimed to determine the genetic transcriptional profile of pigs subsequent to infection with PCV2, but mainly to evaluate the feasibility of using this approach. Therefore, the high reproducibility of the data generated across replicate hybridizations in two different tissues provides a basis for further gene screenings, involving a larger sample size, which may provide more conclusive evidence regarding the genetic background of the immune response efficiency of an individual pig to deal with PCV2 infection.

CHAPTER 4

STUDY II

Time course differential gene expression in response to porcine circovirus type 2 subclinical infection

4.1. Introduction

Some experimental infections have been able to reproduce the histopathological lesions observed in naturally PCV2-SD-affected pigs; however, reproduction of disease has been limited to a few experiments (Tomás *et al*., 2008). In many cases, PCV2-SD development requires a trigger such as coinfection with other pathogens (porcine parvovirus (PPV), porcine respiratory and reproductive syndrome virus (PRRSV), *Mycoplasma hyopneumoniae*, among others), or immune stimulation of the host (Tomás *et al*., 2008). Host genetics may also affect the outcome of PCV2 infection. In this sense, a genetic predisposition to suffer from PCV2-SD has been pointed out since field observations and recent experimental studies identified certain genetic lines of pigs that tended to be more or less susceptible to PCV2 infection (Madec *et al*., 2000; Lopez-Soria *et al*., 2005; Rose *et al*., 2005; Opriessnig *et al*., 2006; 2009a). In addition to breed susceptibility/resistance to suffer from the disease, other individual genetic factors may also be underlying the observed differences in the ability of mounting a good adaptive immune response between susceptible and diseased pigs (Ladekjaer-Mikkelsen *et al*., 2002; Sanchez *et al*., 2003; Meerts *et al*., 2005b; 2006; Fort *et al*., 2007).

The microarray technology has been successfully applied to the study of the porcine immune response against several swine pathogens such as *Salmonella* (Zhao *et al*., 2006; Wang *et al*., 2008), *Actinobacillus pleuropneumoniae* (Hedegaard *et al*., 2007), PRRSV (Lee *et al*., 2004; Lewis *et al*., 2007; Gennini *et al*., 2008), and pseudorabies virus (Flori *et al*., 2008a; 2008b). In Chapter 3, an exploratory microarray study was performed using lung and mesenteric lymph node samples from PCV2-inoculated Duroc pigs at 23 days p.i., thereby identifying several genes closely related to the immune response such as cytokines, CD8, immunoglobulin, and T cell receptor (TCR)-alpha molecules which were mostly up-regulated in the PCV2-inoculated group.

The present work is aimed at characterizing the early and late molecular mechanisms underlying the immune response of CDCD piglets subclinically infected with PCV2 using a genome-wide expression approach. Mediastinal lymph node (MLN) and peripheral blood RNA samples were collected at five different time points, and were hybridized to the Affymetrix Porcine Genechip®. This study gives new insights into the knowledge of

PCV2 host-pathogen interaction and the mechanisms by which an effective immune response occurs.

4.2. Materials and methods

4.2.1. Experimental design

All experimental procedures and animal care were undertaken in accordance with the guidelines of the Good Experimental Practices, under the supervision of the Ethical and Animal Welfare Committee of the Universitat Autònoma de Barcelona.

Specifically, 24 seven-day-old, Landrace CDCD piglets were used. The selection of Landrace pigs was done due to the fact that this pig breed has been shown to be more susceptible to suffer from PCV2-SD disease (Opriessnig *et al*., 2006; 2009). A first group of pigs (n = 8) was kept as un-inoculated controls and the rest of the pigs (n = 16) were oronasally inoculated with $10^{5.2}$ $TCID_{50}$ of the Burgos isolate of PCV2 (Fort *et al*., 2008). The piglets used in the present work belonged to previous studies in which the virological, clinico-pathological and immunological outcomes were evaluated (Fernandes *et al*., 2007; Fort *et al*., 2009a). Briefly, all pigs remained clinically healthy during the experimental period. PCV2 subclinical infection was confirmed in all virus-inoculated pigs by qPCR. The PCV2 genome was detected from 7 days p.i. to the end of the experimental period and all pigs had seroconverted by the end of the study. Microscopic examination revealed mild PCV2-SD-like lesions mostly in the MLN of almost all PCV2-inoculated pigs. Control piglets remained free of PCV2 infection throughout the experiment and no histological lesions were detected.

One control pig and three inoculated pigs were necropsied on days 1, 2, 5, and 8 p.i.. The remaining pigs (4 of each group) were followed up throughout the experimental period, being bled at days 0, 7, 14, 21, and 29 p.i. (Figure 7). One milliliter of whole blood samples were immediately lysed (referred to as LWB) with nucleic acid purification lysis solution (Applied Biosystems, Warrington, UK) and were immediately frozen at - 96 ºC. At necropsy (days 1, 2, 5, 8, and 29 p.i., Figure 7), samples of MLN were collected by immersion in liquid nitrogen for microarray studies. All collected samples1 were kept at - 80 ºC until usage.

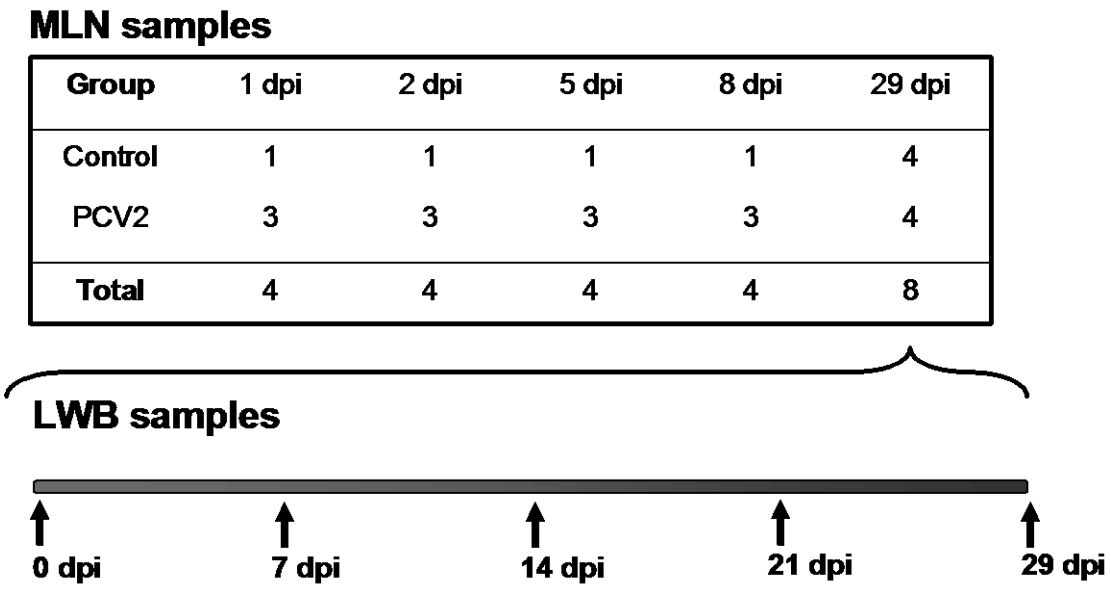

Figure 7. Experimental design. MLN: mediastinal lymph node, LWB: lysed whole blood.

4.2.2. RNA extraction and microarray hybridization

Total RNA extraction from MLN and LWB samples was performed with the RiboPure™ kit (Ambion, Austin, USA), following the manufacturer's instructions. RNA quality was assessed with the RNA Nano 6000 Labchip kit on an Agilent 2100 Bioanalyzer (Agilent Technologies, Palo Alto, USA). RNA was quantified using the NanoDrop ND-1000 spectrophotometer (NanoDrop Technologies, Wilmington, USA). Samples were hybridized to the Affymetrix 24K Genechip® Porcine Genome Array (Affymetrix, Santa Clara, CA, USA) following the standard Affymetrix one-cycle protocol. Reverse transcription, RNA labeling, cRNA amplification, hybridization, and scanning procedures were conducted at the Affymetrix facilities available at the Institut de Recerca Hospital Universitari Vall d'Hebron, Barcelona, Spain (http://www.ir.vhebron.net). In total, 24 MLN samples (8 control and 16 PCV2-inoculated) and 39 LWB samples (corresponding to 2 groups x 4 piglets/group x 5 time points) were hybridized to microarrays. One sample of a PCV2 inoculated pig at day 21 p.i. was discarded due to low RNA quality.

4.2.3. Microarray data analysis

Raw data and statistical analyses were performed with Bioconductor (Gentleman *et al*., 2004) implemented in R 2.6.0 (http://cran.r-project.org/). Data quality was assessed by the QC function implemented in the simpleaffy package (Wilson and Millet, 2005). The Robust Multichip Average (RMA, Irizarry *et al*., 2003a) methodology was used for array normalization. The Empirical Bayes t-test statistic implemented in the limma package was used to determine differential gene expression between control and inoculated pigs (Smyth, 2004). For LWB, a comparison between both groups was performed for each time point. For MLN samples, where only one control pig was available at 1, 2, 5, and 8 dpi, the effect of time was included in the model as a fixed effect. The threshold of significance was set to a false discovery rate (FDR, Benjamini and Hochberg, 1995) of 0.1 and a minimum fold change of 2. Hierarchical clustering was performed with Cluster 3.0 and Java TreeView 1.1 software (www.rana.lbl.gov/Eisen/Software.htm), using the uncentered correlation coefficient and the average linkage method. Probes were annotated based on the chip annotation provided by Affymetrix (NetAffx), Tsai *et al*. (2006a), and the annotation of Iowa State University (Tuggle C., personal communication). However, some of the probes were not coincident between different sources and were, therefore, validated by screening the probe nucleotide sequence available at NetAffx with the nr and EST databases available at NCBI using the Basic Local Alignment Search Tool (BLAST, http://blast.ncbi.nlm.nih.gov/Blast.cgi). These probes that could not be assigned to a known gene were not used for functional analyses. The Database for Annotation, Visualization and Integrated Discovery (DAVID 2008, http://david.abcc.ncifcrf.gov/home.jsp) was used for assessing functional profiles of genes based on the Biological Processes (BP) category of Gene Ontology (GO). The MetaCore platform (GeneGo Inc., http://www.genego.com) was used to map biological processes to canonical pathways and to construct gene interaction networks. Data from this work is available at Gene Expression Omnibus database with accession number GSE14758.

4.2.4. qPCR

Validation of porcine transcripts DE was done by qPCR for five genes (Interferon-gamma, *IFNG*; Immunoglobulin-gamma chain constant region, *IgG*; lectin galactoside-binding soluble 3, *LGALS3*; myxovirus (influenza virus) resistance 1, *Mx1*; and 2',5'-oligoadenylate synthetase 1, *OAS1*) for the MLN samples and one gene (*OAS1*) for the

LWB samples. The hypoxantine phosphoribosyltransferase (*HPRT1*) gene was used as a reference housekeeping gene in the MLN samples. The beta actin gene (*ACTB*) was selected as a reference for qPCR analyses in LWB samples due to the extremely low expression of *HPRT1* gene in blood. Porcine specific primers were designed with the Primer Express software (Applied Biosystems, Warrington, UK). Primer sequences are shown in Table 4. cDNA synthesis was performed with the High Capacity cDNA Reverse Transcription Kit (Applied Biosystems) using 1 µL of total RNA from MLN and LWB. Real-time qPCR was performed in triplicate in a 20 µL final volume reaction containing 4 µL of a 1:20 dilution of the cDNA, 300 nM of each primer, 0.2 µM random hexamers, and 10 µL of Power SYBR Green® PCR Master Mix on an ABI Prism H7000 (Applied Biosystems). The thermal profile consisted of a denaturalization step at 95 ºC for 10 min followed by 40 cycles at 95 ºC/15 s and 60 ºC/1 min. PCR efficiencies between target and housekeeping genes were validated for their relative quantification following the comparative Ct method described by Livak and Schmittgen (2001). Resulting qPCR data were Log2 transformed and analyzed, on a gene-by-gene basis, with the proc GLM method of SAS software (Statistics, V 9.1; SAS Institute, Inc., Cary, NC, USA) following the models used for microarray data analysis. The significance threshold was set at a < 0.05.

Table 4. List of primers used for quantitative PCR analysis.

Name	Sequence 5' → 3'	Amplicon size (bp)	GenBank accession number
ACTB-F	CGCCCAGCACGATGAAG	63	DQ845171
ACTB-R	CCGATCCACACGGAGTACTTG		
HPRT1-F	TCATTATGCCGAGGATTTGGA	90	DQ136030
HPRT1-R	CTCTTTCATCACATCTCGAGCAA		
IgG-F	CAAGAGCTACACCTGCAATGTCA	59	U03778-82
IgG-R	CACGCTTGTCCACCTTGGT		
MX1-F	CCCCTCCATAGCCGAGATCT	55	DQ095779
MX1-R	TGCCGACCTCCTGATGGTA		
OAS1-F	CTGTCGTTGGACGATGTATGCT	63	NM_214303
OAS1-R	GCCGGGTCCAGAATCACA		
LGALS3-F	AACAATTCTGGGCACAGTAAAGC	71	NM_001097501
LGALS3-R	CAACATCATTCCCCTTCTTGAAA		
IFNG-F	GAATGACTTCGAAAAGCTGATTAAAA	61	EU118363
IFNG-R	TGGCTTTGCGCTGGATCT		

4.3. Results

4.3.1. Microarray analysis

The comparison of the gene expression level between control and infected pigs in MLN samples revealed 43 DE probes (FDR < 0.1, Log2 fold change > 2, Table 5). Gene expression differences varied with time and three differentiated clusters were identified (Figure 8A). One cluster grouped eight probes that were globally down-regulated, from day 2 p.i. to the end of the study (cluster a). Among the up-regulated probes, two patterns were identified (clusters b and c). Cluster b grouped 23 probes that were up-regulated at early time-points after infection (5–8 dpi), while cluster c grouped 12 probes up-regulated at later stages of infection (29 days p.i.). Thirty-five out of 43 DE probes corresponded to well annotated genes and were, therefore, used for functional analyses. The 35 DE genes were assigned to eight biological processes ($p < 0.05$, Figure 9A). The most significant biological processes over-represented in the MLN dataset were mainly related to immune system response, catabolic processes and apoptosis.

In LWB samples, maximal differences in gene expression between control and PCV2-inoculated pigs were found at 7 days p.i. (Table 6). Only three probes were found DE on day 21 p.i., two of them up-regulated (DEP domain containing 1B, involved in the intracellular signaling cascade, and DC2 protein, a membrane component) and one down-regulated (Exportin 7, involved in protein export from the nucleus) in PCV2-inoculated pigs. No significant differences were found at any of the remaining time-points. Among the 54 DE probes in LWB samples at 7 dpi, 35 probes were up-regulated and 19 probes were down-regulated in the PCV2-inoculated group (Figure 8B). DE probes corresponded to 42 confirmed unique genes. Figure 9B shows the most significant biological processes of the LWB dataset, which were mainly related to the immune system response, protein metabolism and cellular organization and biogenesis.

Table 5. List of differentially expressed genes between PCV2-inoculated and control pigs in mediastinal lymph node samples with the Affymetrix Porcine Genechip.

Probe ID	Gene Symbol	Gene Name	Log2 FC	FDR	Biological Processes
Globally down-regulated genes					
Ssc.17815.1.S1_at	*LGALS3*	Lectin, galactoside-binding, soluble, 3	-1.50	0.009	extracellular matrix organization
Ssc.575.1.S1_at	*ACP5*	Acid phosphatase 5, tartrate resistant	-1.24	0.009	response to stimulus
Ssc.22441.1.A1_at	-	annotation not clear	-1.20	0.024	
Ssc.300.1.S1_at	*SLC11A1*	Solute carrier family 11, member 1	-1.08	0.097	immune response
Ssc.20870.1.S1_at	*FBLN1*	Fibulin-1	-1.07	0.007	cell adhesion
Ssc.7212.1.A1_at	*TFPI*	Tissue factor pathway inhibitor)	-1.07	0.051	blood coagulation
Ssc.115.1.S1_s_at	*HMOX1*	Heme oxygenase (decycling) 1	-1.05	0.028	apoptosis, cytokine production, catabolic process
Ssc.13115.1.A1_at	*CXADR*	Coxsackie virus and adenovirus receptor	-1.01	0.008	cell adhesion
Early up-regulated genes					
Ssc.19089.1.A1_at		annotation not clear	1.00	0.037	
Ssc.10588.1.A1_at	*H28*	Histocompatibility 28	1.01	0.048	immune response
Ssc.30724.1.S1_at	*HERC6*	Hect domain and RLD 6	1.03	0.069	ubiquitin-cycle
Ssc.29054.3.S1_at	*GBP1*	Guanylate binding protein 1	1.03	0.044	immune response
Ssc.7116.1.A1_at	*NT5C3*	5'-nucleotidase, cytosolic III	1.05	0.045	metabolic process
Ssc.26189.1.S1_a_at	*RTP4*	Receptor (chemosensory) transporter protein 4	1.07	0.097	response to stimulus
Ssc.2641.1.S1_at	*UBE2L6*	Ubiquitin-conjugating enzyme E2L 6	1.08	0.045	ubiquitin cycle
Ssc.883.1.S1_a_at	*GBP2*	Guanylate binding protein 2	1.12	0.051	immune response
Ssc.336.1.S1_at	*USP18*	Ubiquitin specific peptidase 18	1.13	0.083	ubiquitin cycle
Ssc.6433.2.S1_at	-	annotation not clear	1.13	0.084	
Ssc.26009.1.S1_at	-	annotation not clear	1.16	0.082	

Ssc.10593.1.S1_at	*H28*	Histocompatibility 28	1.17	0.051	immune response
Ssc.9327.1.A1_at	*HSH2D*	Hematopoietic SH2 domain containing	1.18	0.031	leukocyte activation
Ssc.7558.1.A1_at	-	annotation not clear	1.20	0.033	
Ssc.29054.2.S1_at	*GBP1*	Guanylate binding protein 1	1.30	0.033	immune response
Ssc.221.1.S1_at	*MX1*	Myxovirus (influenza virus) resistance 1	1.41	0.070	response to virus, apoptosis
Ssc.17894.1.A1_at	-	annotation not clear	1.47	0.042	
Ssc.5020.1.S1_at	*SERPINA3*	Serpin peptidase inhibitor, clade A	1.50	0.057	response to stimulus
Ssc.11557.1.A1_at	*ISG15*	ISG15 ubiquitin-like modifier	1.78	0.090	ubiquitin cycle
Ssc.1031.1.S1_at	*OAS1*	2'-5'-oligoadenylate synthetase 1	1.82	0.089	immune response
SscAffx.1.1.S1_at	*ISG20*	Interferon stimulated exonuclease gene 20 kDa	1.88	0.031	response to virus
Ssc.286.1.S1_s_at	*RSAD2*	Radical S-adenosyl methionine domain containing 3	2.16	0.052	response to virus
AFFX-Ss_IRP_3_at	*RSAD2*	Radical S-adenosyl methionine domain containing 2	2.29	0.064	response to virus
Late up-regulated genes					
Ssc.23658.1.S1_at	*PACAP*	Proapoptotic caspase adaptor protein	1.00	0.019	apoptosis
Ssc.21217.1.A1_at	*GCUD2*	Gastric cancer up-regulated-2	1.01	0.019	unknown
Ssc.24982.1.S1_at	*FABP7*	Fatty acid-binding protein 7, brain	1.03	0.041	cell proliferation
Ssc.19400.2.A1_at	-	annotation not clear	1.03	0.041	
Ssc.11070.1.S1_at	*IgG*	Immunoglobulin G	1.13	0.098	immune response
Ssc.10498.1.A1_at	*EAF2*	ELL associated factor 2	1.14	0.019	apoptosis, regulation of transcription
Ssc.13778.1.S1_at	*IgG*	Immunoglobulin G	1.15	0.024	
Ssc.12505.1.A1_at	*CLGN*	Calmegin	1.28	0.007	protein binding
Ssc.15942.2.S1_x_at	*Ig VDJ*	Ig heavy chain variable region (VDJ)	1.38	0.046	immune response
Ssc.15942.3.S1_x_at	*Ig VDJ*	Ig heavy chain variable region (VDJ)	1.47	0.051	immune response
Ssc.4093.1.A1_at	*IFNG*	Interferon gamma	1.54	0.009	Cytokine production, apoptosis
Ssc.23408.1.A1_s_at	-	annotation not clear	1.63	0.024	

LogFC: Log Fold change, FDR: False discovery rate.

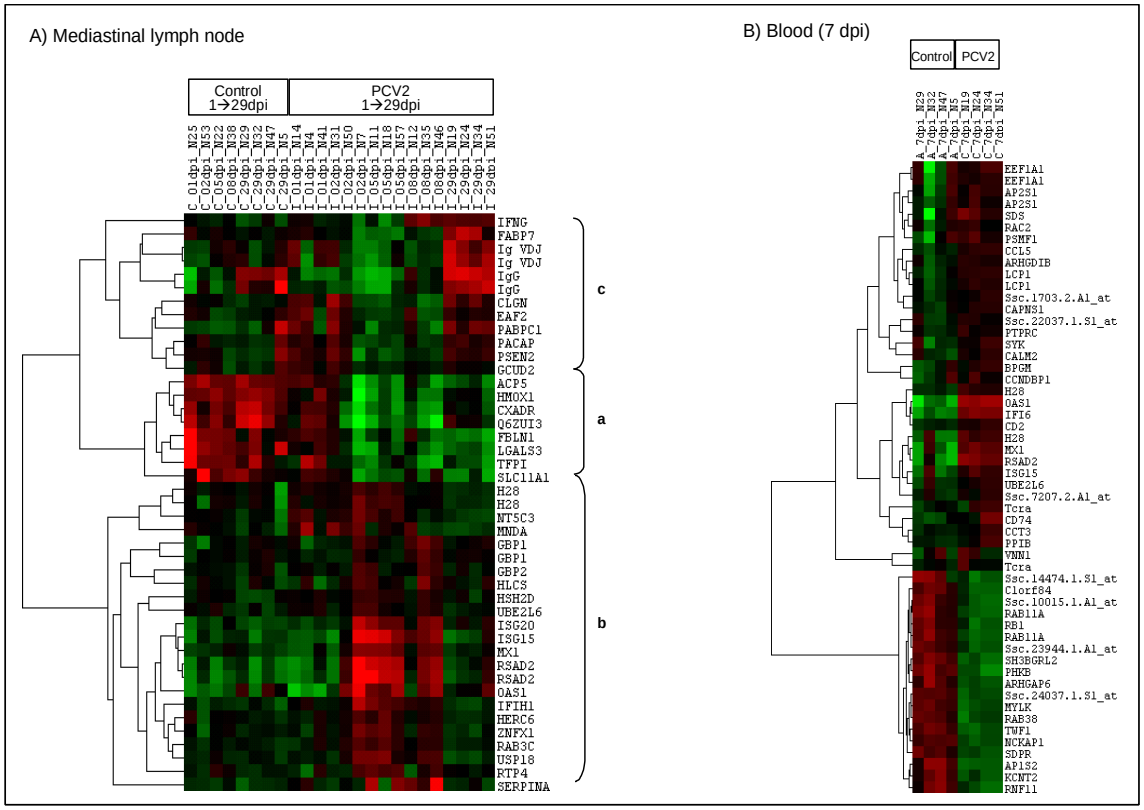

Figure 8. Heat maps of the differentially expressed probes between control (C) and PCV2-inoculated (I) pigs in A) mediastinal lymph node, where a, b, and c, represent clusters for globally down-regulated probes, and early and late up-regulated probes in the mediastinal lymph node dataset, respectively; and B) blood samples. Red represents up-regulation and green shows down-regulation for differentially expressed genes (FDR < 0.1, FC > 2.0).

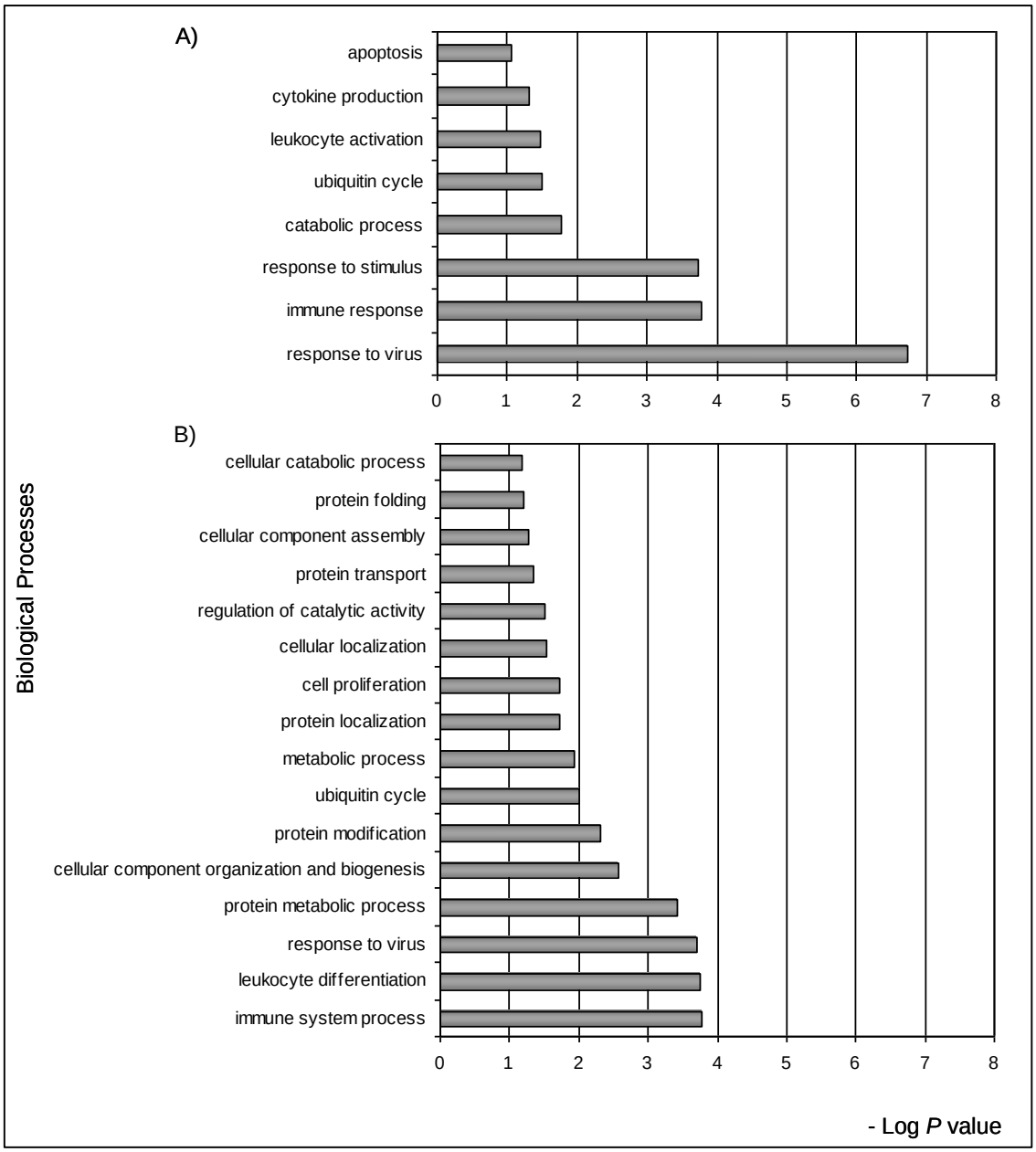

Figure 9. Biological process gene ontology (GO) categorization of the significant differentially expressed genes between control and PCV2-inoculated pigs in A) mediastinal lymph node and B) blood samples.

Table 6. List of differentially expressed genes between PCV2-inoculated and control pigs in blood samples with the Affymetrix Porcine Genechip.

Probe ID	Gene symbol	Gene name	log2 FC	FDR	Biological Processes
Ssc.4717.1.S1_at	*PHKB*	Phosphorylase kinase beta	-1.59	0.024	metabolic process
Ssc.14474.1.S1_at	-	annotation not clear	-1.36	0.066	
Ssc.10889.1.A1_s_at	*RAB11A*	RAB11A, member RAS oncogene family	-1.27	0.041	cellular component organization and biogenesis
Ssc.3657.1.A1_at	*SH3BGRL2*	SH3 domain-binding glutamic acid-rich-like protein 2	-1.26	0.05	unknown
Ssc.4572.1.S1_at	*RNF11*	RING finger protein 11	-1.24	0.026	protein metabolic process
Ssc.21114.1.S1_at	*TWF1*	Twinfilin 1	-1.19	0.034	protein metabolic process
Ssc.4135.2.A1_at	*AP1S2*	Adaptor-related protein complex 1, sigma 2 subunit	-1.19	0.034	cellular component organization and biogenesis
Ssc.951.1.S1_at	*RAB11A*	RAB11A, member RAS oncogene family	-1.19	0.06	cellular component organization and biogenesis
Ssc.23247.1.S1_at	*MYLK*	Myosin light chain kinase	-1.15	0.097	Protein metabolic process
Ssc.23944.1.A1_at	-	annotation not clear	-1.09	0.09	
Ssc.10015.1.A1_at	-	annotation not clear	-1.06	0.071	
Ssc.9586.2.S1_at	*SDPR*	Serum deprivation response protein	-1.05	0.044	unknown
Ssc.9244.1.A1_at	*NCKAP1*	NCK-associated protein 1	-1.05	0.055	Protein metabolic process
Ssc.24037.1.S1_at	-	annotation not clear	-1.05	0.096	
Ssc.17063.1.A1_at	*RB1*	Retinoblastoma 1	-1.03	0.017	leukocyte differentiation
Ssc.494.1.S2_at	*KCNT2*	Potassium channel, subfamily T, member 2	-1.03	0.024	metabolic process
Ssc.20188.2.S1_at	*C1orf84*	Chromosome 1 open reading frame 84	-1.02	0.004	unknown
Ssc.9708.1.A1_at	*ARHGAP6*	Rho-GTPase-activating protein 6	-1.01	0.025	cellular component organization and biogenesis
Ssc.6940.1.A1_s_at	*RAB38*	RAB38, member RAS oncogene family	-1.01	0.042	protein transport
Ssc.7392.1.S1_at	*CALM2*	calmodulin 2	1	0.064	unknown
Ssc.2641.1.S1_at	*UBE2L6*	ubiquitin-conjugating enzyme E2L 6	1.01	0.07	ubiquitin cycle
Ssc.902.1.S1_a_at	*CCT3*	Chaperonin containing TCP1, subunit 3 (gamma)	1.03	0.004	protein folding
Ssc.428.10.A1_at	*Tcra*	T-cell receptor alpha chain	1.04	0.067	immune system process
Ssc.22037.1.S1_at	-	annotation not clear	1.04	0.088	
Ssc.7207.2.A1_at	-	annotation not clear	1.05	0.037	
Ssc.1703.2.A1_at	-	annotation not clear	1.05	0.094	
Ssc.23248.1.S1_at	*PTPRC*	Protein tyrosine phosphatase, receptor type, C	1.07	0.027	leukocyte differentiation
Ssc.9839.1.S1_at	*PPIB*	Peptidylprolyl isomerase B	1.08	0.02	protein folding
Ssc.11742.2.S1_at	*SYK*	Spleen tyrosine kinase	1.09	0.099	leukocyte activation differentiation

Ssc.17304.3.S1_at	*RAC2*	Ras-related C3 botulinum toxin substrate 2	1.11	0.073	cellular component organization and biogenesis
Ssc.7158.2.A1_a_at	*CAPNS1*	Calpain small subunit 1	1.16	0.019	cell proliferation
Ssc.428.6.S1_a_at	*Tcra*	T-cell receptor alpha chain	1.16	0.076	immune system process
Ssc.15890.1.S1_at	*VNN1*	Vanin 1	1.17	0.078	metabolic process
Ssc.18389.3.S1_at	*AP2S1*	Adaptor-related protein complex 2, sigma 1 subunit	1.22	0.081	cellular component organization and biogenesis
Ssc.23774.3.S1_at	*LCP1*	Lymphocyte cytosolic protein 1	1.23	0.019	cellular component organization and biogenesis
Ssc.1230.2.S1_at	*ARHGDIB*	Rho GDP-dissociation inhibitor 2	1.27	0.048	
Ssc.13961.2.A1_at	*EEF1A1*	Eukaryotic translation elongation factor 1 alpha 1	1.28	0.09	protein metabolic process
Ssc.26249.2.S1_at	*CCNDBP1*	Cyclin D-type binding-protein 1	1.32	0.097	
Ssc.23774.2.S1_at	*LCP1*	Lymphocyte cytosolic protein 1	1.32	0.098	cellular component organization and biogenesis
Ssc.22500.1.S1_at	*BPGM*	2,3-bisphosphoglycerate mutase	1.33	0.096	cellular catabolic process
Ssc.23793.1.S1_at	*CD2*	CD2 molecule	1.38	0.005	leukocyte differentiation
Ssc.10593.1.S1_at	*H28*	histocompatibility 28	1.39	0.005	immune system process
Ssc.6222.1.S1_a_at	*CD74*	CD74 molecule, major histocompatibility complex, class II invariant chain	1.42	0.05	leukocyte differentiation
Ssc.22030.1.S1_at	*CCL5*	Chemokine (C-C motif) ligand 5	1.44	0.018	immune system process
Ssc.18389.2.S1_a_at	*AP2S1*	Adaptor-related protein complex 2, sigma 1 subunit	1.46	0.055	cellular component organization and biogenesis
AFFX-Ssc-ef1a-5_at	*EEF1A1*	Eukaryotic translation elongation factor 1 alpha 1	1.55	0.096	protein metabolic process
Ssc.11557.1.A1_at	*ISG15*	ISG15 ubiquitin-like modifier	1.83	0.018	ubiquitin cycle
Ssc.10588.1.A1_at	*H28*	histocompatibility 28	1.88	0.004	immune system process
Ssc.6353.2.S1_at	*PSMF1*	proteasome (prosome, macropain) inhibitor subunit 1	1.98	0.055	protein metabolic process
Ssc.221.1.S1_at	*MX1*	Myxovirus (influenza virus) resistance 1	2.31	0.004	response to virus
Ssc.11076.1.S1_at	*SDS*	Serine dehydratase	2.42	0.08	metabolic process
Ssc.20101.1.S1_at	*IFI6*	Interferon, alpha-inducible protein 6	2.99	0.001	
Ssc.286.1.S1_s_at	*RSAD2*	radical S-adenosyl methionine domain containing 2	3.04	0.004	response to virus
Ssc.1031.1.S1_at	*OAS1*	2'-5'-oligoadenylate synthetase 1	3.78	0.004	response to virus

LogFC: Log Fold change, FDR: False discovery rate.

The comparison between MLN and LWB datasets revealed six common DE genes (*OAS1*, *Mx1*, *ISG15*, *UBE2L6*, *RSAD2*, and *H28*). Both datasets were jointly analyzed with the Pathway analysis option of the Metacore™ platform and revealed that the top scored map ($p < 0.0001$) corresponded to the antiviral action of interferons. A gene interaction network could be constructed using the common gene set as a starting point and allowing the entrance of other DE genes, unique either to the MLN or to the LWB datasets, which were proven to be involved in the same pathway (Figure 10).

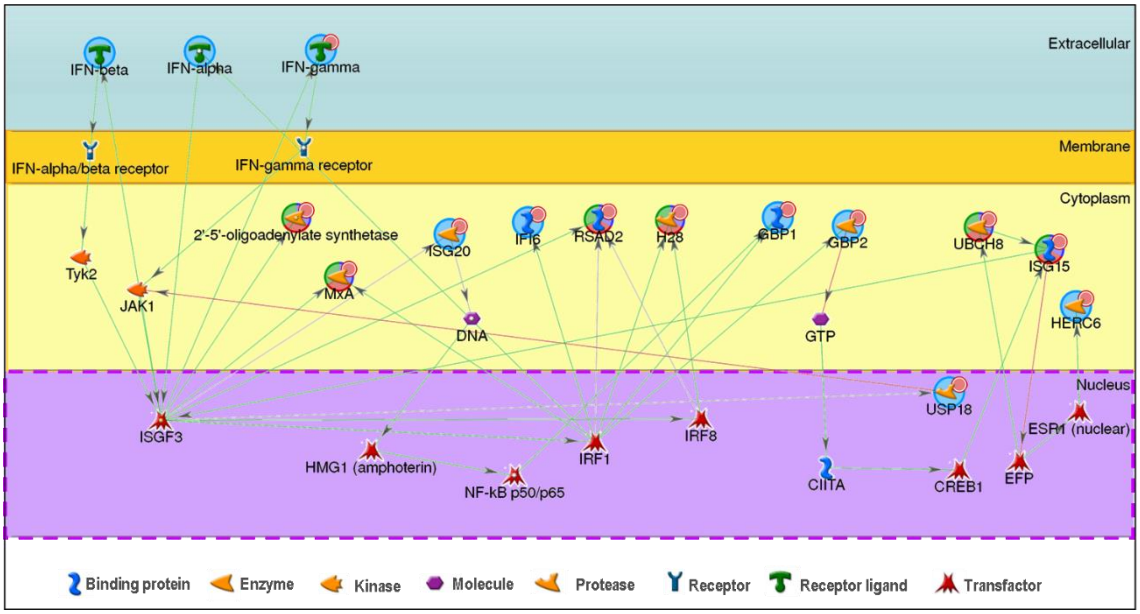

Figure 10. Gene interaction network representing the interferon-induced antiviral effectors differentially expressed in both mediastinal lymph node and blood datasets. Small red circles indicate up-regulated genes. The Metacore software (GeneGO Inc.) was used to create the network. The six common genes to mediastinal lymph node and blood datasets, indicated by tricolour circles, were the starting nodes. Blue circles represent genes manually added. Red, green and grey arrows indicate activation, inhibition and unspecified interactions between connected genes, respectively.

4.3.2. Validation of microarray experiments by qPCR

To confirm the DE genes in the microarray experiment, five (*IFNG*, *IgG*, *OAS1*, *Mx1*, *LGALS3*) and one (*OAS1*) genes were selected for real-time qPCR validation in the MLN and LWB datasets, respectively. Real-time qPCR results are shown in Table 7. All qPCR

validated genes displayed significant differences in gene expression between control and PCV2-inoculated pigs and showed similar fold changes as the ones obtained by the microarray analysis (Table 7), thus indicating that the microarray data was highly reliable.

Table 7. Results of the quantitative PCR validation of differentially expressed genes between PCV2-inoculated and control pigs and comparison with microarray gene expression data.

Genes	Quantitative PCR				Microarrays			
	FC	**Log2 FC**	**S.E.**	***P* value**	**Probes**	**FC**	**Log2 FC**	***P* value**
Mediastinal Lymph node								
IFNG	3.63	1.86	0.38	0.0001	Ssc.4093.1.A1_at	2.91	1.54	0.0086
IgG	2.93	1.55	0.44	0.0026	Ssc.11070.1.S1_at	2.19	1.13	0.0981
					Ssc.13778.1.S1_at	2.22	1.15	0.0236
LGALS3	-3.70	-1.89	0.53	0.0023	Ssc.17815.1.S1_at	-2.86	-1.50	0.0086
Mx1	2.62	1.39	0.66	0.0501	Ssc.221.1.S1_at	2.67	1.41	0.0699
OAS1	3.92	1.97	0.69	0.0103	Ssc.1031.1.S1_at	3.53	1.82	0.0887
Blood (7 days p.i.)								
OAS1	11.96	3.58	1.07	0.0156	Ssc.1031.1.S1_at	13.69	3.78	0.0039

4.4. Discussion

The most important challenge for PCV2 researchers nowadays is the understanding of PCV2-SD pathogenesis. The reason why all animals become infected but only a small percentage develops the disease is a question that remains unsolved. Several authors suggest that the complex host-virus interaction and the final ability of the pig to mount an effective immune response may be the key factors (Meerts *et al*., 2006; Stevenson *et al*., 2006; Vincent *et al*., 2007). Here, the transcriptional profile of CDCD pigs subclinically infected with PCV2 in MLN and LWB samples was characterized to gain insight into the early and late molecular events taking place during PCV2 infection.

Overall, three patterns of gene expression were identified in MLN samples: globally down-regulated genes, and up-regulated genes at early and late stages of infection; whereas in LWB samples DE genes were mostly identified at day 7 p.i. Most down-regulated genes in MLN encoded for molecules that participate in cell adhesion and migration processes such as *LGALS3* (Ochieng *et al*., 2004), *FBLN1* (Timpl *et al*., 2003),

TFPI (Provençal *et al*., 2008), *HMOX1* (Alcaraz *et al*., 2003), and *CXADR* (Fok *et al*., 2007). These gene products mainly act as inhibitors of migration and cell proliferation and, therefore, the sustained reduction in their expression, found from day 2 p.i. onwards in all PCV2-inoculated pigs, may be related to the inflammatory processes (granulomatous infiltration) occurring in animals suffering PCV2-SD.

The first days after PCV2 infection appeared to be the moment in which a higher number of genes were up-regulated both in MLN and LWB samples. The vast majority of these upregulated genes were involved in a common pathway, the interferon-mediated antiviral effector pathway. This result agrees well with the fact that a peak of IFN-α was detected at day 5 p.i. in the PCV2-inoculated pigs from this experiment (Fort *et al*., 2009a). However, differences in *IFNA* gene expression in PCV2-inoculated pigs could not be detected, probably due to the fact that its expression took place in a different time point to those herein analyzed. Activation of interferons in response to viral infection leads to the activation of a cascade of intracellular signaling events that, ultimately, induce the expression of hundreds of genes, commonly known as interferon-stimulated genes (ISG). Most of these ISG have been shown to display antiviral properties (Sadler and Williams, 2008). The most prominent interferon-mediated antiviral effectors represented in the present study were *OAS1*, *Mx1*, and *ISG15*. The OAS1 protein catalyzes the synthesis of 2',5'-oligomers of adenosine that bind to and activate RNase L, which degrades viral and cellular RNA, leading to the inhibition of cellular protein synthesis and impairment of viral replication (Sadler and Williams, 2008). Mx1 belongs to the dynamin superfamily of large GTPases and has been shown to exert their antiviral function by binding viral essential components, thereby blocking viral replication (Sadler and Williams, 2008). ISG15 has been recognized as an ubiquitin-like protein (Herrmann *et al*., 2007). Protein ubiquitylation implies the post-translational labelling of a protein by covalent attachment of an ubiquitin monomer for its degradation in the proteasome. This mechanism has been shown to exert a crucial role in the regulation of immune response (Petrosky, 2008). Several ubiquitin (*UBE2L6*, *HERC6*, and *USP18*) and proteasome (*PSMF1*) related enzymes were up-regulated in PCV2-inoculated pigs. Recently, it has been shown that the PCV2 open reading frame (ORF) 3 interferes with porcine ubiquitin E3 ligase Pirh2 (Liu *et al*., 2007). The ubiquitin proteasome system plays a key role in host pathogen interactions and many viruses have developed different immune evasion strategies by altering this pathway (Gao and Luo, 2006). The activation of several ubiquitin-

proteasome related genes in PCV2 subclinically infected pigs may indicate that this pathway is crucial for the control of PCV2 pathogenesis. Other interferon-inducible genes found differentially regulated either in MLN or LWB datasets were *RSAD2, H28, IFI44L, ISG20, GBP1, GBP2,* and *IFI6*. Overall, these results indicate that an effective activation of the immune response was produced early (first week) after infection with PCV2 in lymph nodes (at least in the MLN), which is also reflected in blood samples, where a number of genes directly related to the activation of the immune system were also found up-regulated (*TCRA, CCL5, CD2, CD74,* and *SYK*).

In LWB samples at 7 days p.i., several genes implicated in the organization and biogenesis of cellular components were DE between control and PCV2-inoculated pigs, such as the members of the Rab (*RAB11A* and *RAB38*) and Rho (*RAC2, ARHGDIB,* and *ARHGP6*) small GTPases, and the clathrin-associated adaptor complexes (*AP1S2* and *AP2S1*). These genes appeared mostly down-regulated except for *AP2S1* and *ARHGDIB* transcripts, which were up-regulated. These genes have been shown to participate in endocytosis-related processes. PCV2 internalization is produced by endocytosis, mainly through actin and Rho-GTPase mediated, dynamin-independent pathways (Misinzo *et al*., 2005; 2009). Furthermore, antigen (Ag) presentation by professional antigen presenting cells involves an active uptake of superficial Ag through macropinocytosis and/or phagocytosis processes followed by a complete arrest of this process to Ag processing and presentation to T cells in secondary lymphoid organs (Sallusto *et al*., 1995; West *et al*., 2004; Fauré-Andre *et al*., 2008). The fact that some of these genes were up-regulated while others were down-regulated might be explained by the fact that a mixture of cells at different stages can be found in LWB, and both processes (virus internalization and Ag presentation) can occur simultaneously.

In late stages of infection, a relatively low number of DE probes were found compared to the results reported in study I. In that experiment, different pig breed, tissue samples, necropsy days, and statistical analysis were used, which may explain the differences found between both experiments. However, an increase of certain cytokines (*CCL4L, CXCL9,* and *CXCL11* in study I, and *IFNG* in the present work) and IgG mRNA was detected in PCV2- inoculated pigs from both studies, thus indicating that similar immunological responses against PCV2 were obtained in Duroc (study I) and Landrace (this study) subclinically infected pigs. Furthermore, the expression of *IFNG* and *IgG*

genes in MLN samples correlated well with the immunological results obtained by Fort *et al*., (2009a), using animal material from the present experiment. In this work, a peak of IFN-γ was detected between days 14 and 21 p.i. and seroconversion took place between days 7 and 14 p.i. in all PCV2-inoculated pigs. In the current experiment, expression of *IFNG* gene started increasing from day 8 p.i. and was mainly over-expressed in pigs infected with PCV2 at day 29 p.i., which agrees well with its role in the early immune response against viruses.

A relatively low number of DE probes were found for both MLN and LWB datasets. This may probably be due to two main reasons. First, tissues are heterogeneous, composed by a mixture of different cell types, each with a specific transcriptional profile. Second, the low number of samples used for microarray analyses may increase data variability and reduce the statistical power to detect DE genes. This aspect might be the case for the analyses of MLN samples, since only one control pig was used for each timepoint.

Overall, this study has allowed the characterization, for the first time, of the genes that are involved in the molecular events underlying an effective immune response to counteract an infection with PCV2 and, more importantly, to control disease progression. The results from this study provide new insights into the complex host-PCV2 interaction, from a subclinical point of view. Given the difficulties in reproducing PCV2-SD disease experimentally, further studies should be performed in healthy and naturally PCV2-SD-affected pigs to explore the host-virus molecular interactions upon disease status.

CHAPTER 5

Study III

Microarray analysis of mediastinal lymph node of pigs naturally affected by porcine circovirus type 2-systemic disease

5.1. Introduction

To date, although different aspects of the PCV2 infection have been elucidated (Finsterbusch and Mankertz, 2009), many questions are still unanswered. It is of paramount importance to further explore the molecular basis underlying the pathogenesis of the infection, such as the mechanisms by which the virus interacts with its host and the events triggered by this interaction. Recently, several porcine gene products and proteins interacting with PCV2 have been identified using in vitro and in vivo models (Bratanich and Blanchetot, 2006; Finsterbusch *et al*., 2009; Karlskov-Mortensen *et al*., 2008; Liu *et al*., 2007). Although these studies are informative, they are based on relatively low-throughput techniques, and the whole picture of PCV2-host interactions is still missing.

In studies I and II, the microarray technology was used to characterize the events taking place after PCV2 experimental infection in a subclinical model. Several gene products were found to be involved in the early and late immune responses against PCV2 infection. However, due to the difficulty of reproducing the full clinical expression of PCV2-SD on an experimental model (Tomás *et al*., 2008), it was considered relevant to carry out studies in diseased pigs. Therefore, in the present study, the Affymetrix 24K Genechip® Porcine Genome Array was used to examine the transcriptome in mediastinal lymph nodes (MLN) from PCV2-SD naturally affected pigs and healthy counterparts.

5.2. Materials and methods

5.2.1. Case selection

A total of 25 conventional 13–15-week-old pigs were used in this study. Animals were selected from three farms with historical records of PCV2-SD and free from major immunomodulatory/ immunosuppressive diseases such as those caused by Porcine reproductive and respiratory syndrome virus (PRRSV) and Pseudorabies virus (PRV) infections. Moreover, one farm was also free from *Mycoplasma hyopneumoniae*, while the other two vaccinated against this pathogen; no clinical and pathological signs of this bacterial infection was observed in any of them. All pigs were euthanized and subsequent necropsy was performed at the farm. MLN samples used for microarray studies were immediately collected and immersed in liquid nitrogen. These samples were kept at

−80ºC until usage. Samples for histopathology were taken and fixed by immersion in 10% neutral buffered formalin.

Twelve out of the 25 pigs fulfilled the PCV2-SD diagnosis, based on the 3 individual disease case definition criteria (Segalés *et al*., 2005): (i) clinical signs including growth retardation and wasting, (ii) moderate (score 2) to severe (score 3) histopathological lesions in lymphoid tissues, including lymphocyte depletion with granulomatous inflammation, and (iii) moderate (score 2) to high (score 3) amount of PCV2 within microscopic lesion detected by in situ hybridization (ISH) (Rosell *et al*., 1999). The remaining thirteen pigs were selected for their good clinical condition, and showed none (score 0) or slight (score 1) PCV2-SD-like histopathological lymphoid lesions and none (score 0) or low (score 1) amount of PCV2 DNA within lymphoid tissues as detected by ISH. These animals were kept as healthy, control animals. At least one case and one control pigs were used from each farm. Microarray and qPCR studies were performed on MLN, as described in study II.

5.2.2. PCV2 genome quantification and sequencing

DNA from MLN samples collected during necropsy was extracted from a 50 mg of tissue using a commercial kit (Nucleospin tissue, Macherey-Nagel®, Bethlehem, PA). The PCV2 genome was quantified by qPCR targeting as previously described by Olvera *et al*. (2004). Statistical analyses to compare mean viral loads among groups were performed using the general linear model (GLM) method of SAS software (Statistics, V 9.1; SAS Institute, Inc., Cary, NC). Significance level (α) was set at 0.05.

The PCV2 genotype (Segalés *et al*., 2008) of each sample was assessed by sequencing of the PCR products obtained by a previously described standard PCR (Quintana *et al*., 2001). Briefly, an internal PCR fragment was amplified and purified (MiniElute®, Qiagen). Secondly, both strands were sequenced using the same specific primers. Cycle sequencing was carried out with BigDye® Terminator v3.1 cycle sequencing kit (Applied Biosystems, Foster City, CA, USA) and an ABI 3730 DNA sequencer (Applied Biosystems) following manufacturers' instructions. Nucleotide sequences were assembled using BioEdit 7.0.5.3 software (Hall, 1999) and aligned using Clustal W method to 3 PCV2 genotype a (GenBank IDs: AF109398, AY180397, AY201310), 3

PCV2 genotype b (GenBank IDs: AY484416, AY847748, AY682996) and one PCV2 genotype c (GenBank ID: EU148503) sequences. Phylogenetic relationships among sequences were analyzed as described in Olvera *et al*. (2007) using parsimony and nucleotide distance methods. Confidence in the Neighbor-Joining (NJ) tree was estimated by 1000 bootstrap replicates.

5.2.3. RNA extraction

Total RNA was isolated from MLN using RiboPureTM kit (Ambion, Austin, USA) according to the manufacturer's instructions and quantified by spectrophotometry (ND-1000 NanoDrop Technologies, Wilmington, DE, USA). RNA quality was assessed by capillary electrophoresis analysis on an Agilent 2100 Bioanalyser (Agilent Technologies, Palo Alto, CA, USA). Only total RNA with RNA integrity number (RIN) $\geq$ 8.0 was used for microarray and quantitative real-time PCR analyses.

5.2.4. Microarray hybridisations and data analysis

Microarray targets were prepared with 5 µg of total RNA from MLN of 13 healthy control and 12 PCV2-SD affected pigs. RNA labelling, hybridization and scanning were conducted by a commercial Affymetrix array service (Institut de Recerca Hospital Universitari Vall d'Hebron, Barcelona, Spain). Reverse transcription of RNA and synthesis of biotin-labelled cRNA with one round of amplification were carried out following the standard Affymetrix one-cycle protocol according to the manufacturer's instructions. Samples were hybridized to the Affymetrix 24 K Genechip® Porcine Genome Array (Affymetrix, Santa Clara, CA, USA). In total, 25 microarrays were used in the experiment.

Data analysis was performed with Bioconductor (Gentleman *et al*., 2004) implemented in R 2.6.0 (http://cran.r-project.org/). Data quality control assessments were performed with *affyQCReport* implemented in the *simpleaffy* package (Wilson and Miller, 2005). The raw data were background corrected, normalized and converted to expression-level data using the Robust Multichip Average (RMA) algorithm (Irizarry *et al*., 2003a). To assess differential expression (changes in transcripts abundance), the Empirical Bayes method implemented in the *limma* package (Smyth, 2004) was used. The effect of farm

was included in the model as a fixed effect. Significance threshold was set to a false discovery rate (FDR, Benjamini and Hochberg, 1995) of 0.05 and a minimum fold change (FC) of 2. Hierarchical clustering analysis was performed using Cluster 3.0 and Java TreeView 1.1 software (www.rana.lbl.gov/Eisen/Software.htm). The uncentered correlation coefficient and the average linkage parameters were applied to cluster genes. Samples were distributed in ascending order based on scores for the lymphocyte depletion (LD) and granulomatous inflammation (GI) (LD score 2/GI score 2; LD 2/GI 3, LD 3/GI 2, LD 3/GI 3) (Rosell *et al*., 1999).

Differentially expressed (DE) mRNAs with significant similarities to transcripts in nr and EST databases available on Basic Local Alignment Search Tool (BLAST) (http://blast.ncbi. nlm.nih.gov/Blast.cgi) were selected for functional classification using the Database for Annotation, Visualization and Integrated Discovery (DAVID 2008, http://david.abcc.ncifcrf.gov/home.jsp).

5.2.5. Primary microarray data

The microarray data are available in the Gene Expression Omnibus repository (www.ncbi.nlm.nih.gov/projects/geo/) under accession Nº. GSE19083.

5.2.6. qPCR

To confirm microarray data, primers for *PLAU, IL10RB, IL8, LGALS3, OAS1* and *HPRT1* (the endogenous control for sample normalization) were designed for qPCR using Primer Express 2.0 software (Applied Biosystems Inc., Foster City, CA) with available public sequences. Primer sequences are listed in Table 8. cDNA was synthesized from one microgram of total RNA from samples used in the microarray analysis, using the High Capacity cDNA Transcription Kit (Applied Biosystems, Inc., Foster City, CA) according to the manufacturer's instructions. The PCR conditions and the relative quantification method were previously described in study I. Resulting qPCR data were Log2 transformed and analyzed using the GLM method of SAS. Differences were considered significant at $P < 0.05$.

Table 8. Primer sequences for quantitative PCR analysis of selected genes.

Gene Symbol[a]	GenBank accession number	Amplicon Size (bp)	Sequence 5' → 3'
PLAU-F	NM_213945.1	61	CCTTGCTCACCACAATGATATTG
PLAU-R			GTGCACACTGGCCCTTGTC
IL10RB-F	NM_213771.1	63	CAGACTGGATAAACATCACCTTCTGT
IL10RB-R			TGCATTCCAGGAGGTCCAA
IL-8-F	NM_213867	84	GTGCAGAAGGTTGTACAGATATTTTTG
IL-8-R			GAGAATGGGTTTTTGCTTGTTGT
LGALS3-F	NM_001097501	71	AACAATTCTGGGCACAGTAAAGC
LGALS3-R			CAACATCATTCCCCTTCTTGAAA
OAS1-F	NM_214303	63	CTGTCGTTGGACGATGTATGCT
OAS1-R			GCCGGGTCCAGAATCACA
HPRT1-F	DQ136030	90	TCATTATGCCGAGGATTTGGA
HPRT1-F			CTCTTTCATCACATCTCGAGCAA

[a] *PLAU*: urokinase-type plasminogen activator precursor; *IL10RB*: interleukin-10 receptor beta chain precursor; *IL-8*: interleukin-8 precursor; *LGALS3*: galectin-3; *OAS1*: 2'-5'-oligoadenylate synthetase; *HPRT1*: hypoxanthine phosphoribosyltransferase 1.

5.3. Results

5.3.1. Pathological findings

The most relevant macroscopic feature found in all PCV2-SD affected pigs (n = 12) was thymus atrophy. Other gross lesions found in the diseased pigs were enlargement of lymph nodes (n = 6), non-collapsed lungs (n = 8), pulmonary craneo-ventral consolidation (n = 9), soft to liquid faeces in the rectum (n = 2) and serous atrophy of the fat (n = 1). As expected, no gross lesions were observed in the healthy pigs, except for mild pulmonary craneo-ventral consolidation in two animals.

Histopathological evaluation of lymphoid tissues from PCV2-SD affected pigs revealed moderate to extensive loss of the normal follicular architecture with lymphocyte depletion and replacement by an infiltrate of macrophages. Occasionally, multinucleate giant cells and PCV2 characteristic cytoplasmic inclusion bodies were also observed. Only one

animal of the healthy group had very slight PCV2-SD-like lymphoid lesions. The presence of moderate to high amount of PCV2 DNA was detected by ISH in lymphoid tissues of all affected pigs and in low amount in two healthy pigs. Table 9 summarizes the severity of lymphocyte depletion, granulomatous inflammation, and the ISH scores for all studied pigs.

Table 9. Scores for amount of PCV2 by ISH, lymphocyte depletion and granulomatous infiltration in lymphoid tissues of the 25 studied animals.

Animal	Origin Herd	PCV2_SD status	ISH	Lymphocyte depletion (LD)	Granulomatous infiltration (GI)	Groups LD/GI
H_A2	1	Healthy	0	0	0	Healthy
H_B6	1	Healthy	0	0	0	Healthy
H_B7	1	Healthy	1	0	0	Healthy
H_C7	2	Healthy	0	0	0	Healthy
H_C8	2	Healthy	1	0	0	Healthy
H_D2	3	Healthy	0	0	0	Healthy
H_D3	3	Healthy	0	0	0	Healthy
H_D4	3	Healthy	0	0	0	Healthy
H_D5	3	Healthy	0	0	0	Healthy
H_D6	3	Healthy	0	0	0	Healthy
H_D7	3	Healthy	0	0	0	Healthy
H_D8	3	Healthy	0	0	0	Healthy
H_D9	3	Healthy	0	1	1	Healthy
C_B4	1	PCV2_SD	2	2	2	PCV2_SD 1
C_C1	2	PCV2_SD	3	2	2	PCV2_SD 1
C_C6	2	PCV2_SD	3	2	2	PCV2_SD 1
C_D1	3	PCV2_SD	2	2	2	PCV2_SD 1
C_B3	1	PCV2_SD	3	2	3	PCV2_SD 2
C_B5	1	PCV2_SD	2	2	3	PCV2_SD 2
C_A1	1	PCV2_SD	2	3	2	PCV2_SD 3
C_B2	1	PCV2_SD	3	3	2	PCV2_SD 3
C_C4	2	PCV2_SD	3	3	2	PCV2_SD 3
C_C5	2	PCV2_SD	3	3	2	PCV2_SD 3
C_C2	2	PCV2_SD	3	3	3	PCV2_SD 4
C_C3	2	PCV2_SD	3	3	3	PCV2_SD 4

Score: Absent (0), mild (1), moderate (2) and high (3).

5.3.2. PCV2 genomic load and PCV2 genotyping

PCV2 viral load in MLN was significantly higher ($P < 0.001$) in PCV2-SD affected pigs compared to the healthy group. PCV2 mean concentration in MLN was 9.33 ± 0.53 and 6.24 ± 0.51 log10 of PCV2 copies/ng of DNA for pigs from PCV2-SD and control groups, respectively. All pigs from the PCV2-SD group were positive by qPCR while PCV2 DNA was detected in 12 out of 13 healthy animals. Based on the phylogenetic

study, all PCV2 sequences found in both groups of animals were assigned to genotype b (data not shown).

5.3.3. Microarray analysis

The global mRNA expression profile of MLN from PCV2-SD cases was compared with that of the healthy control group. Taking a FC > 2.0 and the FDR < 0.05 as criteria, a total of 366 transcripts showed significant differential abundance: a set of 229 transcripts with significantly higher abundance and another set of 137 transcripts with lower abundance in PCV2-SD pigs relative to healthy animals. Of these, putative identities could be determined for 302 transcripts, coded by 252 unique genes, based on BLAST searches. A complete list of the differentially expressed (DE) transcripts is shown in Table S1 (Supplementary material presented at the end of the chapter).

Hierarchical clustering analyses of the 366 transcripts showed that the expression profiles from PCV2-SD affected pigs were not homogeneous (Figure 11). The change in the expression level of some genes could not be found for all diseased animals at the same time. This feature was particularly evident in animals with moderate degree of lymphocyte depletion and high degree of granulomatous inflammation (PCV2-SD group 2), which displayed patterns similar to the ones of healthy pigs for some genes. However, for all genes the number of PCV2-SD animals showing a modification in the expression level was higher than those resembling the healthy controls profile. Thus, suggesting that the altered gene expression was due to disease status. This observation is highlighted in Figure 12, where the individual values of expression for 6 transcripts among those from the most extreme mRNA levels from PCV2-SD affected animals were compared to the average expression from healthy pigs.

Based on the DAVID analysis, which classifies genes by their ontological groups, 217 out of a total of 252 unique genes were grouped into 95 biological processes ($P < 0.01$, Supplementary Table S2). The immune response and related processes were, as expected, the most represented categories. A detailed description of the genes belonging to these functional categories can be found in Table 10. In summary, a large set of mRNAs with increased abundance in PCV2-SD affected pigs were coded by genes involved in inflammatory response including inflammatory mediators, transcriptional regulators and

acute phase proteins. Moreover, in PCV2-SD affected animals, an increased abundance of mRNA transcribed by genes of innate immunity as IFN-related pathway, pattern recognition receptors, immunoglobulin Fc receptors (FcR) and metal ion transporter (*NRAMP1*) was observed. The complement system was also altered in PCV2-SD-affected pigs.

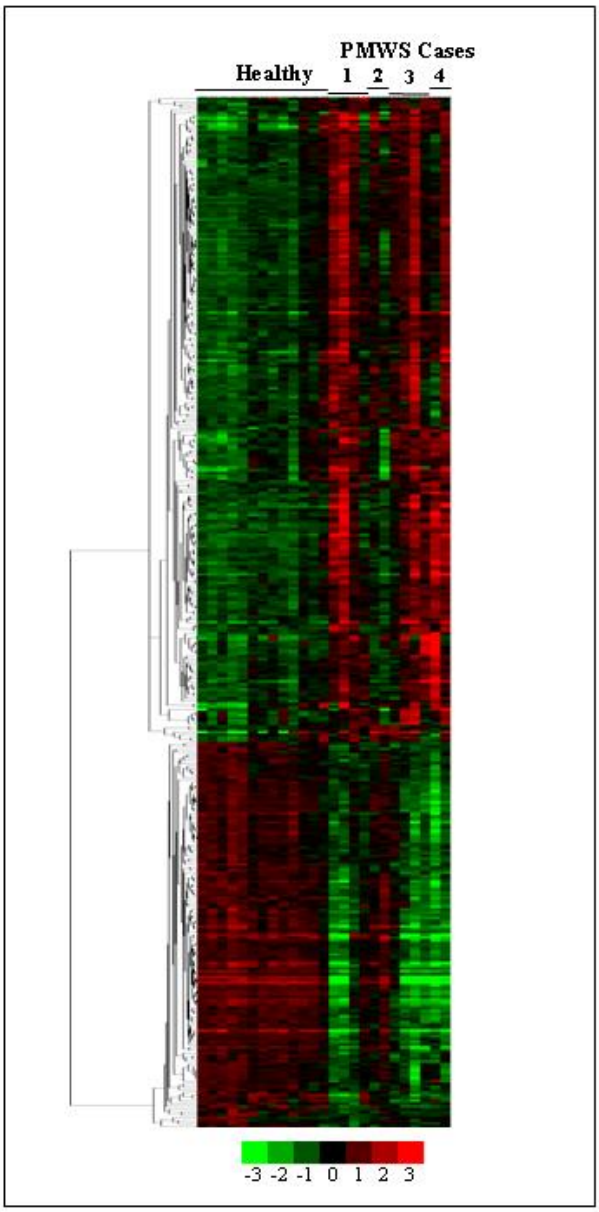

Figure 11. Heat map of the differentially expressed genes between healthy and PCV2-SD affected pigs. In PCV2-SD group, 1, 2, 3 and 4 represent scores for the degree of lymphocyte depletion (LD) and granulomatous inflammation (GI): LD score 2/GI score 2; LD 2/GI 3, LD 3/GI 2 and LD 3/GI 3, respectively. Red represents increased mRNA levels and green shows decrease mRNA levels for differentially expressed genes (FDR < 0.05, FC > 2.0).

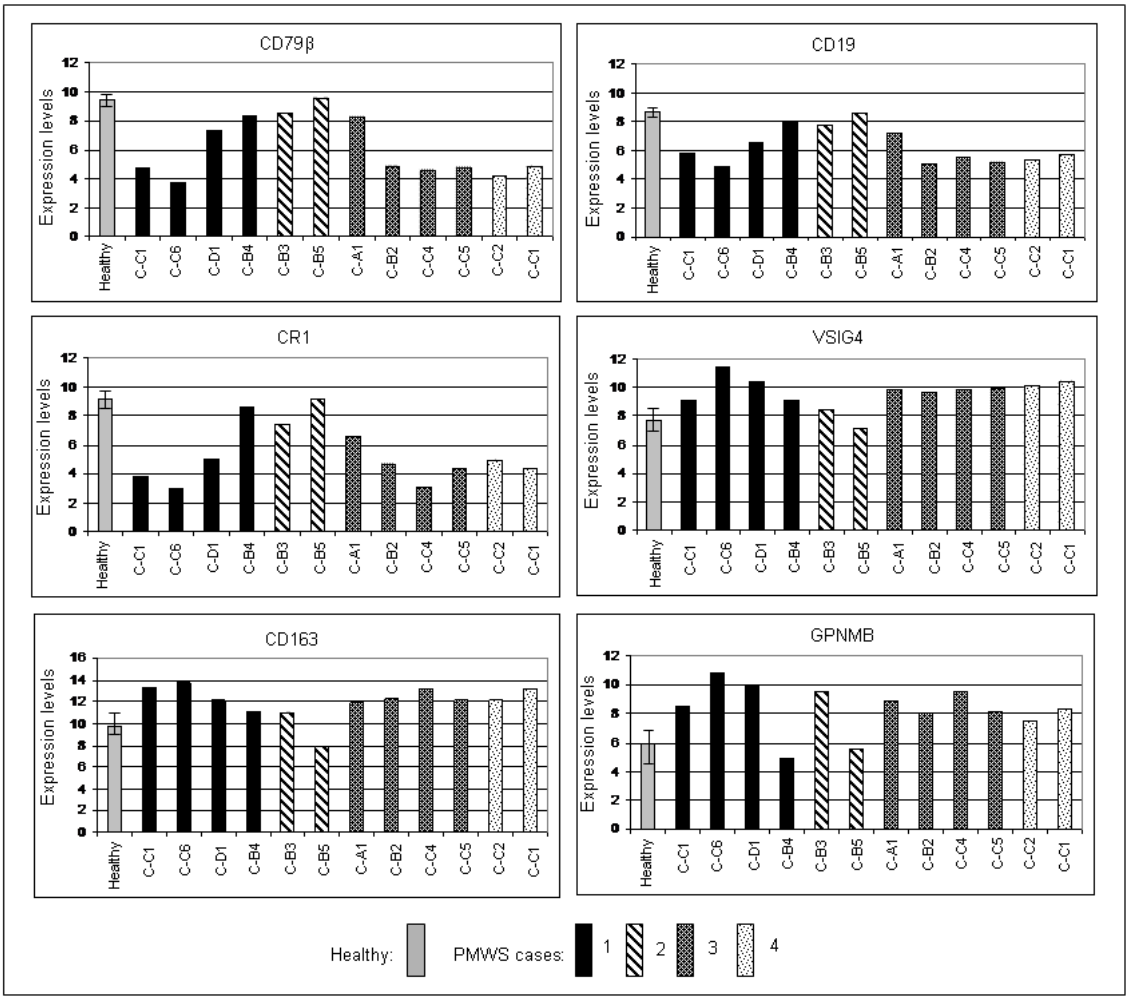

Figure 12. Average expression from healthy pigs and the values of individual levels of expression from PCV2-SD affected animals, for 6 transcripts among those from the most extreme mRNA levels. In PCV2-SD group, 1, 2, 3 and 4 represent scores for the degree of lymphocyte depletion (LD) and granulomatous inflammation (GI): LD score 2/GI score 2; LD 2/GI 3, LD 3/GI 2 and LD 3/GI 3, respectively.

Table 10. Subset of differentially expressed transcripts between PCV2-SD affected and healthy pigs in mediastinal lymph nodes, according to its functional classification.

Functional classification	Gene Symbol	Gene Name	Log2 FC
Inflammatory response	GPNMB	glycoprotein (transmembrane) nmb	3.12
	LGALS3	galectin 3	2.73
	CEBPD	ccaat/enhancer binding protein (c/ebp), delta	1.93
	CEBPB	ccaat/enhancer binding protein (c/ebp), beta	1.55
	JUN	v-jun sarcoma virus 17 oncogene homolog	1.27
	CD163	cd163 antigen	2.58
	IL1RAP	interleukin 1 receptor accessory protein	1.82
	IL8	interleukin 8	1.82
	CXCL3	chemokine (c-x-c motif) ligand 3	1.70
	CCR1	chemokine (c-c motif) receptor 1	1.57
	IL10RB	interleukin 10 receptor, beta	1.34
	CXCL16	chemokine (c-x-c motif) ligand 16	1.15
	CCL4	chemokine (c-c motif) ligand 4, MIP1b	1.08
	CCR5	chemokine (c-c motif) receptor 5	1.07
	CCL3L1	chemokine (c-c motif) ligand 3-like 1	1.06
Acute phase response	PTX3	pentraxin-related gene, rapidly induced by il-1 beta	2.20
	CP	ceruloplasmin (ferroxidase)	1.33
	SAA1	serum amyloid a1	1.13
	ITIH4	inter-alpha (globulin) inhibitor h4	1.12
Innate immune response	NRAMP1	solute carrier family 11, member 1	2.11
	OAS1	2',5'-oligoadenylate synthetase 1, 40/46kda	1.96
	TLR4	Toll-like receptor 4 precursor (hToll).	1.69
	FCGR2C	fc fragment of IgG	1.36
	IFIT3	interferon-induced protein with tetratricopeptide repeats 3	1.29
	FCER1G	fc fragment of IgE	1.21
	TLR8	toll-like receptor 8	1.14
	FCGR3A	fc fragment of IgG	1.02
	SLC15A2	solute carrier family 15, member 2	-2.15
Complement system	CR1	complement component (3b/4b) receptor 1	-3.43
	CR2	complement component receptor 2	-2.19
	DAF	Complement decay-accelerating factor precursor	-1.29
	C5R1	complement component 5a receptor 1	1.16
	CFP	complement factor properdin	1.11
	C2	complement component 2	1.08
	C1R	complement component 1, r subcomponent	1.05
Lymphocyte activation and proliferation	VSIG4	V-set and immunoglobulin domain containing 4;	2.42
	CD79B	cd79b antigen	-3.03
	MYBL1	v-myb myeloblastosis viral oncogene homolog-like 1	-2.64
	CD19	cd19 antigen	-2.51
	LEF1	lymphoid enhancer-binding factor 1	-1.86
	BLK	b lymphoid tyrosine kinase	-1.55
	BCL11A	b-cell cll/lymphoma 11a (zinc finger protein)	-1.50
	LTB	lymphotoxin beta (tnf superfamily, member 3)	-1.48
	CD24	Signal transducer CD24 precursor.	-1.31
	BCL11B	b-cell cll/lymphoma 11b (zinc finger protein)	-1.29
	MYBL2	v-myb myeloblastosis viral oncogene homolog -like 2	-1.17

	SWAP70	swap-70 protein	-1.15
	TRAF5	TNF receptor associated factor 5.	-1.11
	ICOSLG	inducible t-cell co-stimulator ligand	-1.09
	TNFRSF7	tumor necrosis factor receptor superfamily, member 7	-1.08
	TCRB	t cell receptor beta locus	-1.07
	TIMD4	t-cell immunoglobulin and mucin domain containing 4	-1.03
	TRAF5	TNF receptor associated factor 5.	-1.02
Response to stress	RRM2B	ribonucleotide reductase m2 b (tp53 inducible)	-1.41
	SMC6L1	SMC6 protein	-1.15
	TOPO2	topoisomerase (dna) ii alpha 170kda	-1.01
	CYP3A29	Cytochrome P450 3A4	3.27
	PDK4	pyruvate dehydrogenase kinase, isozyme 4	2.53
	CYP3A43	cytochrome p450, family 3, subfamily a, polypeptide 43	2.25
	CYP3A4	cytochrome p450, subfamily iiia, polypeptide 3	2.10
	SOD2	superoxide dismutase 2, mitochondrial	1.64
	GPX3	glutathione peroxidase 3 (plasma)	1.52
	MT2A	metallothionein 2a	1.48
	TXNIP	thioredoxin interacting protein	1.06
	DDIT4L	dna-damage-inducible transcript 4-like	1.04
Apoptosis	P8	p8 protein (candidate of metastasis 1)	2.79
	CASP4	caspase 4, apoptosis-related cysteine peptidase	1.50
	DRAM	hypothetical protein flj11259	1.45
	ANXA1	annexin a1	1.36
	CASP1	caspase 1, apoptosis-related cysteine peptidase	1.27
	TNFSF10	tumor necrosis factor (ligand) superfamily, member 10	1.16
	NQO1	nad(p)h dehydrogenase, quinone 1	1.11
	CTSB	cathepsin b	1.01
Cell adhesion	CDH1	cadherin 1, type 1, e-cadherin (epithelial)	-1.22
	ITGA8	integrin, alpha 8	1.18
Cytoskeleton	ABLIM1	actin binding lim protein 1	-1.31
	CORO1B	coronin, actin binding protein, 1b	-1.25
	PSTPIP2	proline-serine-threonine phosphatase interacting protein 2	1.21
	FGD4	fyve, rhogef and ph domain containing 4	1.13
	SCIN	scinderin	1.00
Extracellular matrix	LAMC2	laminin, gamma 2	-1.40
	XLKD1	extracellular link domain containing 1	1.58
	EMILIN2	elastin microfibril interfacer 2	1.50
	ECM1	Extracellular matrix protein 1 precursor	1.37
Vesicle trafficking	MRC1	mannose receptor, c type 1	1.43
	STX11	syntaxin 11	1.37
	LRP1	low density lipoprotein-related protein 1	1.33
	ANXA8	similar to annexin a8	1.06
	RHOJ	ras homolog gene family, member j	1.01

The relative mRNA levels of genes related to lymphocyte activation, proliferation were largely decreased in diseased pigs. These included transcriptional regulators, members of the TNF family, receptors and signalling molecules.

A set of genes involved in stress response was identified. In diseased animals, genes related to DNA repair showed low mRNA levels, while increased representation were detected for gene products associated to respiratory burst, genes involved in p53-mediated apoptosis and other pro-apoptotic genes (*TNFSF10* and cathepsin B). Finally, a number of altered genes of PCV2-SD affected pigs were involved in cellular adhesion and proliferation, components of extracellular matrix, cytoskeletal reorganization, and genes related to vesicle trafficking. mRNA levels of most of these genes increased in diseased animals.

5.3.4. Validation of microarray results by qPCR

Changes in gene expression identified by microarray were confirmed by qPCR (Table 11). All five selected genes (*PLAU, IL10RB, IL8, LGALS3* and *OAS1*) showed significant differential expression in the qPCR results. Importantly, similar expression patterns of these genes were observed among microarray and qPCR techniques, which indicate the reliability of the microarray findings.

Table 11. Results of the validation of microarray data by quantitative PCR.

Quantitative PCR					Microarrays			
Gene	**FC**	**Log_2 FC**	**Log_2 S.E.**	***P* value**	**Probe**	**FC**	**Log_2 FC**	***P* value**
PLAU	3.24	1.70	0.34	<.0001	Ssc.11194.1.S1_at	3.12	1.64	<.0001
IL10RB	2.32	1.22	0.28	0.0002	Ssc.15484.1.S1_at	2.06	1.05	0.0003
IL8	4.48	2.16	0.74	0.0080	Ssc.658.1.S1_at	3.53	1.82	0.0039
LGALS3	7.62	2.93	0.71	0.0005	Ssc.17815.1.S1_at	6.62	2.73	0.0001
OAS1	3.37	1.75	0.72	0.0233	Ssc.1031.1.S1_at	3.90	1.96	0.0029

5.4. Discussion

The molecular mechanisms underlying PCV2-SD remain largely unknown, in spite of the advance in the general understanding of many aspects of the disease acquired during the last decade. In the present study, the global transcriptional profile of MLN from PCV2-SD naturally affected pigs has been reported for the first time.

Interpretation of transcriptional profiles in diseased tissues can be difficult, in particular when cell compositions are drastically changed. Therefore, it will not be correct to conclude that a specific gene is down-regulated when a specific cell population is virtually absent from the diseased tissue or that a gene is up-regulated while massive infiltrations of a given cell type are observed. For these reasons, in the present study, the terminology "relative abundance of mRNA" has been preferred to "differentially expressed genes". As compared to MLN from healthy animals, which were also infected by PCV2 as usually occurs under field conditions (Grau-Roma *et al*., 2009a), increased abundance of some mRNAs in MLNs of PCV2-SD affected pigs might indicate their capacity to at least retain some original (pre-infection) phenotypes and to express new ones. On the contrary, a much lower mRNA abundance in diseased animals may reflect an impaired capacity to produce some proteins in an affected MLN as a whole. Therefore, a more accurate interpretation of the results obtained here required that not only piglets were classified as PCV2-SD affected or not affected, but also in function of the degree of cell-depletion or infiltration of their respective MLNs. In that respect, particular animals of group PCV2-SD 2, with moderate degree of lymphocyte depletion and high degree of granulomatous inflammation showed similar patterns of mRNA abundance as those of the healthy group. Based on the suggested evolution of microscopic lesions over time (Opriessnig *et al*., 2007), these results might be a reflection of the transition from acute/sub-acute to chronic phases of the disease, where lymph node lesions are being recovered. However, other animals of the groups PCV2-SD 1 and 3 had transcriptional profiles resembling those of group PCV2-SD 4 (severe lymphocyte depletion and severe granulomatous inflammation). From these more severely affected piglets, most of the 10–15 more and less abundant mRNAs in MLNs, when compared to healthy animals, coded for proteins involved in inflammation processes and B cell activation/ differentiation respectively. Therefore, these findings suggest that changes in RNA levels were due to disease status/evolution. Recently, a grading system has been suggested to classify the progression of immunopathological lesions correlated with PCV2 load in lymphoid follicles in the inguinal LNs of PCV2-SD naturally affected pigs by using a tissue microarray (TMA) technology (Lin *et al*., 2011b).

5.4.1. Inflammatory response

An inflammatory response characterized by granulomatous lesions in lymphoid tissues is one of the hallmarks of PCV2-SD. Two major mRNAs (in respect to the relative abundance) found in our study, which code for GPNMB and LGALS3, have antagonistic functions regarding the inflammatory response. In addition to promote inflammation, LGALS3, which can be produced by different cell types, is a chemoattractant to monocytes and an inductor of respiratory burst (Dumic *et al*., 2006). Over-expression of *LGALS3* has been observed in pools of lymph nodes showing moderate lymphocyte depletion and granulomatous lesions from pigs experimentally infected with PCV2 (Lee et al., 2010). Interestingly, in study II, *LGALS3* was down-regulated. This discrepancy indicates that the expression of this gene is modulated by the degree of granulomatous inflammation. Here, indirect evidence of LGALS3 expression is also provided by increased representation of CD163 mRNA (specific marker for monocytes and macrophages), cytochromes and enzyme (*Pdk4*) mRNAs involved in the respiratory burst. Further evidence of an ongoing inflammation process is provided by the relatively abundance of *Ptx3* mRNA, also expressed in macrophages in response to inflammatory cytokines (Deban *et al*., 2009). Although not in the top ranking, *Il-8, Cxcl16, Cxcl3*, and *Ccl4* mRNAs were more abundant in PCV2-SD affected pigs; such mRNAs code for chemoattractants and inflammatory chemokines. Their suspected role in PCV2-SD has already been described (Darwich *et al*., 2003b; Kim and Chae, 2004). On the other hand, GPNMB and CD163 are known to counteract an excessive inflammation (Philippidis *et al*., 2004; Ripoll *et al*., 2007), suggesting that the final outcome of the disease and lesional evolution will depend on a fine regulation of the inflammatory process.

Serum concentrations of several acute phase proteins (APPs) including haptoglobin (HPT), pig-MAP, C-reactive protein (CRP) and serum amyloid A (SAA) are shown to be increased in PCV2-SD affected pigs (Grau-Roma *et al*., 2009b; Wallgren *et al*., 2009; Parra *et al*., 2006; Segalés *et al*., 2004a). Moreover, pig-MAP and HPT responses are correlated to PCV2 viremia (Grau-Roma *et al*., 2009b). In the present study, some APPs encoding genes showed moderate mRNA levels in PCV2-SD affected pigs, which support existing results.

5.4.2. Innate immunity

Interferon-mediated antiviral effectors, such as OAS1, have been already identified as over-expressed in pigs subclinically infected with PCV2 on the first week post-inoculation in study II. Here, *Oas1* mRNA was of relative high abundance indicating that not all antiviral mechanisms of innate immunity are inhibited. In that line, MLNs from diseased pigs had still the potential to express NRAMP1 and to some extent TLR4 and TLR8, which are essentially involved in innate immunity against bacteria and viruses (Forbes and Gros, 2001; Schlaepfer *et al*., 2006; Takeda *et al*., 2003). However, *Slc15A2* was one of the less relative abundant mRNAs and its protein product also recognises pathogen-associated molecular patterns. Therefore, these findings do not entirely explain why opportunistic bacterial infections are commonly observed in PCV2-SD affected pigs (Segalés *et al*., 2004b). Other mechanisms have to be evoked.

An impaired phagocytosis can favour multiple infections and also tissue damage due to deposition of exceeding complement compounds (He *et al*., 2008). In favour of this hypothesis, it was observed that most MLNs with PCV2-SD lesions, even those with moderate lymphocyte depletion, had much lower levels of *Cr1* mRNA than their non-damaged counterparts. Indeed, CR1 is the cellular receptor for C3b and C4b and its lack of expression leads to increased severity of autoimmune and inflammatory diseases (Khera and Das, 2009). However, as indicated by the *Vsig4* mRNAs relative levels, MLNs from diseased pigs produced as much, if no more, Vsig4 (also called CRIg), than their healthy counterparts and independently of the degree of lymphocyte depletion and granulomatous infiltration. In mice and humans, CRIg expression is limited to resting macrophages in peripheral tissues and very low levels are detected in secondary lymphoid organs and inflamed tissues. It acts as a receptor for C3b, iC3b and C3c and is a potent inhibitor of the alternative complement pathway and T-cell responses (He *et al*., 2008). Although providing an alternative to the possible lack of CR1 for clearing C3b and immune complexes, the results obtained here are in clear contradiction with the tissue distribution of CRIg observed in other species (He *et al*., 2008). These discrepancies can be due to species differences in the regulation of the gene *VSIG4* or that PCV2 infection has triggered an alteration of the expression of *VSIG4*. The existence of a mechanism impeding de novo synthesised CRIg to reach the cell surface cannot be also excluded.

5.4.3. Immunosuppression

An impaired adaptive immunity could also explain immunosuppression observed in PCV2-SD affected pigs (Segalés and Mateu, 2006). Indeed, a maintained CRIg expression could impede lymph node residing T-cells to engage cellular activation (Vogt *et al*., 2006). Further evidence for a probable defective immune response was provided by the low mRNAs levels of *Cd79b, Cd19* and *Cd21*, which protein products form the antigen specific B-cell receptor and coreceptor (Erdei *et al*., 2009; Janeway *et al*., 2001). Furthermore, the transcription factor MybL1, which favours B-cell proliferation and primary B-cell antibody responses in germinal centres (Vora *et al*., 2001), was also negatively affected in damaged MLNs.

5.4.4. Apoptosis

It has been shown that the PCV2 ORF3 protein interacts with a porcine ubiquitin E3 ligase pPirh2 to facilitate p53 expression, resulting in apoptosis in vitro (Liu *et al*., 2007). An increase in expression of some p53 apoptotic pathway genes (*P8, NQO1, DRAM* and *ANXA1*) has been observed in PCV2-SD affected animals. This result would suggest a potential apoptotic phenomenon related with the pathogenesis of PCV2-SD related lesions by the p53 apoptotic pathway. In addition, some pro-apoptotic genes, such as *TNFSF10* (Miura *et al*., 2001) and cathepsin B (Chwieralski *et al*., 2006) showed increased expression in diseased pigs. However, the implication of apoptosis in PCV2-SD lymphoid lesion pathogenesis, measured by TUNEL and cleaved-caspase 3 immunohistochemistry, is considered controversial (Krakowka *et al*., 2004; Lin *et al*., 2011; Mandrioli *et al*., 2004; Resendes *et al*., 2004b; Shibahara *et al*., 2000).

5.5. Conclusions

At the light of the results presented here, some hypothesis can be taken into consideration to get new insights into the knowledge of PCV2-SD; however, they would need experimental confirmation. The pathogenesis of PCV2-SD might not be due to a single altered pathway but to the combination of several mechanisms leading to inflammation, lymphocyte depletion through complement deposition and immunosuppression. Moreover, complement receptors, which are also key molecules for the induction of an

adaptive immunity, would be involved in the pathogenesis of PCV2-SD. In that respect, activation of T-cells via the presence of VSIG4 would be compromised as it participates in the specific engagement of a primary B-cell response through its B-cell receptor. However, functional data at the protein level should be conducted to validate the hypotheses presented here.

Table S1. List of differentially expressed genes between PCV2-SD affected and healthy pigs in mediastinal lymph nodes.

Probe ID	Gene Symbol	Gene Name	Log2 FC	FDR
Ssc.26645.1.S1_at	-	annotation not clear	-3.52	0.0017
Ssc.25716.1.S1_at	CR1	complement component (3b/4b) receptor 1 (knops blood group)	-3.43	0.0001
Ssc.12584.1.A1_at	CD79B	cd79b antigen (immunoglobulin-associated beta)	-3.03	0.0006
Ssc.23408.1.A1_s_at	-	annotation not clear	-2.65	0.0015
Ssc.7771.1.A1_at	MYBL1	v-myb myeloblastosis viral oncogene homolog (avian)-like 1	-2.64	0.0004
Ssc.19400.2.A1_at	-	annotation not clear	-2.63	0.0027
Ssc.14471.1.S1_at	CD19	cd19 antigen	-2.51	0.0001
Ssc.22487.1.S1_at	ECRG4	esophageal cancer related gene 4 protein	-2.49	0.0058
Ssc.10498.1.A1_at	EAF2	ell associated factor 2	-2.22	0.0143
Ssc.15327.1.S1_at	CR2	complement component (3d/epstein barr virus) receptor 2	-2.19	0.0039
Ssc.30795.1.S1_at	SLC15A2	solute carrier family 15 (h+/peptide transporter), member 2	-2.15	0.0010
Ssc.20223.1.S1_at	SLC15A2	solute carrier family 15 (h+/peptide transporter), member 2	-2.13	0.0020
Ssc.24382.1.S1_at	TMEM163	hypothetical protein dkfzp566n034	-2.00	0.0001
Ssc.26573.1.S1_at	RALGPS2	ral gef with ph domain and sh3 binding motif 2	-1.94	0.0001
Ssc.17287.1.A1_at	C5orf13	Neuronal protein 3.1 (p311 protein).	-1.87	0.0012
Ssc.14025.1.A1_at	LEF1	lymphoid enhancer-binding factor 1	-1.86	0.0018
Ssc.21236.1.S1_at	RALGPS2	ral gef with ph domain and sh3 binding motif 2	-1.81	0.0002
Ssc.12505.1.A1_at	CLGN	calmegin	-1.81	0.0352
Ssc.4793.1.S1_at	-	annotation not clear	-1.79	0.0005
Ssc.7456.1.A1_at	SLC15A2	solute carrier family 15 (h+/peptide transporter), member 2	-1.77	0.0011
Ssc.2875.1.S1_at	-	annotation not clear	-1.74	0.0004
Ssc.7841.1.A1_at	IGFBPL1	insulin-like growth factor binding protein-like 1	-1.69	0.0013
Ssc.21263.1.S1_at	MEF2B	mads box transcription enhancer factor 2, polypeptide b (myocyte enhancer factor 2b)	-1.67	0.0010
Ssc.6165.1.A1_at	-	annotation not clear	-1.65	0.0009
Ssc.11056.2.S1_a_at	IGHD	immunoglobulin heavy constant delta	-1.57	0.0005
Ssc.17992.1.S1_s_at	-	annotation not clear	-1.57	0.0042
Ssc.11216.1.A1_at	FMR2	af4/fmr2 family, member 2	-1.56	0.0020
Ssc.17975.1.A1_at	BLK	b lymphoid tyrosine kinase	-1.55	0.0010
Ssc.6980.1.A1_at	BCL7A	b-cell cll/lymphoma 7a	-1.52	0.0031

Ssc.18625.1.S1_at	BCL11A	b-cell cll/lymphoma 11a (zinc finger protein)	-1.50	0.0006
Ssc.12209.1.A1_at	PDK1	pyruvate dehydrogenase kinase, isozyme 1	-1.50	0.0002
Ssc.24173.1.S1_at	-	annotation not clear	-1.48	0.0001
Ssc.15277.1.S1_at	LTB	lymphotoxin beta (tnf superfamily, member 3)	-1.48	0.0022
Ssc.25898.1.S1_at	HTRA4	htra serine peptidase 4	-1.48	0.0013
Ssc.2801.1.S1_at	RALGPS2	ral gef with ph domain and sh3 binding motif 2	-1.45	0.0001
Ssc.29855.1.A1_at	CDCA7	cell division cycle associated 7	-1.45	0.0088
Ssc.11601.1.A1_at	DAPL1	similar to death-associated protein	-1.44	0.0149
Ssc.24127.1.S1_a_at	RRM2B	ribonucleotide reductase m2 b (tp53 inducible)	-1.41	0.0040
Ssc.9784.1.S1_at	LAMC2	laminin, gamma 2	-1.40	0.0014
Ssc.6824.1.A1_at	-	annotation not clear	-1.39	0.0031
Ssc.26932.2.A1_at	HVCN1	hypothetical protein mgc15619	-1.38	0.0013
Ssc.26552.1.A1_at	ADAMTS17	adam metallopeptidase with thrombospondin type 1 motif, 17	-1.36	0.0002
Ssc.30637.1.A1_at	TRIM6-TRIM34	tripartite motif-containing 6 and tripartite motif-containing 34	-1.34	0.0009
Ssc.18894.1.S1_a_at	-	annotation not clear	-1.32	0.0009
Ssc.11201.1.A1_at	RASGRP1	ras guanyl releasing protein 1 (calcium and dag-regulated)	-1.31	0.0059
Ssc.17325.1.S1_at	CD24	Signal transducer CD24 precursor.	-1.31	0.0013
Ssc.19823.2.S1_at	ABLIM1	actin binding lim protein 1	-1.31	0.0059
Ssc.27102.1.A1_at	-	annotation not clear	-1.30	0.0004
Ssc.7698.1.S1_at	DAF	Complement decay-accelerating factor precursor (CD55 antigen).	-1.29	0.0025
Ssc.8725.1.A1_at	BCL11B	b-cell cll/lymphoma 11b (zinc finger protein)	-1.29	0.0171
Ssc.24015.1.S1_at	-	annotation not clear	-1.28	0.0001
Ssc.7785.1.S1_at	TMEM123	transmembrane protein 123	-1.28	0.0006
Ssc.2493.1.S1_at	RAB3IP	hypothetical protein flj22548 similar to gene trap pat 12	-1.27	0.0013
Ssc.30849.1.A1_at	ZNF318	zinc finger protein 318	-1.27	0.0007
Ssc.25862.1.S1_at	KLK7	kallikrein 7 (chymotryptic, stratum corneum)	-1.26	0.0168
Ssc.19823.3.S1_at	ABLIM1	actin binding lim protein 1	-1.26	0.0026
Ssc.13176.2.S1_at	CORO1B	coronin, actin binding protein, 1b	-1.25	0.0028
Ssc.17420.1.A1_at	SEP3	septin 3	-1.25	0.0023
Ssc.11721.1.A1_at	-	annotation not clear	-1.25	0.0039
Ssc.20917.1.S1_at	-	annotation not clear	-1.24	0.0028
Ssc.7538.1.S1_at	CDH1	cadherin 1, type 1, e-cadherin (epithelial)	-1.22	0.0166

Ssc.5538.1.S1_at	CA2	carbonic anhydrase ii	-1.21	0.0189
Ssc.4411.1.S1_at	-	annotation not clear	-1.20	0.0010
Ssc.19823.1.A1_at	ABLIM1	actin binding lim protein 1	-1.20	0.0079
Ssc.29645.1.A1_at	RRM2B	ribonucleotide reductase m2 b (tp53 inducible)	-1.19	0.0006
Ssc.13360.1.A1_at	AFF3	af4/fmr2 family, member 3	-1.19	0.0020
Ssc.4076.1.S1_at	BNIP2	bcl2/adenovirus e1b 19kda interacting protein 2	-1.19	0.0011
Ssc.936.1.S1_at	CNN2	calponin 2	-1.18	0.0013
Ssc.9560.2.S1_a_at	ABLIM1	actin binding lim protein 1	-1.18	0.0060
Ssc.26893.1.A1_at	HMCN1	hemicentin 1	-1.18	0.0457
Ssc.1843.1.S1_at	MYBL2	v-myb myeloblastosis viral oncogene homolog (avian)-like 2	-1.17	0.0097
Ssc.14375.1.A1_at	RRM2B	ribonucleotide reductase m2 b (tp53 inducible)	-1.16	0.0013
Ssc.9560.1.S1_at	ABLIM1	actin binding lim protein 1	-1.16	0.0155
Ssc.15382.1.S1_at	CNR2	cannabinoid receptor 2 (macrophage)	-1.15	0.0018
Ssc.271.1.A1_at	DAF	Complement decay-accelerating factor precursor (CD55 antigen).	-1.15	0.0033
Ssc.7867.1.S1_at	SMC6L1	SMC6 protein	-1.15	0.0005
Ssc.9212.1.A1_at	SWAP70	swap-70 protein	-1.15	0.0001
Ssc.10988.1.S1_at	ABLIM1	actin binding lim protein 1	-1.15	0.0088
Ssc.14031.1.S1_at	CD1B	cd1b antigen	-1.15	0.0002
Ssc.9063.1.A1_at	-	annotation not clear	-1.14	0.0078
Ssc.22565.1.A1_at	-	annotation not clear	-1.14	0.0128
Ssc.5467.1.A1_at	S1PR2	endothelial differentiation, sphingolipid g-protein-coupled receptor, 5	-1.13	0.0003
Ssc.10369.1.A1_at	-	annotation not clear	-1.12	0.0016
Ssc.27488.1.S1_at	CHD7	chromodomain helicase dna binding protein 7	-1.12	0.0002
Ssc.15727.1.A1_at	SC5DL	sterol-c5-desaturase (erg3 delta-5-desaturase homolog, fungal)-like	-1.12	0.0035
Ssc.26331.1.S1_at	CCR9	chemokine (c-c motif) receptor 9	-1.12	0.0077
Ssc.24232.1.S1_at	STATIP1	signal transducer and activator of transcription 3 interacting protein 1	-1.12	0.0045
Ssc.4430.1.S1_at	SHCBP1	shc sh2-domain binding protein 1	-1.12	0.0353
Ssc.13176.1.S1_at	CORO1B	coronin, actin binding protein, 1b	-1.11	0.0044
Ssc.19728.1.S1_at	TRAF5	TNF receptor associated factor 5.	-1.11	0.0008
Ssc.11289.1.A1_at	-	annotation not clear	-1.10	0.0013
Ssc.8385.1.A1_at	SQLE	squalene epoxidase	-1.10	0.0025
Ssc.24113.1.A1_at	-	annotation not clear	-1.10	0.0003
Ssc.18720.1.A1_at	-	annotation not clear	-1.10	0.0358

Ssc.21986.1.S1_at	ZNF238	zinc finger protein 238	-1.10	0.0001
Ssc.8288.1.A1_at	ZCCHC12	zinc finger, cchc domain containing 12	-1.10	0.0046
Ssc.24148.1.S1_at	SMC6L1	SMC6 protein	-1.09	0.0011
Ssc.28328.2.A1_at	RCAN3	down syndrome critical region gene 1-like 2	-1.09	0.0032
Ssc.11718.1.S1_at	ICOSLG	inducible t-cell co-stimulator ligand	-1.09	0.0010
Ssc.22495.1.S1_at	OACT2	o-acyltransferase (membrane bound) domain containing 2	-1.09	0.0124
Ssc.21711.1.A1_at	-	annotation not clear	-1.09	0.0035
Ssc.15335.1.S1_at	FAM65B	chromosome 6 open reading frame 32	-1.09	0.0024
Ssc.23513.1.S1_at	-	annotation not clear	-1.08	0.0026
Ssc.122.1.S1_at	DGKA	diacylglycerol kinase, alpha 80kda	-1.08	0.0026
Ssc.19928.1.S1_a_at	DUT	dutp pyrophosphatase	-1.08	0.0092
Ssc.19817.1.S1_at	TNFRSF7	tumor necrosis factor receptor superfamily, member 7	-1.08	0.0057
Ssc.27469.1.S1_at	-	annotation not clear	-1.08	0.0013
Ssc.21592.1.S1_at	TCRB	t cell receptor beta locus	-1.07	0.0010
Ssc.7413.1.A1_at	DNMT3B	dna (cytosine-5-)-methyltransferase 3 beta	-1.07	0.0040
Ssc.5407.2.S1_at	FAM134B	hypothetical protein flj20152	-1.07	0.0308
Ssc.272.1.S1_a_at	DAF	Complement decay-accelerating factor precursor (CD55 antigen).	-1.06	0.0006
Ssc.24795.1.A1_at	-	annotation not clear	-1.06	0.0023
Ssc.26098.1.S1_at	RLTPR	rgd, leucine-rich repeat, tropomodulin and proline-rich containing protein	-1.05	0.0027
Ssc.22309.1.S1_at	CAMK4	calcium/calmodulin-dependent protein kinase iv	-1.05	0.0256
Ssc.9238.1.A1_at	-	annotation not clear	-1.05	0.0046
Ssc.12009.1.A1_at	-	annotation not clear	-1.05	0.0049
Ssc.8406.1.S1_at	-	annotation not clear	-1.04	0.0013
Ssc.23221.1.S1_at	APON	Apolipoprotein F precursor (Apo-F).	-1.04	0.0131
Ssc.16976.2.S1_at	SREBF2	sterol regulatory element binding transcription factor 2	-1.04	0.0001
Ssc.7380.1.A1_at	TIMD4	t-cell immunoglobulin and mucin domain containing 4	-1.03	0.0063
Ssc.19664.2.S1_at	LBH	hypothetical protein dkfzp566j091	-1.03	0.0034
Ssc.19453.1.S1_at	SPIB	spi-b transcription factor (spi-1/pu.1 related)	-1.03	0.0068
Ssc.17988.1.S1_at	-	annotation not clear	-1.03	0.0009
Ssc.19583.1.A1_at	ABCA7	atp-binding cassette, sub-family a (abc1), member 7	-1.02	0.0051
Ssc.25908.1.S1_at	TRAF5	TNF receptor associated factor 5.	-1.02	0.0010
Ssc.5376.3.S1_at	CD3Z	cd3z antigen, zeta polypeptide (tit3 complex)	-1.02	0.0153
Ssc.18806.1.A1_at	-	annotation not clear	-1.02	0.0187

Ssc.16453.1.S1_at	-	annotation not clear	-1.02	0.0063
Ssc.19664.1.S1_at	LBH	hypothetical protein dkfzp566j091	-1.02	0.0021
Ssc.25064.1.S1_at	DYRK2	dual-specificity tyrosine-(y)-phosphorylation regulated kinase 2	-1.02	0.0101
Ssc.1535.1.S1_at	FAM113B	family with sequence similarity 113, member b	-1.01	0.0059
Ssc.13930.1.S1_at	ECOP	egfr-coamplified and overexpressed protein	-1.01	0.0011
Ssc.5376.1.A1_at	CD3Z	cd3z antigen, zeta polypeptide (tit3 complex)	-1.01	0.0101
Ssc.14525.1.S1_at	ZP3	zona pellucida glycoprotein 3	-1.01	0.0219
Ssc.6714.1.A1_at	IDI1	isopentenyl-diphosphate delta isomerase 1	-1.01	0.0040
Ssc.5001.2.A1_at	SNX29	similar to riken cdna 4933437k13	-1.01	0.0015
Ssc.14506.1.S1_at	TOPOII	topoisomerase (dna) ii alpha 170kda	-1.01	0.0285
Ssc.19691.1.S1_at	PLA2G7	phospholipase a2, group vii (platelet-activating factor acetylhydrolase, plasma)	1.00	0.0397
Ssc.31102.1.A1_at	SCIN	scinderin	1.00	0.0234
Ssc.2697.1.S1_at	-	annotation not clear	1.00	0.0334
Ssc.158.1.S1_at	TBXAS1	thromboxane a synthase 1 (platelet, cytochrome p450, family 5, subfamily a)	1.00	0.0405
Ssc.26253.1.S1_at	-	annotation not clear	1.01	0.0009
Ssc.12059.1.A1_at	DLG5	discs, large homolog 5 (drosophila)	1.01	0.0016
Ssc.22342.1.A1_s_at	-	annotation not clear	1.01	0.0015
Ssc.12344.1.S1_at	RHOJ	ras homolog gene family, member j	1.01	0.0203
Ssc.26879.2.S1_at	TNFSF12-TNFSF13	tumor necrosis factor (ligand) superfamily, member 12-member 13	1.01	0.0125
Ssc.1181.1.S1_at	CTSB	cathepsin b	1.01	0.0003
Ssc.9108.2.S1_at	WFDC1	wap four-disulfide core domain 1	1.01	0.0185
Ssc.5743.2.A1_at	HK3	hexokinase 3 (white cell)	1.02	0.0462
Ssc.3214.1.S1_at	-	annotation not clear	1.02	0.0032
Ssc.167.2.S1_a_at	FCGR3A	fc fragment of igg, low affinity iiia, receptor (cd16a)	1.02	0.0052
Ssc.22550.1.A1_at	JUN	v-jun sarcoma virus 17 oncogene homolog (avian)	1.02	0.0027
Ssc.8269.1.A1_at	RAPH1	ras association (ralgds/af-6) and pleckstrin homology domains 1	1.02	0.0029
Ssc.22010.1.A1_at	ALDH1L2	aldehyde dehydrogenase 1 family, member l2	1.02	0.0138
Ssc.888.1.A1_at	MIG-6	erbb receptor feedback inhibitor 1	1.02	0.0050
Ssc.7314.1.A1_at	PTGS2	prostaglandin-endoperoxide synthase 2 (prostaglandin g/h synthase and cyclooxygenase)	1.03	0.0318
Ssc.907.1.A1_at	P2RY5	purinergic receptor p2y, g-protein coupled, 5	1.03	0.0081
Ssc.23009.1.S1_at	ABCC9	atp-binding cassette, sub-family c (cftr/mrp), member 9	1.03	0.0170

Ssc.9637.1.S2_at	GLUL	glutamate-ammonia ligase (glutamine synthetase)	1.04	0.0041
Ssc.12911.1.A1_a_at	TSCOT	thymic stromal co-transporter [Homo sapiens].	1.04	0.0034
Ssc.11079.1.A1_at	RNASE4	ribonuclease, rnase a family, 4	1.04	0.0047
Ssc.14361.1.A1_at	OLFM1	olfactomedin 1	1.04	0.0088
Ssc.11437.1.A1_at	DDIT4L	dna-damage-inducible transcript 4-like	1.04	0.0395
Ssc.983.1.S1_at	C1R	complement component 1, r subcomponent	1.05	0.0002
Ssc.15484.1.S1_at	IL10RB	interleukin 10 receptor, beta	1.05	0.0071
Ssc.16932.1.S1_at	B3GNT3	udp-glcnac:betagal beta-1,3-n-acetylglucosaminyltransferase 3	1.05	0.0009
Ssc.16354.1.S1_at	NR1H3	nuclear receptor subfamily 1, group h, member 3	1.05	0.0008
Ssc.16882.1.A1_at	NFIL3	nuclear factor, interleukin 3 regulated	1.05	0.0053
Ssc.15722.1.S1_at	LRPAP1	low density lipoprotein receptor-related protein associated protein 1	1.05	0.0004
Ssc.24695.1.A1_at	CANP	cancer-associated nucleoprotein	1.05	0.0110
Ssc.19389.1.A1_at	NMES1	chromosome 15 open reading frame 48	1.06	0.0415
Ssc.30833.1.S1_at	CCL3L1	chemokine (c-c motif) ligand 3-like 1	1.06	0.0023
Ssc.16648.1.S1_at	TXNIP	thioredoxin interacting protein	1.06	0.0001
Ssc.1191.1.S1_at	ANXA8	similar to annexin a8 (annexin viii) (vascular anticoagulant-beta) (vac-beta)	1.06	0.0386
Ssc.11457.1.A1_at	PPT1	palmitoyl-protein thioesterase 1 (ceroid-lipofuscinosis, neuronal 1, infantile)	1.07	0.0014
Ssc.26328.1.S1_at	CCR5	chemokine (c-c motif) receptor 5	1.07	0.0265
Ssc.6676.1.S1_at	-	annotation not clear	1.07	0.0471
Ssc.26957.1.S1_at	SLC1A3	solute carrier family 1 (glial high affinity glutamate transporter), member 3	1.07	0.0208
Ssc.14129.1.A1_at	ABAT	4-aminobutyrate aminotransferase	1.07	0.0392
Ssc.26005.1.S1_at	-	annotation not clear	1.07	0.0493
Ssc.16573.1.S1_at	-	annotation not clear	1.08	0.0119
Ssc.9461.1.A1_at	-	annotation not clear	1.08	0.0064
Ssc.23797.1.S1_at	CCL4	chemokine (c-c motif) ligand 4, MIP1b	1.08	0.0038
Ssc.31104.1.A1_at	FKBP5	fk506 binding protein 5	1.08	0.0007
Ssc.19364.1.S1_at	C2	complement component 2	1.08	0.0068
Ssc.21998.2.S1_at	MCF2L	mcf.2 cell line derived transforming sequence-like	1.09	0.0016
Ssc.12616.1.A1_at	CYP1B1	cytochrome p450, family 1, subfamily b, polypeptide 1	1.09	0.0077
Ssc.12446.1.A1_at	CASP4	caspase 4, apoptosis-related cysteine peptidase	1.09	0.0103
Ssc.30512.1.A1_at	-	annotation not clear	1.09	0.0285
Ssc.16664.1.A1_at	KLF9	kruppel-like factor 9	1.09	0.0117
Ssc.16451.1.A1_at	ADAMTS2	adam metallopeptidase with thrombospondin type 1 motif, 2	1.09	0.0022

Ssc.15638.1.A1_at	AMPD3	adenosine monophosphate deaminase (isoform e)	1.09	0.0120
Ssc.6169.2.S1_at	ECM1	Extracellular matrix protein 1 precursor (Secretory component p85).	1.10	0.0064
Ssc.2502.1.S1_at	PTGIS	prostaglandin i2 (prostacyclin) synthase	1.10	0.0159
Ssc.13556.1.A1_at	CCDC128	smooth muscle myosin heavy chain 11 isoform sm1-like	1.10	0.0010
Ssc.15973.1.S1_at	CD39	ectonucleoside triphosphate diphosphohydrolase 1	1.11	0.0068
Ssc.1142.1.S1_at	NQO1	nad(p)h dehydrogenase, quinone 1	1.11	0.0061
Ssc.3214.2.S1_at	RNASET2	ribonuclease t2	1.11	0.0301
Ssc.20009.1.S1_at	EPS8	epidermal growth factor receptor pathway substrate 8	1.11	0.0078
Ssc.27474.1.S1_at	CFP	complement factor properdin	1.11	0.0094
Ssc.4217.1.S1_at	ITIH4	inter-alpha (globulin) inhibitor h4 (plasma kallikrein-sensitive glycoprotein)	1.12	0.0252
Ssc.15224.1.S1_at	FOSL2	Fos-related antigen 2.	1.12	0.0026
Ssc.15224.2.S1_at	FOSL2	Fos-related antigen 2.	1.12	0.0058
Ssc.2571.1.S1_at	PLD3	phospholipase d family, member 3	1.12	0.0083
Ssc.26819.1.A1_at	FGD4	fyve, rhogef and ph domain containing 4	1.13	0.0064
Ssc.9679.2.S1_at	LIPA	Lysosomal acid lipase/cholesteryl ester hydrolase precursor (EC 3.1.1.13) (LAL)	1.13	0.0000
Ssc.18948.1.S1_at	SAA1	serum amyloid a1	1.13	0.0017
Ssc.29841.1.A1_at	-	annotation not clear	1.14	0.0024
Ssc.17224.1.S1_at	TLR8	toll-like receptor 8	1.14	0.0130
Ssc.6583.1.S1_at	CXCL16	chemokine (c-x-c motif) ligand 16	1.15	0.0033
Ssc.22050.1.S1_s_at	FGL2	Fibroleukin precursor (Fibrinogen-like protein 2) (pT49).	1.15	0.0098
Ssc.8436.1.S1_at	-	annotation not clear	1.15	0.0123
Ssc.10449.1.S1_at	-	annotation not clear	1.16	0.0026
Ssc.5822.1.S1_at	ALOX5AP	arachidonate 5-lipoxygenase-activating protein	1.16	0.0097
Ssc.9679.1.A1_at	LIPA	lipase a, lysosomal acid, cholesterol esterase (wolman disease)	1.16	0.0001
Ssc.15950.1.S1_at	C5R1	complement component 5a receptor 1	1.16	0.0071
Ssc.1986.1.S1_at	PTGS1	prostaglandin-endoperoxide synthase 1 (prostaglandin g/h synthase and cyclooxygenase)	1.16	0.0016
Ssc.18955.2.A1_at	-	annotation not clear	1.16	0.0017
Ssc.20883.1.S1_at	SELENBP1	selenium binding protein 1	1.16	0.0070
Ssc.12829.1.A1_at	TNFSF10	tumor necrosis factor (ligand) superfamily, member 10	1.16	0.0041
Ssc.6785.1.S1_at	LRP1	low density lipoprotein-related protein 1 (alpha-2-macroglobulin receptor)	1.17	0.0123
Ssc.19596.2.S1_at	AYTL1	acyltransferase like 1	1.17	0.0169
Ssc.22033.1.S1_at	ACP2	acid phosphatase 2, lysosomal	1.18	0.0004

Ssc.1377.2.S1_at	ITGA8	integrin, alpha 8	1.18	0.0101
Ssc.8212.1.A1_at	-	annotation not clear	1.18	0.0105
Ssc.26060.1.A1_at	MAFB	v-maf musculoaponeurotic fibrosarcoma oncogene homolog b (avian)	1.19	0.0040
Ssc.16380.1.A1_at	-	annotation not clear	1.19	0.0036
Ssc.2474.1.S1_at	HIST1H2BE	histone 1, h2bd	1.19	0.0098
Ssc.8604.1.A1_at	SNX24	sorting nexing 24	1.19	0.0115
Ssc.314.1.S1_at	ADM	adrenomedullin	1.20	0.0020
Ssc.3037.1.S1_at	SCPEP1	serine carboxypeptidase 1	1.20	0.0170
Ssc.18261.1.S1_at	PSTPIP2	proline-serine-threonine phosphatase interacting protein 2	1.21	0.0140
Ssc.508.1.S1_at	FCER1G	fc fragment of ige, high affinity i, receptor for; gamma polypeptide	1.21	0.0020
Ssc.2746.1.A1_at	CDS1	cdp-diacylglycerol synthase (phosphatidate cytidylyltransferase) 1	1.21	0.0068
Ssc.12781.1.A1_s_at	TLR4	Toll-like receptor 4 precursor (hToll).	1.22	0.0061
Ssc.20974.1.A2_at	GNS	N-acetylglucosamine-6-sulfatase precursor (EC 3.1.6.14) (G6S)	1.22	0.0007
Ssc.29177.1.A1_at	TMEM26	transmembrane protein 26	1.22	0.0276
Ssc.26608.1.A1_at	-	annotation not clear	1.23	0.0120
Ssc.21343.1.S1_at	LTR	34 kDa protein	1.23	0.0431
Ssc.13187.1.A1_at	CTTNBP2NL	cttnbp2 n-terminal like	1.23	0.0002
Ssc.14368.1.A1_at	MMRN1	multimerin 1	1.24	0.0445
Ssc.26291.1.S1_at	-	annotation not clear	1.24	0.0074
Ssc.18610.1.A1_at	-	annotation not clear	1.26	0.0005
Ssc.5708.1.A1_at	PLSCR4	phospholipid scramblase 4	1.26	0.0020
Ssc.9075.1.A1_at	JUN	v-jun sarcoma virus 17 oncogene homolog (avian)	1.27	0.0003
Ssc.8585.1.A1_at	PLSCR4	phospholipid scramblase 4	1.27	0.0038
Ssc.16012.1.S1_at	CASP1	caspase 1, apoptosis-related cysteine peptidase (interleukin 1, beta, convertase)	1.27	0.0321
Ssc.16769.1.S1_at	CTSZ	cathepsin z	1.28	0.0011
Ssc.11170.1.S1_at	PDXK	pyridoxal (pyridoxine, vitamin b6) kinase	1.28	0.0029
Ssc.27201.1.S1_a_at	CCRL2	chemokine (c-c motif) receptor-like 2	1.29	0.0128
Ssc.31140.1.S1_at	IFIT3	interferon-induced protein with tetratricopeptide repeats 3	1.29	0.0344
SscAffx.9.1.S1_at	FGL2	Fibroleukin precursor (Fibrinogen-like protein 2) (pT49).	1.31	0.0032
Ssc.29679.1.A1_at	-	annotation not clear	1.32	0.0069
Ssc.17861.1.A1_at	-	annotation not clear	1.32	0.0393
Ssc.23305.1.S1_at	TMEM144	hypothetical protein flj11155	1.32	0.0073
Ssc.23505.1.S1_at	MAOA	monoamine oxidase a	1.33	0.0088

Ssc.10453.1.S1_at	CP	ceruloplasmin (ferroxidase)	1.33	0.0372
Ssc.19596.1.A1_at	AYTL1	acyltransferase like 1	1.33	0.0041
Ssc.3219.1.S1_at	LRP1	low density lipoprotein-related protein 1 (alpha-2-macroglobulin receptor)	1.33	0.0042
Ssc.7331.1.S1_at	-	annotation not clear	1.33	0.0081
Ssc.6566.1.A1_at	AXL	axl receptor tyrosine kinase	1.34	0.0018
Ssc.25844.1.S1_at	-	annotation not clear	1.34	0.0194
Ssc.10965.2.S1_at	MAFB	v-maf musculoaponeurotic fibrosarcoma oncogene homolog b (avian)	1.34	0.0002
Ssc.5955.1.A1_at	IL10RB	interleukin 10 receptor, beta	1.34	0.0014
Ssc.8909.1.A1_at	INHBB	inhibin, beta b (activin ab beta polypeptide)	1.35	0.0027
Ssc.8868.1.S1_at	FCGR2C	fc fragment of igg, low affinity iic, receptor for (cd32)	1.36	0.0250
Ssc.24411.3.S1_a_at	-	annotation not clear	1.36	0.0056
Ssc.14559.1.S1_at	ANXA1	annexin a1	1.36	0.0032
Ssc.12579.1.A1_s_at	FGL2	Fibroleukin precursor (Fibrinogen-like protein 2) (pT49).	1.36	0.0020
Ssc.670.2.S1_at	LYZ	lysozyme (renal amyloidosis)	1.36	0.0030
Ssc.18802.1.A1_at	STX11	syntaxin 11	1.37	0.0013
Ssc.6169.1.S1_at	ECM1	Extracellular matrix protein 1 precursor (Secretory component p85).	1.37	0.0078
Ssc.4081.1.A1_at	FAM13A1	family with sequence similarity 13, member a1	1.37	0.0003
Ssc.17343.1.S1_at	XLKD1	lymphatic vessel endothelial hyaluronan receptor 1;	1.39	0.0035
Ssc.1027.1.S1_at	ASAH1	n-acylsphingosine amidohydrolase (acid ceramidase) 1	1.39	0.0013
Ssc.19703.1.S1_s_at	TLR4	Toll-like receptor 4 precursor (hToll).	1.39	0.0046
Ssc.30532.1.A1_at	-	annotation not clear	1.39	0.0393
Ssc.29841.1.A1_s_at	-	annotation not clear	1.39	0.0025
Ssc.6797.1.S1_at	STXBP1	syntaxin binding protein 1	1.41	0.0025
Ssc.15332.1.S1_at	FAM46A	family with sequence similarity 46, member a	1.41	0.0009
Ssc.11528.1.A1_at	bcsc1	loss of heterozygosity, 11, chromosomal region 2, gene a	1.42	0.0058
Ssc.24337.1.S1_at	HGF	hepatocyte growth factor (hepapoietin a; scatter factor)	1.42	0.0001
Ssc.9229.1.S1_at	MRC1	mannose receptor, c type 1	1.43	0.0204
Ssc.670.1.S1_at	LYZ	lysozyme (renal amyloidosis)	1.43	0.0109
Ssc.10965.1.A1_at	MAFB	v-maf musculoaponeurotic fibrosarcoma oncogene homolog b (avian)	1.43	0.0003
Ssc.16057.2.S1_a_at	CAPN3	calpain 3, (p94)	1.43	0.0064
Ssc.16981.1.S1_at	ITIH3	inter-alpha (globulin) inhibitor h3	1.44	0.0077
Ssc.4978.1.S1_at	CD14	cd14 antigen	1.45	0.0088
Ssc.8956.2.A1_at	PLZF	zinc finger and btb domain containing 16	1.45	0.0402

Ssc.9726.1.A1_at	DRAM	hypothetical protein flj11259	1.45	0.0010
Ssc.8261.1.A1_at	-	annotation not clear	1.45	0.0405
Ssc.11257.1.S1_at	TIMP2	timp metallopeptidase inhibitor 2	1.46	0.0016
Ssc.9329.1.A1_at	-	annotation not clear	1.46	0.0075
Ssc.810.1.S1_at	SCARB2	scavenger receptor class b, member 2	1.47	0.0008
Ssc.26599.1.A1_at	GAB2	grb2-associated binding protein 2	1.47	0.0001
Ssc.8808.1.A1_at	PTPLAD2	protein tyrosine phosphatase-like a domain containing 2	1.47	0.0123
Ssc.15640.1.S1_at	MT2A	metallothionein 2a	1.48	0.0075
Ssc.3271.1.A1_at	ABCA1	atp-binding cassette, sub-family a (abc1), member 1	1.48	0.0000
Ssc.4679.1.S1_at	ANG1	angiogenin, ribonuclease, rnase a family, 5	1.49	0.0024
Ssc.1137.1.S1_at	-	annotation not clear	1.49	0.0017
Ssc.4779.1.A1_at	CPM	carboxypeptidase m	1.49	0.0026
Ssc.140.1.S1_at	AMBN	ameloblastin, enamel matrix protein	1.49	0.0020
Ssc.3139.1.A1_at	RGS2	regulator of g-protein signalling 2, 24kda	1.49	0.0000
Ssc.13053.1.A1_at	CASP4	caspase 4, apoptosis-related cysteine peptidase	1.50	0.0024
Ssc.3016.1.S1_at	EMILIN2	elastin microfibril interfacer 2	1.50	0.0022
Ssc.12781.1.A2_at	TLR4	Toll-like receptor 4 precursor (hToll).	1.50	0.0013
Ssc.6709.1.S1_at	LGMN	legumain	1.50	0.0023
Ssc.1588.1.S1_at	NAGK	n-acetylglucosamine kinase	1.51	0.0005
Ssc.7146.1.A1_at	ABCA1	atp-binding cassette, sub-family a (abc1), member 1	1.52	0.0000
Ssc.31189.1.S1_at	CHPT1	choline phosphotransferase 1	1.52	0.0028
Ssc.3706.1.S1_at	SOD2	superoxide dismutase 2, mitochondrial	1.52	0.0045
Ssc.19694.1.S1_at	GPX3	glutathione peroxidase 3 (plasma)	1.52	0.0301
Ssc.16008.1.S1_at	FCNB	ficolin (collagen/fibrinogen domain containing) 1	1.53	0.0203
Ssc.20974.1.A1_at	GNS	N-acetylglucosamine-6-sulfatase precursor (EC 3.1.6.14) (G6S)	1.53	0.0003
Ssc.5743.1.S1_a_at	HK3	hexokinase 3 (white cell)	1.53	0.0158
Ssc.11439.1.A1_at	TMEM26	transmembrane protein 26	1.53	0.0033
Ssc.7158.1.A1_a_at	CAPNS1	calpain, small subunit 1	1.54	0.0214
Ssc.19059.1.A1_at	AGTR1	angiotensin ii receptor, type 1	1.54	0.0018
Ssc.13241.1.A1_at	-	annotation not clear	1.55	0.0299
Ssc.17042.1.A1_at	SOD2	superoxide dismutase 2, mitochondrial	1.55	0.0008
Ssc.9738.1.A1_at	CEBPB	ccaat/enhancer binding protein (c/ebp), beta	1.55	0.0008
Ssc.11779.1.S1_at	FBP	folate receptor 1 (adult)	1.56	0.0014

Ssc.11746.1.A1_at	MSTP150	mstp150	1.56	0.0000
Ssc.5022.1.A1_at	NNMT	nicotinamide n-methyltransferase	1.57	0.0240
Ssc.18359.1.S1_at	CCR1	chemokine (c-c motif) receptor 1	1.57	0.0032
Ssc.5047.1.A1_at	XLKD1	extracellular link domain containing 1; lymphatic vessel endothelial hyaluronan receptor 1;	1.58	0.0006
Ssc.11145.1.A1_at	CD5L	cd5 antigen-like (scavenger receptor cysteine rich family)	1.60	0.0027
Ssc.3706.1.S2_at	SOD2	superoxide dismutase 2, mitochondrial	1.64	0.0010
Ssc.11194.1.S1_at	PLAU	plasminogen activator, urokinase	1.64	0.0003
Ssc.10025.1.S1_at	CEBPD	ccaat/enhancer binding protein (c/ebp), delta	1.67	0.0006
Ssc.12781.1.A1_at	TLR4	Toll-like receptor 4 precursor (hToll).	1.69	0.0019
Ssc.4871.1.S1_at	CXCL3	chemokine (c-x-c motif) ligand 3	1.70	0.0087
Ssc.26345.1.S1_at	F13A1	coagulation factor xiii, a1 polypeptide	1.73	0.0163
Ssc.14028.1.S1_at	AOAH	acyloxyacyl hydrolase (neutrophil)	1.75	0.0026
Ssc.29905.1.A1_at	-	annotation not clear	1.76	0.0002
Ssc.83.1.S1_at	ANPEP	alanyl (membrane) aminopeptidase (aminopeptidase n, microsomal aminopeptidase, cd13, p150)	1.77	0.0013
Ssc.12972.1.S1_at	ASAH1	n-acylsphingosine amidohydrolase (acid ceramidase) 1	1.77	0.0156
Ssc.11145.2.S1_at	CD5L	cd5 antigen-like (scavenger receptor cysteine rich family)	1.79	0.0027
Ssc.658.1.S1_at	IL8	interleukin 8	1.82	0.0363
Ssc.7864.1.A1_at	IL1RAP	interleukin 1 receptor accessory protein	1.82	0.0014
Ssc.12825.1.A1_at	-	annotation not clear	1.86	0.0007
Ssc.10025.3.S1_at	CEBPD	ccaat/enhancer binding protein (c/ebp), delta	1.93	0.0002
Ssc.21663.1.A1_at	LIPG	lipase, endothelial	1.94	0.0025
Ssc.1031.1.S1_at	OAS1	2',5'-oligoadenylate synthetase 1, 40/46kda	1.96	0.0303
Ssc.16640.3.S1_at	VSIG4	V-set and immunoglobulin domain containing 4;	1.97	0.0009
Ssc.16981.2.S1_at	ITIH3	inter-alpha (globulin) inhibitor h3	2.00	0.0020
Ssc.709.1.S1_at	GLRX	glutaredoxin (thioltransferase)	2.03	0.0014
Ssc.1126.1.A1_at	SMPDL3A	sphingomyelin phosphodiesterase, acid-like 3a	2.04	0.0018
Ssc.9114.1.S1_at	STEAP4	steap family member 4	2.05	0.0011
Ssc.30334.1.A1_at	CYP3A4	cytochrome p450, subfamily iiia (niphedipine oxidase), polypeptide 3	2.10	0.0083
Ssc.300.1.S1_at	NRAMP1	solute carrier family 11 (proton-coupled divalent metal ion transporters), member 1	2.11	0.0025
Ssc.30077.1.A1_at	-	annotation not clear	2.15	0.0148
Ssc.1206.1.A1_at	GLRX1	ADAMTS-19 precursor (EC 3.4.24.-)	2.16	0.0002

Ssc.8162.1.S1_at	PTX3	pentraxin-related gene, rapidly induced by il-1 beta	2.20	0.0054
Ssc.26326.1.S1_at	CYP3A43	cytochrome p450, family 3, subfamily a, polypeptide 43	2.25	0.0088
Ssc.16640.1.A1_at	VSIG4	V-set and immunoglobulin domain containing 4;	2.42	0.0001
Ssc.18572.2.S1_at	GPNMB	glycoprotein (transmembrane) nmb	2.46	0.0001
Ssc.10131.1.A1_at	PDK4	pyruvate dehydrogenase kinase, isozyme 4	2.49	0.0194
Ssc.1121.1.S1_at	PDK4	pyruvate dehydrogenase kinase, isozyme 4	2.53	0.0105
Ssc.5053.1.S1_at	CD163	cd163 antigen	2.58	0.0006
Ssc.17815.1.S1_at	LGALS3	lectin, galactoside-binding, soluble, 3 (galectin 3)	2.73	0.0032
Ssc.11991.1.A1_at	-	annotation not clear	2.74	0.0004
Ssc.5104.1.S1_at	P8	p8 protein (candidate of metastasis 1)	2.79	0.0007
Ssc.18572.1.S1_at	GPNMB	glycoprotein (transmembrane) nmb	3.10	0.0003
Ssc.16639.3.S1_at	GPNMB	glycoprotein (transmembrane) nmb	3.12	0.0016
Ssc.204.1.S1_at	CYP3A29	Cytochrome P450 3A4	3.27	0.0026

Log2 FC: Log Fold change, FDR: False discovery rate.

Table S2. Biological processes associated with differentially expressed transcripts.

Biological process	*P* value	Number of genes	
		Increased mRNA abundance	Decreased mRNA abundance
response to wounding	7.40E-21	36	4
response to external stimulus	1.61E-19	41	5
inflammatory response	1.96E-15	26	3
response to stress	3.40E-14	42	9
response to stimulus	6.27E-14	68	24
defense response	2.21E-13	30	6
immune system process	3.03E-11	33	15
immune response	8.53E-10	27	13
response to chemical stimulus	3.03E-08	26	3
acute inflammatory response	9.17E-08	8	3
behavior	1.97E-07	15	5
positive regulation of biological process	2.34E-07	26	13
immune effector process	5.46E-07	7	5
immunoglobulin mediated immune response	8.02E-07	4	5
B cell mediated immunity	1.07E-06	4	5
taxis	1.29E-06	12	1
chemotaxis	1.29E-06	12	1
adaptive immune response based on somatic recombination of immune receptors built from immunoglobulin superfamily domains	1.78E-06	5	5
adaptive immune response	1.78E-06	5	5
biological regulation	3.50E-06	73	34
locomotory behavior	4.60E-06	12	2
lymphocyte mediated immunity	9.13E-06	4	5
regulation of body fluid levels	9.24E-06	10	1
blood coagulation	1.05E-05	9	1
coagulation	1.24E-05	9	1
hemostasis	1.57E-05	9	1
leukocyte mediated immunity	1.63E-05	4	5
positive regulation of immune response	2.34E-05	5	4
positive regulation of immune system process	2.55E-05	5	4
lipid metabolic process	2.75E-05	23	4
developmental process	4.27E-05	50	22
regulation of biological quality	4.49E-05	25	4
activation of immune response	4.62E-05	4	4
cytokine production	5.27E-05	9	1
positive regulation of cellular process	6.31E-05	23	8
regulation of immune response	7.68E-05	5	4
wound healing	8.68E-05	9	1
regulation of immune system process	8.85E-05	5	4
innate immune response	1.02E-04	6	3
activation of plasma proteins during acute inflammatory response	1.21E-04	3	3
complement activation	1.21E-04	3	3
positive regulation of multicellular organismal process	1.33E-04	5	4
regulation of apoptosis	2.19E-04	14	6
regulation of programmed cell death	2.52E-04	14	6
death	2.90E-04	19	7
cell death	2.90E-04	19	7

prostaglandin biosynthetic process	3.06E-04	4	0
prostanoid biosynthetic process	3.06E-04	4	0
elevation of cytosolic calcium ion concentration	3.82E-04	5	2
cytosolic calcium ion homeostasis	3.82E-04	5	2
complement activation, classical pathway	5.18E-04	2	3
lipid biosynthetic process	5.84E-04	10	3
humoral immune response mediated by circulating immunoglobulin	6.85E-04	2	3
apoptosis	6.89E-04	17	7
programmed cell death	7.78E-04	17	7
icosanoid biosynthetic process	7.82E-04	5	0
cellular cation homeostasis	1.06E-03	8	2
cation homeostasis	1.10E-03	8	2
negative regulation of biological process	1.14E-03	25	6
negative regulation of cellular process	1.22E-03	24	6
cellular lipid metabolic process	1.32E-03	16	4
regulation of biological process	1.41E-03	58	31
phagocytosis	1.57E-03	4	1
prostaglandin metabolic process	1.61E-03	4	0
prostanoid metabolic process	1.61E-03	4	0
cell differentiation	1.72E-03	32	10
cellular developmental process	1.72E-03	32	10
regulation of cell proliferation	1.89E-03	13	4
membrane invagination	1.91E-03	9	1
endocytosis	1.91E-03	9	1
cellular di-, tri-valent inorganic cation homeostasis	1.93E-03	7	2
di-, tri-valent inorganic cation homeostasis	2.00E-03	7	2
response to other organism	2.19E-03	10	0
regulation of multicellular organismal process	2.87E-03	6	6
icosanoid metabolic process	3.06E-03	5	0
membrane organization and biogenesis	3.12E-03	11	1
cellular chemical homeostasis	3.33E-03	8	2
cellular ion homeostasis	3.33E-03	8	2
positive regulation of biosynthetic process	3.42E-03	4	2
positive regulation of secretion	3.47E-03	4	0
humoral immune response	3.63E-03	3	3
leukocyte chemotaxis	3.95E-03	4	0
cytokine biosynthetic process	4.08E-03	5	1
cytokine metabolic process	4.32E-03	5	1
proteolysis	4.83E-03	16	6
cell development	4.89E-03	22	8
multi-organism process	5.71E-03	12	0
ion homeostasis	6.30E-03	8	2
calcium ion homeostasis	7.27E-03	5	2
cellular calcium ion homeostasis	7.27E-03	5	2
negative regulation of cell proliferation	7.36E-03	10	0
multicellular organismal process	7.47E-03	49	21
regulation of inflammatory response	7.65E-03	4	0
regulation of defense response	7.65E-03	4	0
regulation of biosynthetic process	9.04E-03	7	2

CHAPTER 6

GENERAL DISCUSSION

Due to the multifactorial basis of PCV2-SD, a more global understanding about the mechanisms involved in the host-PCV2 interaction has not yet been achieved, despite the traditional approaches used to study the pathogenesis of PCV2 infection over the last two decades. At the beginning of this Thesis, a number of works had been published using the microarray technology for gene expression profiling to explore the effects of bacterial (Hammamieh *et al*., 2004; Niewold *et al*., 2005) and viral (Afonso *et al*., 2004; Lee *et al*., 2004; Miller *et al*., 2004; Moser *et al*., 2004) infections on swine immune responses. However, at that moment, the porcine transcriptome analysis using this methodology was in the early stages of development. These published works, although provided helpful insights into the molecular basis of the pig response to pathogens, were performed based on in-house made cDNA arrays constructed using a relatively low number of cDNAs or ESTs obtained from swine specific cell-types or tissues, or based on cross-species hybridizations with human cDNA arrays. On the other hand, the analysis of the PCV2 infection from a transcriptional point of view was reported by few studies that aimed at characterizing the mRNA levels of some cytokines in lymphoid organs and PBMCs of pigs naturally affected by PCV2-SD using qPCR techniques (Darwich *et al*., 2003b; Sipos *et al*., 2004). Hence, this Thesis focused on the evaluation of the Affymetrix Porcine Genechip® platform usefulness to study the host transcriptional response against PCV2 infection and the applicability of this technology to gain a more comprehensive picture of the PCV2 infection pathogenesis. This work described, for the first time, changes in the global transcriptome of subclinically PCV2 infected pigs and also of animals naturally affected by PCV2-SD.

The first experiment (study I) provided evidence that the Affymetrix Porcine Genechip® is a reliable and sensitive resource to study the interactions between PCV2 and its host. There are important practical issues associated with the choice of a platform for a large-scale gene expression study. The *in-situ* synthesized technology is considered to be an improvement over cDNA arrays or spotted long oligonucleotide platforms, since chips are synthesized *in silico* based on sequence information alone, without the need for physical intermediates such as clones, PCR products or cDNAs. Such approach further eliminates problems related to clone misidentification and avoid incorrect spot placements occurrence (Jarvinen *et al*., 2004). This latter work indicates that the wide coverage of the swine transcriptome and high reproducibility were other advantages of the technology, since it allowed accurate detection and comparison of changes in gene

expression of RNA samples from complex organs under different experimental conditions. Indeed, among the three studies of this Thesis, four tissues were analyzed (mesenteric and mediastinal lymph nodes, lung and whole blood), all of them composed by a diversity of cell types. Besides, considering the histopathological features of PCV2 infection, while subclinically infected pigs (studies I and II) presented only mild lymphoid lesions characterized by slight lymphocyte depletion with histiocytic infiltration, marked changes on these cell populations occurred in lymphoid tissues from PCV2-SD affected animals (study III).

During the course of the present Thesis, five gene expression microarray studies, three of them using the Affymetrix platform, were carried out to profile the transcriptional response against PCV2 infection both *in vivo* (Ramírez-Boo *et al*., 2009; Lee *et al*., 2010; Andersson *et al*., 2011) and *in vitro* (Li *et al*., 2013; Mavrommatis *et al*., 2014). The results from these works were mostly in accordance with the observations made in this Thesis, confirming the good reproducibility of this technology. Furthermore, some of the DE genes were shared between them; a finding that not only suggests a disruption in common pathways but also supports the notion that connections between datasets are possible (Tsai *et al*., 2006b; Badaoui *et al*., 2013). Differences in the number of DE genes between these works and studies from the present Thesis could be due to several factors, including the age and origin of animals, tissue samples and cell types, microarray platform, experimental design or data analysis. Additionally, results obtained from the cluster analysis in study III indicate that the microarray technique would be able to discriminate stages of infection within natural cases of PCV2-SD. This aspect deserves further studies with controlled experiments reproducing the disease and relating the chronology of lymphoid lesions with the transcriptome of the lymphoid tissues.

The lack of an appropriate probe annotation on the array was a limitation detected in this Thesis. The need to re-annotate a list of DE transcripts using the BLAST database in a gene-per-gene basis, or even with related programs such as the Blast2GO (Conesa *et al*., 2005) or ANEXdb (Couture *et al*., 2009) was time-consuming. Furthermore, the interpretation of the results could be affected, as probes lacking annotation were not included on the subsequent analyses, such as gene ontology and pathway analysis. Thus, the present Thesis highlights the relevance to improve the annotation of the chip, which

would increase the amount of biological information that can be derived from the Porcine Genechip datasets and enhance its usefulness for swine genomic studies.

In the first part of this Thesis, the molecular events taking place in response to a subclinical PCV2 infection were investigated, initially with a single time-point experiment (study I) and, subsequently, these earlier efforts were expanded with an improved time course study (study II). However, PCV2-SD could not be reproduced in any of the abovementioned experimental inoculations, reinforcing the notion that disease reproduction by using PCV2 alone is difficult and the achievement of a reproducible model of PCV2-SD under experimental conditions remains a crucial challenge to this field of research (Tomás *et al*., 2008). For this reason, pigs naturally affected by PCV2-SD were chosen for the third study, which represents, so far, the only attempt to profile the global transcriptional changes in natural cases of the disease.

The balance between the host immune system reacting to the presence of the PCV2 and the ability of the virus to interfere with the immune response development seems critical to determine if the infectious process may remain subclinical or may progress towards PCV2-SD. Some of the potential mechanisms underlying this concept were investigated in the present Thesis.

The innate immunity represents the first defense against infecting pathogens. Cellular recognition of viral products by pattern recognition receptors (PRRs) induces the activation of multiple intracellular signaling pathways, which ultimately leads to transcription of several genes encoding proteins, including IFNs and pro-inflammatory cytokines that restrict viral replication and stimulates the initiation of adaptive responses. IFNs exert antiviral function by binding to their receptors on the cell surface, and thereby activating, among others, the JAK (Janus kinase)-STAT (signal transducer and activator of transcription) signaling cascade. The outcome of the pathway activation is the establishment of an antiviral state characterized by the expression of a wide array of ISGs (Takaoka and Yanai, 2006). An increased expression of ISGs was demonstrated in all three studies of the present Thesis. Specifically, in study II, a relative high over-expression of 12 ISGs was detected between MLN and blood from PCV2-inoculated pigs during the first week of infection. To corroborate this result, a transient detection of IFN-α in serum of PCV2-inoculated pigs was observed at day 5 p.i (Fort *et al*., 2009a). These

findings suggest that interferon-mediated antiviral effectors participate in the immune response against PCV2 and, more importantly, an early induction of ISGs may represent a relevant mechanism used by the innate immunity to counteract PCV2 infection and avoid disease progression. Recently, the up-regulation of a set of ISGs was detected in intestine of pigs experimentally co-infected with PCV2 and PPV (Andersson *et al*., 2011). Although some animals from this study showed clinical signs and displayed gross and histological lesions consistent with PCV2-SD, only mild to moderate depletion of Peyer´s patches was observed in the intestine. This result indicates that, at least locally, the severe effects of the disease could be controlled, supporting the participation of ISGs in this process, which is in agreement with the results presented in this Thesis.

It is well documented that different virus families have developed multiple strategies to evade the IFN system, including the disruption of cellular pathways leading to IFN synthesis, subversion of JAK-STAT signaling to limit ISGs expression or blocking their antiviral functions (García-Sastre and Biron, 2006). Recent *in vitro* studies have shown that PCV2 affects the cellular transcription of important components involved in the IFN signaling pathway, such as the NF-κB and members of the MAPK cascades (Wei *et al*., 2008; Wei and Liu, 2009; Wei *et al*., 2009). Moreover, it has been reported that the NF-κB plays a complex role in the regulation of ISGs (Pfeffer *et al*., 2011). In this context, the ability of PCV2 to modify molecular mechanisms to impair an early expression of IFNs, and subsequently a high number of ISGs, is likely to influence the outcome of PCV2 infection. Furthermore, genetic variations in ISGs have to be taken into account as possible factors contributing to an individual susceptibility to PCV2-SD. As demonstrated in study III, although PCV2-SD affected animals were able to produce a moderate to high abundance of some ISG mRNAs (*Oas1* and *Ifit3*), their expression seems not to be entirely effective or sufficient to counteract the disease. Literature shows that polymorphisms in the *MxA* gene and members of the *OAS* group were associated with the IFN response in chronic hepatitis C virus (HCV) and B virus (HBV) infections, respectively (Suzuki *et al*., 2004; Ren *et al*., 2011). Moreover, a mutation in the *OAS1* gene may have the potential to influence the risk of infection in response to West Nile virus (WNV) exposure in humans (Lim *et al*., 2009). Thus, it would be of interest to further investigate the specific roles of ISGs in the PCV2 infection and the underlying mechanisms involved in their regulation.

Finally, among the ISGs genes over-expressed detected in the study II, the *ISG15* and its conjugated proteins USP18, UBE2L6 and HERC6 are also related to the ubiquitin-proteasome system (UPS). This system plays important roles in a variety of fundamental cellular processes such as regulation of cell cycle, apoptosis, cell trafficking, and modulation of the immune responses (Loureiro and Ploegh, 2006). Two other ubiquitin-proteasome associated genes, *UBD* and *PSMF1* were found with increased expression in studies I and II, respectively, suggesting that this pathway is altered in PCV2 subclinically infected pigs and may be relevant in controlling the infection. It has already been described that the PCV2 ORF3 protein modify the UPS, specifically interacting with the porcine E3 ubiquitin ligase (pPirh2) and the regulator of G protein signaling 16 (RGS16). These interactions can ultimately lead to increased apoptosis mediated by p53 and excessive inflammatory response by increased production of IL-6 and IL-8, respectively (Liu *et al*., 2007; Cheng *et al*., 2014).

The complement system, which is an intricate enzymatic cascade, is also one of the major effector mechanisms of innate immune defense and plays a crucial role in shaping the acquired immune response. When working properly, complement provides essential protection against infections and supports tissue homeostasis. However, alterations in the balance between complement activation and regulation may render this system into a harmful player in tissue damage and disease severity (Ricklin *et al*., 2011). The study III demonstrated that the complement system was altered in PCV2-SD affected pigs, with eight genes DE and, notably, by the lower and higher levels of the complement receptors *Cr1* and *Vsig4* mRNAs, respectively. The *CR1* attenuates complement amplification by removing C3b/C4b immune complexes, while simultaneously allows the access of opsonins by other complement receptors and promotes downstream immune responses (Khera and Das, 2009). Thus, the reduction on its expression might favor both complement deposition leading to tissue damage and secondary infections by impairing phagocytosis. Apparently contradictory, expression of *VSIG4* has been associated to increase phagocytosis by recognizing cell-bound C3 compounds and to inhibit the alternative complement pathway. In addition, this gene is believed to play a role in tissue homeostasis and resolution rather than initiation of inflammatory response (He *et al*., 2008). An over-expression of this gene could represent a compensatory mechanism used by macrophages to clear excessive immune complexes in damaged lymphoid tissues. On the other hand, as observed in diverse human infections, pathogens and predominantly

viruses use the complement system to enter cells by binding to cell-bound complement receptors and regulators, which allows their evasion from immune defenses and persistence in the host (Lambris *et al*., 2008). In this sense, results obtained through yeast and bacterial two-hybrid approaches indicated that complement compounds C1qR and its ligand C1qB interact with the Cap protein of PCV2 (Timmusk *et al*., 2006; Finsterbusch *et al*., 2009). These authors suggested that these interactions could facilitate the uptake of PCV2 by phagocytic cells or also contribute to produce immune complex-mediated lesions. Overall, the fine tune between complement components in the pathogenesis of PCV2-SD has yet to be determined.

In the presence of detrimental stimuli, such as infection or tissue injury, an inflammatory response is initiated to further engage the immune system and promote clearance of infectious agents and tissue repair (Medzhitov, 2010). The inflammatory response represents a highly regulated biological program that involves a wide range of components: the sensors that detect the inflammatory inducers, the inflammatory mediators and the target tissues. The combination of different components results in activation of distinct molecular pathways. The usual outcome of the inflammatory events is the successful removal of offending factors and restoration of tissue structure and physiological function. However, the sustained inflammation resulting in tissue damage implies persistence of an inflammatory inducer or a failure in normal resolution mechanisms (Medzhitov, 2010). As stated in the Introduction of this Thesis, the inflammatory response characterized by granulomatous lesions observed in lymphoid tissues from diseased pigs is one of the hallmarks of PCV2-SD. On the other hand, subclinical PCV2 infections apparently only produce mild PCV2-SD-like lesions in infected tissues. Thus, as expected, significant differences regarding the inflammatory responses were observed among the three studies presented in this Thesis. The most noticeable changes detected in subclinically infected pigs were the increased expression of genes encoding for the chemoattractants CCL4, CXCL9, CXCL11 (study I), CCL5 (study II) and the down-regulation of *LGALS3* (study II). In contrast, the inflammatory response was one of the biological functions most altered in PCV2-SD affected animals (study III), including the increased mRNA levels of a wide variety of inflammatory mediators (cytokines, chemokines, prostaglandins), acute phase proteins, transcriptional regulators, and genes related to stress response and tissue remodeling. This latter result

demonstrates that an ongoing and persistent inflammation mediated by different mechanisms is occurring in diseased pigs.

It has been described both in *in vitro* and *in vivo* studies that PCV2 modulates the production of cytokines/chemokines (Darwich *et al*., 2003a; Chang *et al*., 2006; Vincent *et al*., 2005; 2007; Tsai *et al*., 2010). The over-expression of several genes encoding for cytokines/chemokines with chemoattractant properties in the studies of the present Thesis suggests that PCV2 may regulate the recruitment and migration of leucocytes to the sites of inflammation. Specifically, the *CCL4* gene (MIP-1) was over-expressed in pigs from studies I and III. The MIP-1 is a powerful chemoattractant with activation properties for monocytes and has previously been suggested to be involved in the pathogenesis of PCV2-SD by mediating the granulomatous inflammation induced by PCV2 (Kim and Chae, 2004; Tsai *et al*., 2010). Recently, in a microarray analysis of superficial lymph nodes from the same pigs used in the study II, but only at 29 days p.i., the *CCL4* gene was over-expressed in subclinically PCV2-infected animals (Ramirez-Boo, 2009). Therefore, it is tempting to speculate that some mechanisms underlying the development of granulomatous inflammation may be similar in subclinical PCV2 infection and PCV2-SD, at least in lymph nodes.

Galectin-3 (LGALS3) is expressed by virtually all immune cell types, modulates a plethora of biological processes, and has been largely reported to have a pro-inflammatory role. It has been described that LGALS3 may attract and activate inflammatory cells or contribute to their retention by increasing cellular interactions with extracellular matrix glycoproteins. Moreover, the protein encoded by this gene has the ability to induce IL-1 and superoxide production by monocytes, mast cell degranulation and IL-8 generation by neutrophils (Norling *et al*., 2009). Opposite expression levels of this gene was observed in studies II and III. While in subclinically PCV2-infected pigs the *LGALS3* gene was down-regulated from 2 days p.i until the end of the experiment (29 days p.i), its expression was highly increased in diseased animals. In addition, over-expression of *LGALS3* was detected by microarray analysis in pools of lymph nodes showing moderate lymphocyte depletion and granulomatous lesions from pigs experimentally infected with PCV2 (Lee *et al*., 2010). This discrepancy could be related to the stages of the infection and the degree of granulomatous inflammation. Similar results were obtained by profiling the gene expression of lymph nodes during HIV infection (Li *et al*., 2009). Therefore, the

LGALS3 may play an important role in the development of granulomatous lesions observed in PCV2 infections and could be used as a potential marker to study the progression of the PCV2-SD.

Changes in the expression of genes linked to tissue remodelling observed in diseased pigs from study III, such as extracellular matrix components, adhesion molecules and growth factors, suggest that in the state of persistent inflammation from ongoing PCV2 replication, damage and disruption to the lymphoid tissue microenvironment occur. These events could lead to an inability of the tissue to support the normal resident population of cells, and also impairs the recruitment, retention and proliferation of certain cell types, such as lymphocytes. This mechanism has been suggested as one potential explanation for the $CD4^+$ T cell depletion observed during HIV infections (Schacker *et al*., 2002), and may apply in cases of PCV2 infection leading to clinical disease.

The acquired phase of the immune response is triggered when innate responses are not sufficient to control a pathogen. The adaptive immunity is characterized by T and B cells clonally expressing a large repertoire of antigen receptors, that is, T cell receptor (TCR) and B cell receptor (BCR), and subsequent activation and clonal expansion of cells carrying the appropriate antigen-specific receptors. Induction of this type of response depends on direct antigen recognition by the antigen receptors and signals that are delivered by the innate immune system (Janeway *et al*., 2001; Huang and Wange, 2004). The present Thesis demonstrates that cell-mediated and humoral immunity developed over the course of a subclinical PCV2 infection. A number of genes encoding proteins associated with the activation of T cells (*TCRa*, *CD8a*, *LCK*, *CD2, RASSF2*), B cells (*SYK, CD74*) and NK cells (*KLRK1*) showed increased mRNA levels in subclinically infected pigs (studies I and II). Only the variable TCRa chain showed over expression, and could indicate an epitope-driven selection of limited T-cell clones in lung and blood of PCV2 subclinically infected pigs. Moreover, the level of IgG mRNA was increased in the lymph nodes of infected pigs of both studies. Seroconversion occurred in all PCV2-inoculated animals between the second and third week p.i, in agreement with the observations made by other researchers (Pogranichnyy *et al*., 2000; Bolin *et al*., 2001). Finally, the increased expression of the *IFNG* from day 8 p.i until 29 days p.i (study II) and also the interferon-gamma inducible chemokines *CXCL9* and *CXCL11* (study I) highlights once more the importance of the IFN system throughout PCV2 infection.

Overall, the prompt over-expression of these genes related to the activation of humoral and cell-mediated immune responses could be key events to avoid the progression of PCV2 infection.

Another defining feature of the PCV2-SD is the marked lymphocyte depletion in lymphoid tissues (Chapter 1). Thus, not surprisingly, a large number of genes implicated in several mechanisms involved in lymphocyte development, proliferation, activation and homing, showed low mRNA levels in diseased pigs from study III. Although reduced expression could be due to loss of cells expressing these genes, decreased expression in a particular cell type, or both, the global effect is a dysfunctional host defences due to decreased expression of various genes, such as BCR (*Cd79b*, *Cd19*, *Cd21*, *BLK*) and TCR (*TCRB*, *LEF1*) components, and activation/proliferation of B and T cells (*MYBL1*, *MYBL2*, *SWAP70*, *ICOSLG* and *TIMD4*).

In addition to its role as a complement receptor, as discussed above, VSIG4 acts as a strong negative regulator of $CD4^+$ and $CD8^+$ T-cell activation and proliferation (Vogt *et al*., 2006). It has been described that the protein encoded by this gene, expressed in macrophages, participates in the induction and maintenance of liver T- and NK-cell tolerance (Jung *et al*., 2012) and may be a potential inhibitor of adaptive immunity in chronic HBV infection by regulating IFN-γ production in T cells (Guo *et al*., 2010). In this latter report, IFN-γ could down-regulate the expression of *VSIG4 in vivo* and *in vitro*, weakening the effect of negative co-stimulatory signals delivered by macrophages to T cells. Another gene coding for a protein with immunosuppressive properties is the type I transmembrane receptor *GPNMB*, and its mRNA levels were highly increased in diseased pigs (study III). When expressed in macrophages, the GPNMB acts as a potent inhibitor of inflammatory responses, possibly by suppressing pro-inflammatory mediators (Ripoll *et al*., 2007). In DC, GPNMB acts as a co-inhibitory molecule strongly inhibiting responses of T cells by binding syndecan-4 on activated T cells in mice and humans. This binding strongly attenuates the T-cell response to anti-CD3 antibody, thereby blocking the T-cell production of pro-inflammatory cytokines and T-cell entry into the cell cycle (Chung *et al*., 2007; 2009). Interestingly, its expression on primary human moDC was dramatically up-regulated upon treatment with IL-10 (Schwarzbich *et al*., 2012). This latter cytokine is frequently associated with PCV2 infection (Darwich *et al*., 2003b; Stevenson *et al*., 2006). In the microarray analysis mentioned above, performed by Lee

et al. (2010), over-expression of *GPNMB* was detected in PCV2 infected pigs. Taking together, these observations might help to elucidate the mechanisms behind the immunosuppression observed in PCV2-SD affected pigs. Therefore, since these two genes have been only recently identified and so far, little is known about their functions in immune responses, the determination of the biological relevance of these molecules in the PCV2-SD pathogenesis warrants further investigation.

Apoptosis, or programmed cell death, is a highly regulated process modulated by both pro-apoptotic and anti-apoptotic cellular factors and activated by various stimuli that disturb cell metabolism and physiology (Hetts, 1998). Despite numerous studies examining the possible implication of apoptosis in the pathogenesis of the PCV2-SD, it remains unclear if PCV2 infection modulates apoptotic pathways (Shibahara *et al*., 2000; Kiupel *et al*., 2001; Mandrioli *et al*., 2004; Resendes *et al*., 2004b; Juhan *et al*., 2010; Lv *et al*., 2012). A number of potential mechanisms have been proposed, many of them suggesting the participation of the PCV2 ORF3 in mediating the virus-induced apoptosis (Liu *et al*., 2005; 2006; 2007; Karuppannan *et al*., 2010; 2011; Lin *et al*., 2011a,b). In PCV2-SD affected pigs (study III), cell death and apoptosis processes were altered, including 24 DE genes, most of them showing increased expression. These apoptosis-related genes were implicated in different canonical pathways, such as p53 apoptotic pathway (*P8, NQO1, DRAM, ANXA1, BCL11A* and *BCL7A*), caspase-mediated pathway (*CASP1* and *CASP4*) and death receptor mediated apoptosis (*TNFSF10* – TRAIL). Viruses have been shown to manipulate these pathways to induce their replication and/or to avoid immune responses (Jault *et al*., 1995; Miura *et al*., 2001; Gao *et al*., 2013). Therefore, these results indicate that apoptosis may play an important role in the pathogenesis of PCV2-SD and its specific mechanisms should be further investigated. The fact that apoptosis was not a biological function highly altered in studies I and II suggests that, in subclinical PCV2 infections, other mechanisms might be used to counteract the ability of the virus to modulate apoptotic pathways, thus controlling its replication and avoiding lymphocyte depletion.

In conclusion, the microarray technology used in this Thesis allowed obtaining valuable information about the transcriptional profile of pigs under PCV2 subclinical infection as well as animals affected by PCV2-SD. The identification of potential genes, pathways and biological processes involved in the PCV2 pathogenesis should help to better

understand why some pigs remain subclinically infected while others develop the clinical disease. In this context, it is important to remark the early activation of the immune responses, and especially the induction of ISGs and genes related to lymphocyte activation within the first week p.i in the subclinical model. Moreover, the effective development of cell-mediated and humoral responses at late stages of infection should provide virus clearance and limit the disease progression. On the other hand, in animals affected by PCV2-SD the immune response was impaired and potential genes and pathways were identified underlying the inflammation and lymphocyte depletion in lymph nodes. Although these findings contributed to improve the understanding of the PCV2 pathogenesis, no single approach can fully unravel the complexity of the molecular events that occur in response to infectious diseases. Therefore, the integration of data from additional studies encompassing deep-sequencing technologies, such as RNA and miRNA sequencing, should provide a more comprehensive picture of the interaction between PCV2 and its host, from a transcriptional point of view. Very recently, three works have been published using the miRNAseq technique to study PCV2-host interactions, and are mostly in accordance with the results presented in this Thesis (Hong *et al*., 2015; Núñez-Hernández *et al*., 2015a; 2015b). Ultimately, they should help to reveal novel control mechanisms, target genes, and pathway functions that encode PCV2 resistance and provide protective anti-viral responses.

CHAPTER 7

CONCLUSIONS

1. The microarray platform Affymetrix Porcine Genechip® is a reliable and sensitive resource to study the interactions between PCV2 and the pig. This technique allowed accurate detection and comparison of changes in gene expression of RNA samples from complex organs under different experimental conditions and was able to discriminate stages of infection within natural cases of PCV2-SD.

2. In subclinically PCV2-infected pigs, the innate immune response develops during the first week p.i. and is characterized by over-expression of ISGs.

3. In the course of a subclinical PCV2 infection, the adaptive immunity starts within the first week p.i trough the up-regulation of genes associated with the lymphocyte activation in blood. At late stages of infection, cell-mediated and humoral immune responses are characterized mostly by the over-expression of *IFNG* and interferon-gamma inducible genes, and of *IGHG*, respectively. Moreover, subclinically infected Duroc and Landrace pigs develop similar immunological responses against PCV2.

4. In PCV2-SD affected pigs, changes in the gene expression is related to the progression of microscopic lesions. Lymph nodes of animals showing moderate degree of lymphocyte depletion and high degree of granulomatous inflammation have similar patterns of expression to those from healthy pigs.

5. The complement system is altered in PCV2-SD affected pigs, notably by the lower and high levels of the complement receptors Cr1 and Vsig4 mRNAs, respectively.

6. In the course of PCV2-SD, an ongoing and persistent inflammation occurs and this process is mediated by different mechanisms, which are characterized by the increased mRNA levels of inflammatory mediators, acute phase proteins, transcriptional regulators, genes related to stress response and tissue remodeling.

7. PCV2-SD affected animals experience an impaired adaptive immunity response, which is characterized by the increased expression of *VSIG4* and low mRNA levels of genes involved in lymphocyte development, proliferation, activation and homing.

8. Cell death and apoptosis processes are altered in PCV2-SD affected pigs, which are characterized by the increased expression of genes implicated in the p53 apoptotic pathway, caspase-mediated pathway and death receptor mediated apoptosis.

CHAPTER 8

REFERENCES

Affymetrix, Inc., 2002. Statistical Algorithms Description Document. Technical Report. (http://www.affymetrix.com/support/technical/whitepapers/sadd_whitepaper.pdf), 28p.

Affymetrix, Inc., 2005. Guide to Probe Logarithmic Intensity Error (PLIER) Estimation. Technical Note. (http://media.affymetrix.com/support/technical/technotes/plier_technote.pdf), 10p.

Afonso, C.L., Piccone, M.E., Zaffuto, K.M., Neilan, J., Kutish, G.F., Lu, Z., Balinsky, C.A., Gibb, T.R., Bean, T.J., Zsak, L., Rock, D.L., 2004. African swine fever virus multigene family 360 and 530 genes affect host interferon response. J Virol 78, 1858-1864.

Alarcon, P., Velasova, M., Werling, D., Stark, K.D., Chang, Y.M., Nevel, A., Pfeiffer, D.U., Wieland, B., 2011. Assessment and quantification of post-weaning multi-systemic wasting syndrome severity at farm level. Preventive veterinary medicine 98, 19-28.

Alberti, K.A., Estienne, M.J., Meng, X.J., 2011. Effect of vaccination of boars against porcine circovirus type 2 on ejaculate characteristics, serum antibody titers, viremia, and semen virus shedding. J Anim Sci 89, 1581-1587.

Albina, E., Truong, C., Hutet, E., Blanchard, P., Cariolet, R., L'Hospitalier, R., Mahe, D., Allee, C., Morvan, H., Amenna, N., Le Dimna, M., Madec, F., Jestin, A., 2001. An experimental model for post-weaning multisystemic wasting syndrome (PMWS) in growing piglets. Journal of comparative pathology 125, 292-303.

Alcaraz, M.J., Fernandez, P., Guillen, M.I., 2003. Anti-inflammatory actions of the heme oxygenase-1 pathway. Current pharmaceutical design 9, 2541-2551.

Allan, G., Krakowka, S., Ellis, J., Charreyre, C., 2012. Discovery and evolving history of two genetically related but phenotypically different viruses, porcine circoviruses 1 and 2. Virus Res 164, 4-9.

Allan, G., Meehan, B., Todd, D., Kennedy, S., McNeilly, F., Ellis, J., Clark, E.G., Harding, J., Espuna, E., Botner, A., Charreyre, C., 1998a. Novel porcine circoviruses from pigs with wasting disease syndromes. Vet Rec 142, 467-468.

Allan, G.M., Kennedy, S., McNeilly, F., Foster, J.C., Ellis, J.A., Krakowka, S.J., Meehan, B.M., Adair, B.M., 1999. Experimental reproduction of severe wasting disease by co-infection of pigs with porcine circovirus and porcine parvovirus. Journal of comparative pathology 121, 1-11.

Allan, G.M., McNeilly, F., Ellis, J., Krakowka, S., Meehan, B., McNair, I., Walker, I., Kennedy, S., 2000. Experimental infection of colostrum deprived piglets with porcine circovirus 2 (PCV2) and porcine reproductive and respiratory syndrome virus (PRRSV) potentiates PCV2 replication. Arch Virol 145, 2421-2429.

Allan, G.M., McNeilly, F., Kennedy, S., Daft, B., Clarke, E.G., Ellis, J.A., Haines, D.M., Meehan, B.M., Adair, B.M., 1998b. Isolation of porcine circovirus-like viruses from pigs with a wasting disease in the USA and Europe. J Vet Diagn Invest 10, 3-10.

Allemandou, A., Grasland, B., Hernandez-Nignol, A.C., Keranflec'h, A., Cariolet, R., Jestin, A., 2011. Modification of PCV-2 virulence by substitution of the genogroup motif of the capsid protein. Veterinary research 42, 54.

An, D.J., Song, D.S., Park, B.K., 2008. Systemic cytokine profiles of mice vaccinated with naked DNAs encoding six open reading frame antigens of porcine circovirus type 2 (PCV2). Res Vet Sci 85, 503-509.

Andersson, M., Ahlberg, V., Jensen-Waern, M., Fossum, C., 2011. Intestinal gene expression in pigs experimentally co-infected with PCV2 and PPV. Veterinary immunology and immunopathology 142, 72-80.

Arikawa, E., Sun, Y., Wang, J., Zhou, Q., Ning, B., Dial, S.L., Guo, L., Yang, J., 2008. Cross-platform comparison of SYBR Green real-time PCR with TaqMan PCR, microarrays and other gene expression measurement technologies evaluated in the MicroArray Quality Control (MAQC) study. BMC genomics 9, 328.

Ashburner, M., Ball, C.A., Blake, J.A., Botstein, D., Butler, H., Cherry, J.M., Davis, A.P., Dolinski, K., Dwight, S.S., Eppig, J.T., Harris, M.A., Hill, D.P., Issel-Tarver, L., Kasarskis, A., Lewis, S., Matese, J.C., Richardson, J.E., Ringwald, M., Rubin, G.M., Sherlock, G., 2000. Gene ontology: tool for the unification of biology. The Gene Ontology Consortium. Nat Genet 25, 25-29.

Badaoui, B., Tuggle, C.K., Hu, Z., Reecy, J.M., Ait-Ali, T., Anselmo, A., Botti, S., 2013. Pig immune response to general stimulus and to porcine reproductive and respiratory syndrome virus infection: a meta-analysis approach. BMC genomics 14, 220.

Baekbo, P., Kristensen, C.S., Larsen, L.E., 2012. Porcine Circovirus Diseases: A review of PMWS. Transbound Emerg Dis doi: 10.1111/j.1865-1682.2011.01288.x.

Balasch, M., Segales, J., Rosell, C., Domingo, M., Mankertz, A., Urniza, A., Plana-Duran, J., 1999. Experimental inoculation of conventional pigs with tissue homogenates from pigs with post-weaning multisystemic wasting syndrome. Journal of comparative pathology 121, 139-148.

Barrera, L., Benner, C., Tao, Y.C., Winzeler, E., Zhou, Y., 2004. Leveraging two-way probe-level block design for identifying differential gene expression with high-density oligonucleotide arrays. BMC Bioinformatics 5, 42.

Beach, N.M., Meng, X.J., 2012. Efficacy and future prospects of commercially available and experimental vaccines against porcine circovirus type 2 (PCV2). Virus Res 164, 33-42.

Beach, N.M., Smith, S.M., Ramamoorthy, S., Meng, X.J., 2011. Chimeric porcine circoviruses (PCV) containing amino acid epitope tags in the C terminus of the capsid gene are infectious and elicit both anti-epitope tag antibodies and anti-PCV type 2 neutralizing antibodies in pigs. J Virol 85, 4591-4595.

Benjamini, Y., Hochberg, Y., 1995. Controlling the False Discovery Rate: A Practical and Powerful Approach to Multiple Testing. Journal of the Royal Statistical Society 57, Series B (Methodological), 289-300.

Blinkova, O., Victoria, J., Li, Y., Keele, B.F., Sanz, C., Ndjango, J.B., Peeters, M., Travis, D., Lonsdorf, E.V., Wilson, M.L., Pusey, A.E., Hahn, B.H., Delwart, E.L., 2010. Novel circular DNA viruses in stool samples of wild-living chimpanzees. J Gen Virol 91, 74-86.

Bolin, S.R., Stoffregen, W.C., Nayar, G.P., Hamel, A.L., 2001. Postweaning multisystemic wasting syndrome induced after experimental inoculation of cesarean-derived, colostrum-deprived piglets with type 2 porcine circovirus. J Vet Diagn Invest 13, 185-194.

Bolstad, B., 2012. affyPLM: Model Based QC Assessment of Affymetrix GeneChips. http://www.bioconductor.org/packages/2.10/bioc/vignettes/affyPLM/inst/doc/QualityAssess.pdf.

Bolstad, B.M., Irizarry, R.A., Astrand, M., Speed, T.P., 2003. A comparison of normalization methods for high density oligonucleotide array data based on variance and bias. Bioinformatics 19, 185-193.

Bratanich, A., Blanchetot, A., 2006. A gene similar to the human hyaluronan-mediated motility receptor (RHAMM) gene is upregulated during Porcine Circovirus type 2 infection. Virus Genes 32, 145-152.

Brazma, A., Hingamp, P., Quackenbush, J., Sherlock, G., Spellman, P., Stoeckert, C., Aach, J., Ansorge, W., Ball, C.A., Causton, H.C., Gaasterland, T., Glenisson, P., Holstege, F.C., Kim, I.F., Markowitz, V., Matese, J.C., Parkinson, H., Robinson, A., Sarkans, U., Schulze-Kremer, S., Stewart, J., Taylor, R., Vilo, J., Vingron, M., 2001. Minimum information about a microarray experiment (MIAME)-toward standards for microarray data. Nat Genet 29, 365-371.

Brazma, A., Parkinson, H., Sarkans, U., Shojatalab, M., Vilo, J., Abeygunawardena, N., Holloway, E., Kapushesky, M., Kemmeren, P., Lara, G.G., Oezcimen, A., Rocca-Serra, P., Sansone, S.A., 2003. ArrayExpress--a public repository for microarray gene expression data at the EBI. Nucleic Acids Res 31, 68-71.

Calsamiglia, M., Fraile, L., Espinal, A., Cuxart, A., Seminati, C., Martin, M., Mateu, E., Domingo, M., Segales, J., 2007. Sow porcine circovirus type 2 (PCV2) status effect on litter mortality in postweaning multisystemic wasting syndrome (PMWS). Res Vet Sci 82, 299-304.

Canales, R.D., Luo, Y., Willey, J.C., Austermiller, B., Barbacioru, C.C., Boysen, C., Hunkapiller, K., Jensen, R.V., Knight, C.R., Lee, K.Y., Ma, Y., Maqsodi, B., Papallo, A., Peters, E.H., Poulter, K., Ruppel, P.L., Samaha, R.R., Shi, L., Yang, W., Zhang, L., Goodsaid, F.M., 2006. Evaluation of DNA microarray results with quantitative gene expression platforms. Nat Biotechnol 24, 1115-1122.

Carman, S., Cai, H.Y., DeLay, J., Youssef, S.A., McEwen, B.J., Gagnon, C.A., Tremblay, D., Hazlett, M., Lusis, P., Fairles, J., Alexander, H.S., van Dreumel, T., 2008. The emergence of a new strain of porcine circovirus-2 in Ontario and Quebec swine and its association with severe porcine circovirus associated disease--2004-2006. Can J Vet Res 72, 259-268.

Chaiyakul, M., Hsu, K., Dardari, R., Marshall, F., Czub, M., 2010. Cytotoxicity of ORF3 Proteins from a Nonpathogenic and a Pathogenic Porcine Circovirus. J Virol 84, 11440-11447.

Chang, H.W., Jeng, C.R., Lin, T.L., Liu, J.J., Chiou, M.T., Tsai, Y.C., Chia, M.Y., Jan, T.R., Pang, V.F., 2006. Immunopathological effects of porcine circovirus type 2 (PCV2) on swine alveolar macrophages by in vitro inoculation. Veterinary immunology and immunopathology 110, 207-219.

Chen, H., Cheng, L., Yang, S., Liu, X., Liu, Y., Tang, J., Li, X., He, Q., Zhao, S., 2010. Molecular characterization, induced expression, and transcriptional regulation of porcine S100A12 gene. Molecular immunology 47, 1601-1607.

Chen, X., Ren, F., Hesketh, J., Shi, X., Li, J., Gan, F., Huang, K., 2012. Reactive oxygen species regulate the replication of porcine circovirus type 2 via NF-kappaB pathway. Virology 426, 66-72.

Cheng, S., Zhang, M., Li, W., Wang, Y., Liu, Y., He, Q., 2012. Proteomic analysis of porcine alveolar macrophages infected with porcine circovirus type 2. Journal of proteomics 75, 3258-3269.

Cheung, A.K., 2003a. Transcriptional analysis of porcine circovirus type 2. Virology 305, 168-180.

Cheung, A.K., 2012. Porcine circovirus: transcription and DNA replication. Virus Res 164, 46-53.
Cheung, A.K., Bolin, S.R., 2002. Kinetics of porcine circovirus type 2 replication. Arch Virol 147, 43-58.
Cheung, A.K., Lager, K.M., Kohutyuk, O.I., Vincent, A.L., Henry, S.C., Baker, R.B., Rowland, R.R., Dunham, A.G., 2007. Detection of two porcine circovirus type 2 genotypic groups in United States swine herds. Arch Virol 152, 1035-1044.
Chianini, F., Majo, N., Segales, J., Dominguez, J., Domingo, M., 2003. Immunohistochemical characterisation of PCV2 associate lesions in lymphoid and non-lymphoid tissues of pigs with natural postweaning multisystemic wasting syndrome (PMWS). Veterinary immunology and immunopathology 94, 63-75.
Chung, J.S., Bonkobara, M., Tomihari, M., Cruz, P.D., Jr., Ariizumi, K., 2009. The DC-HIL/syndecan-4 pathway inhibits human allogeneic T-cell responses. European journal of immunology 39, 965-974.
Chung, J.S., Sato, K., Dougherty, II, Cruz, P.D., Jr., Ariizumi, K., 2007. DC-HIL is a negative regulator of T lymphocyte activation. Blood 109, 4320-4327.
Chwieralski, C.E., Welte, T., Buhling, F., 2006. Cathepsin-regulated apoptosis. Apoptosis 11, 143-149.
Cino-Ozuna, A.G., Henry, S., Hesse, R., Nietfeld, J.C., Bai, J., Scott, H.M., Rowland, R.R., 2011. Characterization of a new disease syndrome associated with porcine circovirus type 2 in previously vaccinated herds. Journal of clinical microbiology 49, 2012-2016.
Clark, E. 1996. Post-weaning multisystemic wasting syndrome. In: Proceedings of the 27th Annual Meeting of the Western Canadian Association of Swine Practitioners, 19-20.
Clark, E. 1997. Postweaning multisystemic wasting syndrome. In: American association of Swine Practitioners, 499-501.
Clarke, J.D., Zhu, T., 2006. Microarray analysis of the transcriptome as a stepping stone towards understanding biological systems: practical considerations and perspectives. The Plant journal : for cell and molecular biology 45, 630-650.
Conesa, A., Gotz, S., Garcia-Gomez, J.M., Terol, J., Talon, M., Robles, M., 2005. Blast2GO: a universal tool for annotation, visualization and analysis in functional genomics research. Bioinformatics 21, 3674-3676.
Cortey, M., Olvera, A., Grau-Roma, L., Segales, J., 2011. Further comments on porcine circovirus type 2 (PCV2) genotype definition and nomenclature. Vet Microbiol 149, 522-523.
Cortey, M., Segales, J., 2012. Low levels of diversity among genomes of Porcine circovirus type 1 (PCV1) points to differential adaptive selection between Porcine circoviruses. Virology 422, 161-164.
Couture, O., Callenberg, K., Koul, N., Pandit, S., Younes, R., Hu, Z.L., Dekkers, J., Reecy, J., Honavar, V., Tuggle, C., 2009. ANEXdb: an integrated animal ANnotation and microarray EXpression database. Mamm Genome 20, 768-777.
Crisci, E., Ballester, M., Dominguez, J., Segales, J., Montoya, M., 2010. Increased numbers of myeloid and lymphoid IL-10 producing cells in spleen of pigs with naturally occurring postweaning multisystemic wasting syndrome. Veterinary immunology and immunopathology 136, 305-310.
Dallas, P.B., Gottardo, N.G., Firth, M.J., Beesley, A.H., Hoffmann, K., Terry, P.A., Freitas, J.R., Boag, J.M., Cummings, A.J., Kees, U.R., 2005. Gene expression levels assessed by oligonucleotide microarray analysis and quantitative real-time RT-PCR -- how well do they correlate? BMC genomics 6, 59.
Darwich, L., Balasch, M., Plana-Duran, J., Segales, J., Domingo, M., Mateu, E., 2003a. Cytokine profiles of peripheral blood mononuclear cells from pigs with postweaning multisystemic wasting syndrome in response to mitogen, superantigen or recall viral antigens. J Gen Virol 84, 3453-3457.
Darwich, L., Pie, S., Rovira, A., Segales, J., Domingo, M., Oswald, I.P., Mateu, E., 2003b. Cytokine mRNA expression profiles in lymphoid tissues of pigs naturally affected by postweaning multisystemic wasting syndrome. J Gen Virol 84, 2117-2125.
Darwich, L., Segales, J., Mateu, E., 2004. Pathogenesis of postweaning multisystemic wasting syndrome caused by Porcine circovirus 2: An immune riddle. Arch Virol 149, 857-874.
Darwich, L., Segales, J., Resendes, A., Balasch, M., Plana-Duran, J., Mateu, E., 2008. Transient correlation between viremia levels and IL-10 expression in pigs subclinically infected with porcine circovirus type 2 (PCV2). Res Vet Sci 84, 194-198.
Deban, L., Bottazzi, B., Garlanda, C., de la Torre, Y.M., Mantovani, A., 2009. Pentraxins: multifunctional proteins at the interface of innate immunity and inflammation. Biofactors 35, 138-145.
Denyer, M.S., Wileman, T.E., Stirling, C.M., Zuber, B., Takamatsu, H.H., 2006. Perforin expression can define CD8 positive lymphocyte subsets in pigs allowing phenotypic and functional analysis of natural killer, cytotoxic T, natural killer T and MHC un-restricted cytotoxic T-cells. Veterinary immunology and immunopathology 110, 279-292.

Deyholos, M.K., Galbraith, D.W., 2001. High-density microarrays for gene expression analysis. Cytometry 43, 229-238.

Doster, A.R., Subramaniam, S., Yhee, J.Y., Kwon, B.J., Yu, C.H., Kwon, S.Y., Osorio, F.A., Sur, J.H., 2010. Distribution and characterization of IL-10-secreting cells in lymphoid tissues of PCV2-infected pigs. J Vet Sci 11, 177-183.

Dumic, J., Dabelic, S., Flogel, M., 2006. Galectin-3: an open-ended story. Biochim Biophys Acta 1760, 616-635.

Dumur, C.I., Nasim, S., Best, A.M., Archer, K.J., Ladd, A.C., Mas, V.R., Wilkinson, D.S., Garrett, C.T., Ferreira-Gonzalez, A., 2004. Evaluation of quality-control criteria for microarray gene expression analysis. Clinical chemistry 50, 1994-2002.

Dupont, K., Nielsen, E.O., Baekbo, P., Larsen, L.E., 2008. Genomic analysis of PCV2 isolates from Danish archives and a current PMWS case-control study supports a shift in genotypes with time. Vet Microbiol 128, 56-64.

Edgar, R., Domrachev, M., Lash, A.E., 2002. Gene Expression Omnibus: NCBI gene expression and hybridization array data repository. Nucleic Acids Res 30, 207-210.

Eisen, M.B., Spellman, P.T., Brown, P.O., Botstein, D., 1998. Cluster analysis and display of genome-wide expression patterns. Proc Natl Acad Sci U S A 95, 14863-14868.

Ellis, J., Hassard, L., Clark, E., Harding, J., Allan, G., Willson, P., Strokappe, J., Martin, K., McNeilly, F., Meehan, B., Todd, D., Haines, D., 1998. Isolation of circovirus from lesions of pigs with postweaning multisystemic wasting syndrome. Can Vet J 39, 44-51.

Ellis, J., Krakowka, S., Lairmore, M., Haines, D., Bratanich, A., Clark, E., Allan, G., Konoby, C., Hassard, L., Meehan, B., Martin, K., Harding, J., Kennedy, S., McNeilly, F., 1999. Reproduction of lesions of postweaning multisystemic wasting syndrome in gnotobiotic piglets. J Vet Diagn Invest 11, 3-14.

Erdei, A., Isaak, A., Torok, K., Sandor, N., Kremlitzka, M., Prechl, J., Bajtay, Z., 2009. Expression and role of CR1 and CR2 on B and T lymphocytes under physiological and autoimmune conditions. Molecular immunology 46, 2767-2773.

Fachinger, V., Bischoff, R., Jedidia, S.B., Saalmuller, A., Elbers, K., 2008. The effect of vaccination against porcine circovirus type 2 in pigs suffering from porcine respiratory disease complex. Vaccine 26, 1488-1499.

Fan, H., Pan, Y., Fang, L., Wang, D., Wang, S., Jiang, Y., Chen, H., Xiao, S., 2008. Construction and immunogenicity of recombinant pseudotype baculovirus expressing the capsid protein of porcine circovirus type 2 in mice. J Virol Methods 150, 21-26.

Fan, H., Ye, Y., Luo, Y., Tong, T., Yan, G., Liao, M., 2012. Quantitative proteomics using stable isotope labeling with amino acids in cell culture reveals protein and pathway regulation in porcine circovirus type 2 infected PK-15 cells. Journal of proteome research 11, 995-1008.

Faure-Andre, G., Vargas, P., Yuseff, M.I., Heuze, M., Diaz, J., Lankar, D., Steri, V., Manry, J., Hugues, S., Vascotto, F., Boulanger, J., Raposo, G., Bono, M.R., Rosemblatt, M., Piel, M., Lennon-Dumenil, A.M., 2008. Regulation of dendritic cell migration by CD74, the MHC class II-associated invariant chain. Science 322, 1705-1710.

Faurez, F., Dory, D., Grasland, B., Jestin, A., 2009. Replication of porcine circoviruses. Virol J 6, 60.

Fenaux, M., Opriessnig, T., Halbur, P.G., Elvinger, F., Meng, X.J., 2004. Two amino acid mutations in the capsid protein of type 2 porcine circovirus (PCV2) enhanced PCV2 replication in vitro and attenuated the virus in vivo. J Virol 78, 13440-13446.

Fernandes, L.T., Mateu, E., Sibila, M., Fort, M., Andaluz, A., McNeilly, F., Allan, G., Sanchez, A., Segales, J., Stevenson, L., 2007. Lack of in vitro and in vivo effects of lipopolysaccharide on porcine circovirus type 2 infection. Viral immunology 20, 541-552.

Ferraz, A.L., Ojeda, A., Lopez-Bejar, M., Fernandes, L.T., Castello, A., Folch, J.M., Perez-Enciso, M., 2008. Transcriptome architecture across tissues in the pig. BMC genomics 9, 173.

Finsterbusch, T., Mankertz, A., 2009. Porcine circoviruses--small but powerful. Virus Res 143, 177-183.

Finsterbusch, T., Steinfeldt, T., Doberstein, K., Rodner, C., Mankertz, A., 2009. Interaction of the replication proteins and the capsid protein of porcine circovirus type 1 and 2 with host proteins. Virology 386, 122-131.

Firth, C., Charleston, M.A., Duffy, S., Shapiro, B., Holmes, E.C., 2009. Insights into the evolutionary history of an emerging livestock pathogen: porcine circovirus 2. J Virol 83, 12813-12821.

Flori, L., Rogel-Gaillard, C., Cochet, M., Lemonnier, G., Hugot, K., Chardon, P., Robin, S., Lefevre, F., 2008a. Transcriptomic analysis of the dialogue between Pseudorabies virus and porcine epithelial cells during infection. BMC genomics 9, 123.

Flori, L., Rogel-Gaillard, C., Mariani, V., Lemonnier, G., Cochet, M., Hugot, K., Chardon, P., Robin, S., Lefevre, F., 2008b. A combined transcriptomic approach to analyse the dialogue between pseudorabies virus and porcine cells. Developments in biologicals 132, 99-104.

Fodor, S.P., Read, J.L., Pirrung, M.C., Stryer, L., Lu, A.T., Solas, D., 1991. Light-directed, spatially addressable parallel chemical synthesis. Science 251, 767-773.

Fok, P.T., Huang, K.C., Holland, P.C., Nalbantoglu, J., 2007. The Coxsackie and adenovirus receptor binds microtubules and plays a role in cell migration. J Biol Chem 282, 7512-7521.

Forbes, J.R., Gros, P., 2001. Divalent-metal transport by NRAMP proteins at the interface of host-pathogen interactions. Trends Microbiol 9, 397-403.

Fort, M., Fernandes, L.T., Nofrarias, M., Diaz, I., Sibila, M., Pujols, J., Mateu, E., Segales, J., 2009a. Development of cell-mediated immunity to porcine circovirus type 2 (PCV2) in caesarean-derived, colostrum-deprived piglets. Veterinary immunology and immunopathology 129, 101-107.

Fort, M., Olvera, A., Sibila, M., Segales, J., Mateu, E., 2007. Detection of neutralizing antibodies in postweaning multisystemic wasting syndrome (PMWS)-affected and non-PMWS-affected pigs. Vet Microbiol 125, 244-255.

Fort, M., Sibila, M., Allepuz, A., Mateu, E., Roerink, F., Segales, J., 2008. Porcine circovirus type 2 (PCV2) vaccination of conventional pigs prevents viremia against PCV2 isolates of different genotypes and geographic origins. Vaccine 26, 1063-1071.

Fort, M., Sibila, M., Perez-Martin, E., Nofrarias, M., Mateu, E., Segales, J., 2009b. One dose of a porcine circovirus 2 (PCV2) sub-unit vaccine administered to 3-week-old conventional piglets elicits cell-mediated immunity and significantly reduces PCV2 viremia in an experimental model. Vaccine 27, 4031-4037.

Fraile, L., Grau-Roma, L., Sarasola, P., Sinovas, N., Nofrarias, M., Lopez-Jimenez, R., Lopez-Soria, S., Sibila, M., Segales, J., 2012. Inactivated PCV2 one shot vaccine applied in 3-week-old piglets: improvement of production parameters and interaction with maternally derived immunity. Vaccine 30, 1986-1992.

Gagnon, C.A., Music, N., Fontaine, G., Tremblay, D., Harel, J., 2010. Emergence of a new type of porcine circovirus in swine (PCV): a type 1 and type 2 PCV recombinant. Vet Microbiol 144, 18-23.

Gagnon, C.A., Tremblay, D., Tijssen, P., Venne, M.H., Houde, A., Elahi, S.M., 2007. The emergence of porcine circovirus 2b genotype (PCV-2b) in swine in Canada. Can Vet J 48, 811-819.

Gao, G., Luo, H., 2006. The ubiquitin-proteasome pathway in viral infections. Canadian journal of physiology and pharmacology 84, 5-14.

Gao, Y., Wu, H., He, D., Hu, X., Li, Y., 2013. Downregulation of BCL11A by siRNA induces apoptosis in B lymphoma cell lines. Biomedical reports 1, 47-52.

Garcia-Sastre, A., Biron, C.A., 2006. Type 1 interferons and the virus-host relationship: a lesson in detente. Science 312, 879-882.

Gauger, P.C., Lager, K.M., Vincent, A.L., Opriessnig, T., Kehrli, M.E., Jr., Cheung, A.K., 2011. Postweaning multisystemic wasting syndrome produced in gnotobiotic pigs following exposure to various amounts of porcine circovirus type 2a or type 2b. Vet Microbiol 153, 229-239.

Gautier, L., Cope, L., Bolstad, B.M., Irizarry, R.A., 2004. affy--analysis of Affymetrix GeneChip data at the probe level. Bioinformatics 20, 307-315.

Gautier, L., Irizarry, R., Cope, L., Bolstad, B., 2012. Description of affy. http://www.bioconductor.org/packages/release/bioc/vignettes/affy/inst/doc/affy.pdf.

Ge, X., Wang, F., Guo, X., Yang, H., 2012. Porcine circovirus type 2 and its associated diseases in China. Virus Res 164, 100-106.

Genini, S., Delputte, P.L., Malinverni, R., Cecere, M., Stella, A., Nauwynck, H.J., Giuffra, E., 2008. Genome-wide transcriptional response of primary alveolar macrophages following infection with porcine reproductive and respiratory syndrome virus. J Gen Virol 89, 2550-2564.

Gentleman, R.C., Carey, V.J., Bates, D.M., Bolstad, B., Dettling, M., Dudoit, S., Ellis, B., Gautier, L., Ge, Y., Gentry, J., Hornik, K., Hothorn, T., Huber, W., Iacus, S., Irizarry, R., Leisch, F., Li, C., Maechler, M., Rossini, A.J., Sawitzki, G., Smith, C., Smyth, G., Tierney, L., Yang, J.Y., Zhang, J., 2004. Bioconductor: open software development for computational biology and bioinformatics. Genome Biol 5, R80.

Gerber, P.F., Garrocho, F.M., Lana, A.M., Lobato, Z.I., 2011. Serum antibodies and shedding of infectious porcine circovirus 2 into colostrum and milk of vaccinated and unvaccinated naturally infected sows. Veterinary journal 188, 240-242.

Gillespie, D., Spiegelman, S., 1965. A quantitative assay for DNA-RNA hybrids with DNA immobilized on a membrane. Journal of molecular biology 12, 829-842.

Gilpin, D.F., McCullough, K., Meehan, B.M., McNeilly, F., McNair, I., Stevenson, L.S., Foster, J.C., Ellis, J.A., Krakowka, S., Adair, B.M., Allan, G.M., 2003. In vitro studies on the infection and replication of porcine circovirus type 2 in cells of the porcine immune system. Veterinary immunology and immunopathology 94, 149-161.

Grasland, B., Loizel, C., Blanchard, P., Oger, A., Nignol, A.C., Bigarre, L., Morvan, H., Cariolet, R., Jestin, A., 2005. Reproduction of PMWS in immunostimulated SPF piglets transfected with infectious cloned genomic DNA of type 2 porcine circovirus. Veterinary research 36, 685-697.

Grau-Roma, L., Crisci, E., Sibila, M., Lopez-Soria, S., Nofrarias, M., Cortey, M., Fraile, L., Olvera, A., Segales, J., 2008. A proposal on porcine circovirus type 2 (PCV2) genotype definition and their relation with postweaning multisystemic wasting syndrome (PMWS) occurrence. Vet Microbiol 128, 23-35.

Grau-Roma, L., Fraile, L., Segales, J., 2011. Recent advances in the epidemiology, diagnosis and control of diseases caused by porcine circovirus type 2. Veterinary journal 187, 23-32.

Grau-Roma, L., Heegaard, P.M., Hjulsager, C.K., Sibila, M., Kristensen, C.S., Allepuz, A., Pineiro, M., Larsen, L.E., Segales, J., Fraile, L., 2009b. Pig-major acute phase protein and haptoglobin serum concentrations correlate with PCV2 viremia and the clinical course of postweaning multisystemic wasting syndrome. Vet Microbiol 138, 53-61.

Grau-Roma, L., Hjulsager, C.K., Sibila, M., Kristensen, C.S., Lopez-Soria, S., Enoe, C., Casal, J., Botner, A., Nofrarias, M., Bille-Hansen, V., Fraile, L., Baekbo, P., Segales, J., Larsen, L.E., 2009a. Infection, excretion and seroconversion dynamics of porcine circovirus type 2 (PCV2) in pigs from post-weaning multisystemic wasting syndrome (PMWS) affected farms in Spain and Denmark. Vet Microbiol 135, 272-282.

Grau-Roma, L., Stockmarr, A., Kristensen, C.S., Enoe, C., Lopez-Soria, S., Nofrarias, M., Bille-Hansen, V., Hjulsager, C.K., Sibila, M., Jorsal, S.E., Fraile, L., Baekbo, P., Vigre, H., Segales, J., Larsen, L.E., 2012. Infectious risk factors for individual postweaning multisystemic wasting syndrome (PMWS) development in pigs from affected farms in Spain and Denmark. Res Vet Sci 93, 1231-1240.

Gunderson, K.L., Kruglyak, S., Graige, M.S., Garcia, F., Kermani, B.G., Zhao, C., Che, D., Dickinson, T., Wickham, E., Bierle, J., Doucet, D., Milewski, M., Yang, R., Siegmund, C., Haas, J., Zhou, L., Oliphant, A., Fan, J.B., Barnard, S., Chee, M.S., 2004. Decoding randomly ordered DNA arrays. Genome research 14, 870-877.

Guo, L.J., Lu, Y.H., Wei, Y.W., Huang, L.P., Liu, C.M., 2010a. Porcine circovirus type 2 (PCV2): genetic variation and newly emerging genotypes in China. Virol J 7, 273.

Guo, S., Yang, C., Mei, F., Wu, S., Luo, N., Fei, L., Chen, Y., Wu, Y., 2010b. Down-regulation of Z39Ig on macrophages by IFN-gamma in patients with chronic HBV infection. Clinical immunology 136, 282-291.

Hall, T.A., 1999. BioEdit: a user-friendly biological sequence alignment editor and analysis program for Windows 95/98/NT. Nucleic Acids Symposiun Ser 41, 95-98.

Hamel, A.L., Lin, L.L., Nayar, G.P., 1998. Nucleotide sequence of porcine circovirus associated with postweaning multisystemic wasting syndrome in pigs. J Virol 72, 5262-5267.

Hammamieh, R., Bi, S., Das, R., Neill, R., Jett, M., 2004. Modeling of SEB-induced host gene expression to correlate in vitro to in vivo responses. Biosens Bioelectron 20, 719-727.

Hansen, M.S., Pors, S.E., Bille-Hansen, V., Kjerulff, S.K., Nielsen, O.L., 2010. Occurrence and tissue distribution of porcine circovirus type 2 identified by immunohistochemistry in Danish finishing pigs at slaughter. Journal of comparative pathology 142, 109-121.

Harding, J.C., Ellis, J.A., McIntosh, K.A., Krakowka, S., 2010. Dual heterologous porcine circovirus genogroup 2a/2b infection induces severe disease in germ-free pigs. Vet Microbiol 145, 209-219.

Harms, P.A., Sorden, S.D., Halbur, P.G., Bolin, S.R., Lager, K.M., Morozov, I., Paul, P.S., 2001. Experimental reproduction of severe disease in CD/CD pigs concurrently infected with type 2 porcine circovirus and porcine reproductive and respiratory syndrome virus. Vet Pathol 38, 528-539.

Hasslung, F., Wallgren, P., Ladekjaer-Hansen, A.S., Botner, A., Nielsen, J., Wattrang, E., Allan, G.M., McNeilly, F., Ellis, J., Timmusk, S., Belak, K., Segall, T., Melin, L., Berg, M., Fossum, C., 2005. Experimental reproduction of postweaning multisystemic wasting syndrome (PMWS) in pigs in Sweden and Denmark with a Swedish isolate of porcine circovirus type 2. Vet Microbiol 106, 49-60.

He, J., Cao, J., Zhou, N., Jin, Y., Wu, J., Zhou, J., 2013. Identification and functional analysis of the novel ORF4 protein encoded by porcine circovirus type 2. J Virol 87, 1420-1429.

He, J.Q., Wiesmann, C., van Lookeren Campagne, M., 2008. A role of macrophage complement receptor CRIg in immune clearance and inflammation. Molecular immunology 45, 4041-4047.

Hedegaard, J., Skovgaard, K., Mortensen, S., Sorensen, P., Jensen, T.K., Hornshoj, H., Bendixen, C., Heegaard, P.M., 2007. Molecular characterisation of the early response in pigs to experimental infection with Actinobacillus pleuropneumoniae using cDNA microarrays. Acta veterinaria Scandinavica 49, 11.

Herrmann, J., Lerman, L.O., Lerman, A., 2007. Ubiquitin and ubiquitin-like proteins in protein regulation. Circulation research 100, 1276-1291.

Hesse, R., Kerrigan, M., Rowland, R.R., 2008. Evidence for recombination between PCV2a and PCV2b in the field. Virus Res 132, 201-207.

Hetts, S.W., 1998. To die or not to die: an overview of apoptosis and its role in disease. Jama 279, 300-307.

Hirai, T., Nunoya, T., Ihara, T., Saitoh, T., Shibuya, K., Nakamura, K., 2006. Infectivity of porcine circovirus 1 and circovirus 2 in primary porcine hepatocyte and kidney cell cultures. J Vet Med Sci 68, 179-182.

Hong, J.S., Kim, N.H., Choi, C.Y., Lee, J.S., Na, D., Chun, T., Lee, Y.S., 2015. Changes in cellular microRNA expression induced by porcine circovirus type 2-encoded proteins. Veterinary research 46, 39.

Hosack, D.A., Dennis, G., Jr., Sherman, B.T., Lane, H.C., Lempicki, R.A., 2003. Identifying biological themes within lists of genes with EASE. Genome Biol 4, R70.

Huang, D.R., Wang, J., Kivisakk, P., Rollins, B.J., Ransohoff, R.M., 2001. Absence of monocyte chemoattractant protein 1 in mice leads to decreased local macrophage recruitment and antigen-specific T helper cell type 1 immune response in experimental autoimmune encephalomyelitis. The Journal of experimental medicine 193, 713-726.

Huang, D.W., Sherman, B.T., Lempicki, R.A., 2009a. Bioinformatics enrichment tools: paths toward the comprehensive functional analysis of large gene lists. Nucleic Acids Res 37, 1-13.

Huang, D.W., Sherman, B.T., Lempicki, R.A., 2009b. Systematic and integrative analysis of large gene lists using DAVID bioinformatics resources. Nat Protoc 4, 44-57.

Huang, L.P., Lu, Y.H., Wei, Y.W., Guo, L.J., Liu, C.M., 2011. Identification of one critical amino acid that determines a conformational neutralizing epitope in the capsid protein of porcine circovirus type 2. BMC Microbiol 11, 188.

Huang, Y., Wange, R.L., 2004. T cell receptor signaling: beyond complex complexes. J Biol Chem 279, 28827-28830.

Huber, W., von Heydebreck, A., Sultmann, H., Poustka, A., Vingron, M., 2002. Variance stabilization applied to microarray data calibration and to the quantification of differential expression. Bioinformatics 18 Suppl 1, S96-104.

Hughes, T.R., Mao, M., Jones, A.R., Burchard, J., Marton, M.J., Shannon, K.W., Lefkowitz, S.M., Ziman, M., Schelter, J.M., Meyer, M.R., Kobayashi, S., Davis, C., Dai, H., He, Y.D., Stephaniants, S.B., Cavet, G., Walker, W.L., West, A., Coffey, E., Shoemaker, D.D., Stoughton, R., Blanchard, A.P., Friend, S.H., Linsley, P.S., 2001. Expression profiling using microarrays fabricated by an ink-jet oligonucleotide synthesizer. Nat Biotechnol 19, 342-347.

Irizarry, R.A., Bolstad, B.M., Collin, F., Cope, L.M., Hobbs, B., Speed, T.P., 2003b. Summaries of Affymetrix GeneChip probe level data. Nucleic Acids Res 31, e15.

Irizarry, R.A., Hobbs, B., Collin, F., Beazer-Barclay, Y.D., Antonellis, K.J., Scherf, U., Speed, T.P., 2003a. Exploration, normalization, and summaries of high density oligonucleotide array probe level data. Biostatistics 4, 249-264.

Irizarry, R.A., Warren, D., Spencer, F., Kim, I.F., Biswal, S., Frank, B.C., Gabrielson, E., Garcia, J.G., Geoghegan, J., Germino, G., Griffin, C., Hilmer, S.C., Hoffman, E., Jedlicka, A.E., Kawasaki, E., Martinez-Murillo, F., Morsberger, L., Lee, H., Petersen, D., Quackenbush, J., Scott, A., Wilson, M., Yang, Y., Ye, S.Q., Yu, W., 2005. Multiple-laboratory comparison of microarray platforms. Nat Methods 2, 345-350.

Irizarry, R.A., Wu, Z., Jaffee, H.A., 2006. Comparison of Affymetrix GeneChip expression measures. Bioinformatics 22, 789-794.

Jacobsen, B., Krueger, L., Seeliger, F., Bruegmann, M., Segales, J., Baumgaertner, W., 2009. Retrospective study on the occurrence of porcine circovirus 2 infection and associated entities in Northern Germany. Vet Microbiol 138, 27-33.

Janeway, C.A., Travers, P., Walport, M., Shlomchik, M.J., 2001. Immunobiology: The Immune System in Health and Disease, 5th Edition Edition. Garland Science

Jarvinen, A.K., Hautaniemi, S., Edgren, H., Auvinen, P., Saarela, J., Kallioniemi, O.P., Monni, O., 2004. Are data from different gene expression microarray platforms comparable? Genomics 83, 1164-1168.

Jault, F.M., Jault, J.M., Ruchti, F., Fortunato, E.A., Clark, C., Corbeil, J., Richman, D.D., Spector, D.H., 1995. Cytomegalovirus infection induces high levels of cyclins, phosphorylated Rb, and p53, leading to cell cycle arrest. J Virol 69, 6697-6704.

Juhan, N.M., LeRoith, T., Opriessnig, T., Meng, X.J., 2010. The open reading frame 3 (ORF3) of porcine circovirus type 2 (PCV2) is dispensable for virus infection but evidence of reduced pathogenicity is limited in pigs infected by an ORF3-null PCV2 mutant. Virus Res 147, 60-66.

Jung, K., Kang, M., Park, C., Hyun Choi, Y., Jeon, Y., Park, S.H., Seo, S.K., Jin, D., Choi, I., 2012. Protective role of V-set and immunoglobulin domain-containing 4 expressed on kupffer cells during immune-mediated liver injury by inducing tolerance of liver T- and natural killer T-cells. Hepatology 56, 1838-1848.

Kafatos, F.C., Jones, C.W., Efstratiadis, A., 1979. Determination of nucleic acid sequence homologies and relative concentrations by a dot hybridization procedure. Nucleic Acids Res 7, 1541-1552.

Kane, L.P., Lin, J., Weiss, A., 2000. Signal transduction by the TCR for antigen. Curr Opin Immunol 12, 242-249.

Karakach, T.K., Flight, R.M., Douglas, S.E., Wentzell, P.D., 2010. An introduction to DNA microarrays for gene expression analysis. Chemometrics and Intelligent Laboratory Systems 104 28-52.

Karlskov-Mortensen, P., Kristensen, C.S., Grau-Roma, L., Bille-Hansen, V., Mc Neilly, F., Jorgensen, C.B., Baekbo, P., Segalés, J., Fredholm, M., 2008. Closing in on a locus with effect on PMWS susceptibility. *In*: Proceedings of 2nd European conference of pigs genomics.

Karuppannan, A.K., Jong, M.H., Lee, S.H., Zhu, Y., Selvaraj, M., Lau, J., Jia, Q., Kwang, J., 2009. Attenuation of porcine circovirus 2 in SPF piglets by abrogation of ORF3 function. Virology 383, 338-347.

Karuppannan, A.K., Kwang, J., 2011. ORF3 of porcine circovirus 2 enhances the in vitro and in vivo spread of the of the virus. Virology 410, 248-256.

Karuppannan, A.K., Liu, S., Jia, Q., Selvaraj, M., Kwang, J., 2010. Porcine circovirus type 2 ORF3 protein competes with p53 in binding to Pirh2 and mediates the deregulation of p53 homeostasis. Virology 398, 1-11.

Khaiseb, S., Sydler, T., Zimmermann, D., Pospischil, A., Sidler, X., Brugnera, E., 2011. Coreplication of the major genotype group members of porcine circovirus type 2 as a prerequisite to coevolution may explain the variable disease manifestations. J Virol 85, 11111-11120.

Khatri, P., Draghici, S., 2005. Ontological analysis of gene expression data: current tools, limitations, and open problems. Bioinformatics 21, 3587-3595.

Khera, R., Das, N., 2009. Complement Receptor 1: disease associations and therapeutic implications. Molecular immunology 46, 761-772.

Kim, H.K., Luo, Y., Moon, H.J., Park, S.J., Keum, H.O., Rho, S., Park, B.K., 2009. Phylogenetic and recombination analysis of genomic sequences of PCV2 isolated in Korea. Virus Genes 39, 352-358.

Kim, J., Chae, C., 2004. Expression of monocyte chemoattractant protein-1 and macrophage inflammatory protein-1 in porcine circovirus 2-induced granulomatous inflammation. Journal of comparative pathology 131, 121-126.

Kiupel, M., Stevenson, G.W., Choi, J., Latimer, K.S., Kanitz, C.L., Mittal, S.K., 2001. Viral replication and lesions in BALB/c mice experimentally inoculated with porcine circovirus isolated from a pig with postweaning multisystemic wasting disease. Vet Pathol 38, 74-82.

Kixmoller, M., Ritzmann, M., Eddicks, M., Saalmuller, A., Elbers, K., Fachinger, V., 2008. Reduction of PMWS-associated clinical signs and co-infections by vaccination against PCV2. Vaccine 26, 3443-3451.

Kohonen, T., 1997. Self-Organizating MapsNew York.

Krakowka, S., Allan, G., Ellis, J., Hamberg, A., Charreyre, C., Kaufmann, E., Brooks, C., Meehan, B., 2012. A nine-base nucleotide sequence in the porcine circovirus type 2 (PCV2) nucleocapsid gene determines viral replication and virulence. Virus Res 164, 90-99.

Krakowka, S., Ellis, J., McNeilly, F., Meehan, B., Oglesbee, M., Alldinger, S., Allan, G., 2004. Features of cell degeneration and death in hepatic failure and systemic lymphoid depletion characteristic of porcine circovirus-2-associated postweaning multisystemic wasting disease. Vet Pathol 41, 471-481.

Krakowka, S., Ellis, J., McNeilly, F., Waldner, C., Rings, D.M., Allan, G., 2007. Mycoplasma hyopneumoniae bacterins and porcine circovirus type 2 (PCV2) infection: induction of postweaning multisystemic wasting syndrome (PMWS) in the gnotobiotic swine model of PCV2-associated disease. Can Vet J 48, 716-724.

Krakowka, S., Ellis, J.A., McNeilly, F., Ringler, S., Rings, D.M., Allan, G., 2001. Activation of the immune system is the pivotal event in the production of wasting disease in pigs infected with porcine circovirus-2 (PCV-2). Vet Pathol 38, 31-42.

Krakowka, S., Ellis, J.A., Meehan, B., Kennedy, S., McNeilly, F., Allan, G., 2000. Viral wasting syndrome of swine: experimental reproduction of postweaning multisystemic wasting syndrome in gnotobiotic swine by coinfection with porcine circovirus 2 and porcine parvovirus. Vet Pathol 37, 254-263.

Kristensen, C.S., Baadsgaard, N.P., Toft, N., 2011. A meta-analysis comparing the effect of PCV2 vaccines on average daily weight gain and mortality rate in pigs from weaning to slaughter. Preventive veterinary medicine 98, 250-258.

Ladekjaer-Mikkelsen, A.S., Nielsen, J., Stadejek, T., Storgaard, T., Krakowka, S., Ellis, J., McNeilly, F., Allan, G., Botner, A., 2002. Reproduction of postweaning multisystemic wasting syndrome (PMWS) in immunostimulated and non-immunostimulated 3-week-old piglets experimentally infected with porcine circovirus type 2 (PCV2). Vet Microbiol 89, 97-114.

Lambris, J.D., Ricklin, D., Geisbrecht, B.V., 2008. Complement evasion by human pathogens. Nat Rev Microbiol 6, 132-142.

Larochelle, R., Magar, R., D'Allaire, S., 2002. Genetic characterization and phylogenetic analysis of porcine circovirus type 2 (PCV2) strains from cases presenting various clinical conditions. Virus Res 90, 101-112.

Larochelle, R., Magar, R., D'Allaire, S., 2003. Comparative serologic and virologic study of commercial swine herds with and without postweaning multisystemic wasting syndrome. Can J Vet Res 67, 114-120.

Lee, C., Bachand, A., Murtaugh, M.P., Yoo, D., 2004. Differential host cell gene expression regulated by the porcine reproductive and respiratory syndrome virus GP4 and GP5 glycoproteins. Veterinary immunology and immunopathology 102, 189-198.

Lee, G., Han, D., Song, J.Y., Lee, Y.S., Kang, K.S., Yoon, S., 2010. Genomic expression profiling in lymph nodes with lymphoid depletion from porcine circovirus 2-infected pigs. J Gen Virol 91, 2585-2591.

Lefebvre, D., 2009a. Genetic, antigenetic and pathogenic features of porcine circovirus type 2 strains. Ghent University, Belgium.

Lefebvre, D.J., Meerts, P., Costers, S., Misinzo, G., Barbe, F., Van Reeth, K., Nauwynck, H.J., 2008. Increased porcine circovirus type 2 replication in porcine leukocytes in vitro and in vivo by concanavalin A stimulation. Vet Microbiol 132, 74-86.

Lefebvre, D.J., Van Doorsselaere, J., Delputte, P.L., Nauwynck, H.J., 2009b. Recombination of two porcine circovirus type 2 strains. Arch Virol 154, 875-879.

Lekcharoensuk, P., Morozov, I., Paul, P.S., Thangthumniyom, N., Wajjawalku, W., Meng, X.J., 2004. Epitope mapping of the major capsid protein of type 2 porcine circovirus (PCV2) by using chimeric PCV1 and PCV2. J Virol 78, 8135-8145.

Lennon, G.G., Lehrach, H., 1991. Hybridization analyses of arrayed cDNA libraries. Trends in genetics : TIG 7, 314-317.

Lewis, C.R., Ait-Ali, T., Clapperton, M., Archibald, A.L., Bishop, S., 2007. Genetic perspectives on host responses to porcine reproductive and respiratory syndrome (PRRS). Viral immunology 20, 343-358.

Li, C., Wong, W.H., 2001. Model-based analysis of oligonucleotide arrays: expression index computation and outlier detection. Proc Natl Acad Sci U S A 98, 31-36.

Li, J., Yu, Q., Nie, X., Guo, X., Song, Q., Li, H., 2012. Effects of porcine circovirus type 2 on expression of mRNA associated with endogenous antigen processing and presentation in pulmonary alveolar macrophages and circulating T lymphocytes in piglets. Veterinary journal 193, 199-205.

Li, L., Kapoor, A., Slikas, B., Bamidele, O.S., Wang, C., Shaukat, S., Masroor, M.A., Wilson, M.L., Ndjango, J.B., Peeters, M., Gross-Camp, N.D., Muller, M.N., Hahn, B.H., Wolfe, N.D., Triki, H., Bartkus, J., Zaidi, S.Z., Delwart, E., 2010. Multiple diverse circoviruses infect farm animals and are commonly found in human and chimpanzee feces. J Virol 84, 1674-1682.

Li, Q., Smith, A.J., Schacker, T.W., Carlis, J.V., Duan, L., Reilly, C.S., Haase, A.T., 2009. Microarray analysis of lymphatic tissue reveals stage-specific, gene expression signatures in HIV-1 infection. Journal of immunology 183, 1975-1982.

Li, W., Liu, S., Wang, Y., Deng, F., Yan, W., Yang, K., Chen, H., He, Q., Charreyre, C., Audoneet, J.C., 2013. Transcription analysis of the porcine alveolar macrophage response to porcine circovirus type 2. BMC genomics 14, 353.

Lim, J.K., Lisco, A., McDermott, D.H., Huynh, L., Ward, J.M., Johnson, B., Johnson, H., Pape, J., Foster, G.A., Krysztof, D., Follmann, D., Stramer, S.L., Margolis, L.B., Murphy, P.M., 2009. Genetic

variation in OAS1 is a risk factor for initial infection with West Nile virus in man. PLoS Pathog 5, e1000321.

Lin, C.M., Jeng, C.R., Chang, H.W., Guo, I.C., Huang, Y.L., Tsai, Y.C., Chia, M.Y., Pang, V.F., 2008. Characterization of porcine circovirus type 2 (PCV2) infection in swine lymphocytes using mitogen-stimulated peripheral blood lymphocytes from healthy PCV2-carrier pigs. Veterinary immunology and immunopathology 124, 355-366.

Lin, C.M., Jeng, C.R., Hsiao, S.H., Liu, J.P., Chang, C.C., Chiou, M.T., Tsai, Y.C., Chia, M.Y., Pang, V.F., 2011b. Immunopathological characterization of porcine circovirus type 2 infection-associated follicular changes in inguinal lymph nodes using high-throughput tissue microarray. Vet Microbiol 149, 72-84.

Lin, C.M., Jeng, C.R., Liu, J.P., Lin, E.C., Chang, C.C., Huang, Y.L., Tsai, Y.C., Chia, M.Y., Wan, C.H., Pang, V.F., 2013. Immune gene expression profiles in swine inguinal lymph nodes with different viral loads of porcine circovirus type 2. Vet Microbiol 162, 519-529.

Lin, W.L., Chien, M.S., Wu, P.C., Lai, C.L., Huang, C., 2011a. The Porcine Circovirus Type 2 Nonstructural Protein ORF3 Induces Apoptosis in Porcine Peripheral Blood Mononuclear Cells. The open virology journal 5, 148-153.

Lipshutz, R.J., Fodor, S.P., Gingeras, T.R., Lockhart, D.J., 1999. High density synthetic oligonucleotide arrays. Nat Genet 21, 20-24.

Liu, J., Bai, J., Lu, Q., Zhang, L., Jiang, Z., Michal, J.J., He, Q., Jiang, P., 2013. Two-dimensional liquid chromatography-tandem mass spectrometry coupled with isobaric tags for relative and absolute quantification (iTRAQ) labeling approach revealed first proteome profiles of pulmonary alveolar macrophages infected with porcine circovirus type 2. Journal of proteomics 79, 72-86.

Liu, J., Chen, I., Du, Q., Chua, H., Kwang, J., 2006. The ORF3 protein of porcine circovirus type 2 is involved in viral pathogenesis in vivo. J Virol 80, 5065-5073.

Liu, J., Chen, I., Kwang, J., 2005. Characterization of a previously unidentified viral protein in porcine circovirus type 2-infected cells and its role in virus-induced apoptosis. J Virol 79, 8262-8274.

Liu, J., Zhu, Y., Chen, I., Lau, J., He, F., Lau, A., Wang, Z., Karuppannan, A.K., Kwang, J., 2007. The ORF3 protein of porcine circovirus type 2 interacts with porcine ubiquitin E3 ligase Pirh2 and facilitates p53 expression in viral infection. J Virol 81, 9560-9567.

Livak, K.J., Schmittgen, T.D., 2001. Analysis of relative gene expression data using real-time quantitative PCR and the 2(-Delta Delta C(T)) Method. Methods 25, 402-408.

Lockhart, D.J., Dong, H., Byrne, M.C., Follettie, M.T., Gallo, M.V., Chee, M.S., Mittmann, M., Wang, C., Kobayashi, M., Horton, H., Brown, E.L., 1996. Expression monitoring by hybridization to high-density oligonucleotide arrays. Nat Biotechnol 14, 1675-1680.

Loizel, C., Blanchard, P., Grasland, B., Dory, D., Oger, A., Nignol, A.C., Cariolet, R., Jestin, A., 2005. Effect of granulocyte-macrophage colony-stimulating factor on post-weaning multisystemic wasting syndrome in porcine circovirus type-2-transfected piglets. Int J Exp Pathol 86, 33-43.

Lopez-Soria, S., Nofrarias, M., Calsamiglia, M., Espinal, A., Valero, O., Ramirez-Mendoza, H., Minguez, A., Serrano, J.M., Marin, O., Callen, A., Segales, J., 2011. Post-weaning multisystemic wasting syndrome (PMWS) clinical expression under field conditions is modulated by the pig genetic background. Vet Microbiol 149, 352-357.

Lopez-Soria, S., Segales, J., Rose, N., Vinas, M.J., Blanchard, P., Madec, F., Jestin, A., Casal, J., Domingo, M., 2005. An exploratory study on risk factors for postweaning multisystemic wasting syndrome (PMWS) in Spain. Preventive veterinary medicine 69, 97-107.

Loureiro, J., Ploegh, H.L., 2006. Antigen presentation and the ubiquitin-proteasome system in host-pathogen interactions. Advances in immunology 92, 225-305.

Lukert, P., de Boer, G.F., Dale, J.L., Keese, P., McNulty, M.S., Tischer, I. 1995. The Circoviridae. Virus Taxonomy. In: Sixth Report of the International Committee on Taxonomy of Viruses, 166-168.

Lyoo, K., Joo, H., Caldwell, B., Kim, H., Davies, P.R., Torrison, J., 2011. Comparative efficacy of three commercial PCV2 vaccines in conventionally reared pigs. Veterinary journal 189, 58-62.

Ma, C.M., Hon, C.C., Lam, T.Y., Li, V.Y., Wong, C.K., de Oliveira, T., Leung, F.C., 2007. Evidence for recombination in natural populations of porcine circovirus type 2 in Hong Kong and mainland China. J Gen Virol 88, 1733-1737.

MacQueen, J.B. 1967. Some Methods for Classification and Analysis of MultiVariate Observations. In: In: Fifth Berkeley Symposium on Mathematical Statistics and Probability, Berkeley, 281-297.

Madec, F., Eveno, E., Morvan, P., Hamon, L., Blanchard, P., Cariolet, R., Amenna, N., Morvan, H., Truong, C., Mahé, D., Albina, E., Jestin, A., 2000. Post-weaning multisystemic wasting syndrome (PMWS) in pigs in France: clinical observations from follow-up studies on affected farms. Livestock Production Science 63, 223-233.

Madec, F., Rose, N., Eveno, E., Morvan, P., Larour, G., Jolly, J.P., Le Diguerher, G., Cariolet, R., Le Dimna, M., Blanchard, P., Jestin, A. 2001
PMWS: on-farm observations and preliminary analytic epidemiology. In: Proceedings ssDNA Viruses Plants, Birds, Pigs and Primates (ESVV), 86-87.

Madec, F., Rose, N., Grasland, B., Cariolet, R., Jestin, A., 2008. Post-Weaning Multisystemic Wasting Syndrome and Other PCV2-Related Problems in Pigs: a 12-Year Experience. Transbound Emerg Dis.

Madson, D.M., Opriessnig, T., 2011. Effect of porcine circovirus type 2 (PCV2) infection on reproduction: disease, vertical transmission, diagnostics and vaccination. Animal health research reviews / Conference of Research Workers in Animal Diseases 12, 47-65.

Madson, D.M., Patterson, A.R., Ramamoorthy, S., Pal, N., Meng, X.J., Opriessnig, T., 2009b. Effect of porcine circovirus type 2 (PCV2) vaccination of the dam on PCV2 replication in utero. Clinical and vaccine immunology : CVI 16, 830-834.

Madson, D.M., Ramamoorthy, S., Kuster, C., Pal, N., Meng, X.J., Halbur, P.G., Opriessnig, T., 2008. Characterization of shedding patterns of Porcine circovirus types 2a and 2b in experimentally inoculated mature boars. J Vet Diagn Invest 20, 725-734.

Madson, D.M., Ramamoorthy, S., Kuster, C., Pal, N., Meng, X.J., Halbur, P.G., Opriessnig, T., 2009a. Infectivity of porcine circovirus type 2 DNA in semen from experimentally-infected boars. Veterinary research 40, 10.

Magar, R., Muller, P., Larochelle, R., 2000. Retrospective serological survey of antibodies to porcine circovirus type 1 and type 2. Can J Vet Res 64, 184-186.

Mahe, D., Blanchard, P., Truong, C., Arnauld, C., Le Cann, P., Cariolet, R., Madec, F., Albina, E., Jestin, A., 2000. Differential recognition of ORF2 protein from type 1 and type 2 porcine circoviruses and identification of immunorelevant epitopes. J Gen Virol 81, 1815-1824.

Mandrioli, L., Sarli, G., Panarese, S., Baldoni, S., Marcato, P.S., 2004. Apoptosis and proliferative activity in lymph node reaction in postweaning multisystemic wasting syndrome (PMWS). Veterinary immunology and immunopathology 97, 25-37.

Mankertz, A., Caliskan, R., Hattermann, K., Hillenbrand, B., Kurzendoerfer, P., Mueller, B., Schmitt, C., Steinfeldt, T., Finsterbusch, T., 2004. Molecular biology of Porcine circovirus: analyses of gene expression and viral replication. Vet Microbiol 98, 81-88.

Mankertz, A., Domingo, M., Folch, J.M., LeCann, P., Jestin, A., Segales, J., Chmielewicz, B., Plana-Duran, J., Soike, D., 2000. Characterisation of PCV-2 isolates from Spain, Germany and France. Virus Res 66, 65-77.

Maskos, U., Southern, E.M., 1993a. A novel method for the analysis of multiple sequence variants by hybridisation to oligonucleotides. Nucleic Acids Res 21, 2267-2268.

Maskos, U., Southern, E.M., 1993b. A novel method for the parallel analysis of multiple mutations in multiple samples. Nucleic Acids Res 21, 2269-2270.

Maurer, K., Cooper, J., Caraballo, M., Crye, J., Suciu, D., Ghindilis, A., Leonetti, J.A., Wang, W., Rossi, F.M., Stover, A.G., Larson, C., Gao, H., Dill, K., McShea, A., 2006. Electrochemically generated acid and its containment to 100 micron reaction areas for the production of DNA microarrays. PloS one 1, e34.

Mavrommatis, B., Offord, V., Patterson, R., Watson, M., Kanellos, T., Steinbach, F., Grierson, S., Werling, D., 2014. Global gene expression profiling of myeloid immune cell subsets in response to in vitro challenge with porcine circovirus 2b. PloS one 9, e91081.

McKeown, N.E., Opriessnig, T., Thomas, P., Guenette, D.K., Elvinger, F., Fenaux, M., Halbur, P.G., Meng, X.J., 2005. Effects of porcine circovirus type 2 (PCV2) maternal antibodies on experimental infection of piglets with PCV2. Clin Diagn Lab Immunol 12, 1347-1351.

Medzhitov, R., 2010. Inflammation 2010: new adventures of an old flame. Cell 140, 771-776.

Meehan, B.M., McNeilly, F., Todd, D., Kennedy, S., Jewhurst, V.A., Ellis, J.A., Hassard, L.E., Clark, E.G., Haines, D.M., Allan, G.M., 1998. Characterization of novel circovirus DNAs associated with wasting syndromes in pigs. J Gen Virol 79 (Pt 9), 2171-2179.

Meerts, P., Misinzo, G., Lefebvre, D., Nielsen, J., Botner, A., Kristensen, C.S., Nauwynck, H.J., 2006. Correlation between the presence of neutralizing antibodies against porcine circovirus 2 (PCV2) and protection against replication of the virus and development of PCV2-associated disease. BMC Vet Res 2, 6.

Meerts, P., Misinzo, G., McNeilly, F., Nauwynck, H.J., 2005a. Replication kinetics of different porcine circovirus 2 strains in PK-15 cells, fetal cardiomyocytes and macrophages. Arch Virol 150, 427-441.

Meerts, P., Misinzo, G., Nauwynck, H.J., 2005c. Enhancement of porcine circovirus 2 replication in porcine cell lines by IFN-gamma before and after treatment and by IFN-alpha after treatment. J Interferon Cytokine Res 25, 684-693.

Meerts, P., Van Gucht, S., Cox, E., Vandebosch, A., Nauwynck, H.J., 2005b. Correlation between type of adaptive immune response against porcine circovirus type 2 and level of virus replication. Viral immunology 18, 333-341.

Meng, T., Jia, Q., Liu, S., Karuppannan, A.K., Chang, C.C., Kwang, J., 2010. Characterization and epitope mapping of monoclonal antibodies recognizing N-terminus of Rep of porcine circovirus type 2. J Virol Methods 165, 222-229.

Michael, K.L., Taylor, L.C., Schultz, S.L., Walt, D.R., 1998. Randomly ordered addressable high-density optical sensor arrays. Analytical chemistry 70, 1242-1248.

Millenaar, F.F., Okyere, J., May, S.T., van Zanten, M., Voesenek, L.A., Peeters, A.J., 2006. How to decide? Different methods of calculating gene expression from short oligonucleotide array data will give different results. BMC Bioinformatics 7, 137.

Miller, L.C., Fox, J.M., 2004. Apoptosis and porcine reproductive and respiratory syndrome virus. Veterinary immunology and immunopathology 102, 131-142.

Miller, M.B., Tang, Y.W., 2009. Basic concepts of microarrays and potential applications in clinical microbiology. Clin Microbiol Rev 22, 611-633.

Misinzo, G., Delputte, P.L., Lefebvre, D.J., Nauwynck, H.J., 2009. Porcine circovirus 2 infection of epithelial cells is clathrin-, caveolae- and dynamin-independent, actin and Rho-GTPase-mediated, and enhanced by cholesterol depletion. Virus Res 139, 1-9.

Misinzo, G., Delputte, P.L., Meerts, P., Lefebvre, D.J., Nauwynck, H.J., 2006. Porcine circovirus 2 uses heparan sulfate and chondroitin sulfate B glycosaminoglycans as receptors for its attachment to host cells. J Virol 80, 3487-3494.

Misinzo, G., Delputte, P.L., Nauwynck, H.J., 2008. Inhibition of endosome-lysosome system acidification enhances porcine circovirus 2 infection of porcine epithelial cells. J Virol 82, 1128-1135.

Misinzo, G., Meerts, P., Bublot, M., Mast, J., Weingartl, H.M., Nauwynck, H.J., 2005. Binding and entry characteristics of porcine circovirus 2 in cells of the porcine monocytic line 3D4/31. J Gen Virol 86, 2057-2068.

Miura, Y., Misawa, N., Maeda, N., Inagaki, Y., Tanaka, Y., Ito, M., Kayagaki, N., Yamamoto, N., Yagita, H., Mizusawa, H., Koyanagi, Y., 2001. Critical contribution of tumor necrosis factor-related apoptosis-inducing ligand (TRAIL) to apoptosis of human CD4+ T cells in HIV-1-infected hu-PBL-NOD-SCID mice. The Journal of experimental medicine 193, 651-660.

Moser, R.J., Reverter, A., Kerr, C.A., Beh, K.J., Lehnert, S.A., 2004. A mixed-model approach for the analysis of cDNA microarray gene expression data from extreme-performing pigs after infection with Actinobacillus pleuropneumoniae. J Anim Sci 82, 1261-1271.

Naef, F., Hacker, C.R., Patil, N., Magnasco, M., 2002. Empirical characterization of the expression ratio noise structure in high-density oligonucleotide arrays. Genome Biol 3, RESEARCH0018.

Naraballobh, W., Chomdej, S., Murani, E., Wimmers, K., Ponsuksili, S., 2010. Annotation and in silico localization of the Affymetrix GeneChip Porcine Genome Array. Arch Tierz 53, 230-238.

Nauwynck, H.J., Sanchez, R., Meerts, P., Lefebvre, D.J., Saha, D., Huang, L., Misinzo, G., 2012. Cell tropism and entry of porcine circovirus 2. Virus Res 164, 43-45.

Nawagitgul, P., Morozov, I., Bolin, S.R., Harms, P.A., Sorden, S.D., Paul, P.S., 2000. Open reading frame 2 of porcine circovirus type 2 encodes a major capsid protein. J Gen Virol 81, 2281-2287.

Negre, N., Lavrov, S., Hennetin, J., Bellis, M., Cavalli, G., 2006. Mapping the distribution of chromatin proteins by ChIP on chip. Methods in enzymology 410, 316-341.

Nielsen, E.O., Enoe, C., Jorsal, S.E., Barfod, K., Svensmark, B., Bille-Hansen, V., Vigre, H., Botner, A., Baekbo, P., 2008. Postweaning multisystemic wasting syndrome in Danish pig herds: productivity, clinical signs and pathology. Vet Rec 162, 505-508.

Nielsen, J., Vincent, I.E., Botner, A., Ladekaer-Mikkelsen, A.S., Allan, G., Summerfield, A., McCullough, K.C., 2003. Association of lymphopenia with porcine circovirus type 2 induced postweaning multisystemic wasting syndrome (PMWS). Veterinary immunology and immunopathology 92, 97-111.

Niewold, T.A., Kerstens, H.H., van der Meulen, J., Smits, M.A., Hulst, M.M., 2005. Development of a porcine small intestinal cDNA micro-array: characterization and functional analysis of the response to enterotoxigenic E. coli. Veterinary immunology and immunopathology 105, 317-329.

Norling, L.V., Perretti, M., Cooper, D., 2009. Endogenous galectins and the control of the host inflammatory response. The Journal of endocrinology 201, 169-184.

Nunez-Hernandez, F., Perez, L.J., Munoz, M., Vera, G., Tomas, A., Egea, R., Cordoba, S., Segales, J., Sanchez, A., Nunez, J.I., 2015a. Identification of microRNAs in PCV2 subclinically infected pigs by high throughput sequencing. Veterinary research 46, 18.

Nunez-Hernandez, F., Perez, L.J., Vera, G., Cordoba, S., Segales, J., Sanchez, A., Nunez, J.I., 2015b. Evaluation of the capability of the PCV2 genome to encode miRNAs: lack of viral miRNA expression in an experimental infection. Veterinary research 46, 48.

Ochieng, J., Furtak, V., Lukyanov, P., 2004. Extracellular functions of galectin-3. Glycoconjugate journal 19, 527-535.

Okuda, Y., Ono, M., Yazawa, S., Shibata, I., 2003. Experimental reproduction of postweaning multisystemic wasting syndrome in cesarean-derived, colostrum-deprived piglets inoculated with porcine circovirus type 2 (PCV2): investigation of quantitative PCV2 distribution and antibody responses. J Vet Diagn Invest 15, 107-114.

Olvera, A., Cortey, M., Segales, J., 2007. Molecular evolution of porcine circovirus type 2 genomes: phylogeny and clonality. Virology 357, 175-185.

Olvera, A., Sibila, M., Calsamiglia, M., Segales, J., Domingo, M., 2004. Comparison of porcine circovirus type 2 load in serum quantified by a real time PCR in postweaning multisystemic wasting syndrome and porcine dermatitis and nephropathy syndrome naturally affected pigs. J Virol Methods 117, 75-80.

Opriessnig, T., Fenaux, M., Thomas, P., Hoogland, M.J., Rothschild, M.F., Meng, X.J., Halbur, P.G., 2006. Evidence of breed-dependent differences in susceptibility to porcine circovirus type-2-associated disease and lesions. Vet Pathol 43, 281-293.

Opriessnig, T., Halbur, P.G., 2012. Concurrent infections are important for expression of porcine circovirus associated disease. Virus Res 164, 20-32.

Opriessnig, T., Madson, D.M., Schalk, S., Brockmeier, S., Shen, H.G., Beach, N.M., Meng, X.J., Baker, R.B., Zanella, E.L., Halbur, P.G., 2011. Porcine circovirus type 2 (PCV2) vaccination is effective in reducing disease and PCV2 shedding in semen of boars concurrently infected with PCV2 and Mycoplasma hyopneumoniae. Theriogenology 76, 351-360.

Opriessnig, T., Meng, X.J., Halbur, P.G., 2007. Porcine circovirus type 2 associated disease: update on current terminology, clinical manifestations, pathogenesis, diagnosis, and intervention strategies. J Vet Diagn Invest 19, 591-615.

Opriessnig, T., O'Neill, K., Gerber, P.F., de Castro, A.M., Gimenez-Lirola, L.G., Beach, N.M., Zhou, L., Meng, X.J., Wang, C., Halbur, P.G., 2013a. A PCV2 vaccine based on genotype 2b is more effective than a 2a-based vaccine to protect against PCV2b or combined PCV2a/2b viremia in pigs with concurrent PCV2, PRRSV and PPV infection. Vaccine 31, 487-494.

Opriessnig, T., Patterson, A.R., Elsener, J., Meng, X.J., Halbur, P.G., 2008b. Influence of maternal antibodies on efficacy of porcine circovirus type 2 (PCV2) vaccination to protect pigs from experimental infection with PCV2. Clinical and vaccine immunology : CVI 15, 397-401.

Opriessnig, T., Patterson, A.R., Madson, D.M., Pal, N., Rothschild, M., Kuhar, D., Lunney, J.K., Juhan, N.M., Meng, X.J., Halbur, P.G., 2009. Difference in severity of porcine circovirus type two-induced pathological lesions between Landrace and Pietrain pigs. J Anim Sci 87, 1582-1590.

Opriessnig, T., Ramamoorthy, S., Madson, D.M., Patterson, A.R., Pal, N., Carman, S., Meng, X.J., Halbur, P.G., 2008a. Differences in virulence among porcine circovirus type 2 isolates are unrelated to cluster type 2a or 2b and prior infection provides heterologous protection. J Gen Virol 89, 2482-2491.

Opriessnig, T., Thacker, E.L., Yu, S., Fenaux, M., Meng, X.J., Halbur, P.G., 2004. Experimental reproduction of postweaning multisystemic wasting syndrome in pigs by dual infection with Mycoplasma hyopneumoniae and porcine circovirus type 2. Vet Pathol 41, 624-640.

Opriessnig, T., Xiao, C.T., Gerber, P.F., Halbur, P.G., 2013b. Emergence of a novel mutant PCV2b variant associated with clinical PCVAD in two vaccinated pig farms in the U.S. concurrently infected with PPV2. Vet Microbiol 163, 177-183.

Opriessnig, T., Yu, S., Gallup, J.M., Evans, R.B., Fenaux, M., Pallares, F., Thacker, E.L., Brockus, C.W., Ackermann, M.R., Thomas, P., Meng, X.J., Halbur, P.G., 2003. Effect of vaccination with selective bacterins on conventional pigs infected with type 2 porcine circovirus. Vet Pathol 40, 521-529.

Ostanello, F., Caprioli, A., Di Francesco, A., Battilani, M., Sala, G., Sarli, G., Mandrioli, L., McNeilly, F., Allan, G.M., Prosperi, S., 2005. Experimental infection of 3-week-old conventional colostrum-fed pigs with porcine circovirus type 2 and porcine parvovirus. Vet Microbiol 108, 179-186.

Patterson, A.R., Opriessnig, T., 2010. Epidemiology and horizontal transmission of porcine circovirus type 2 (PCV2). Animal health research reviews / Conference of Research Workers in Animal Diseases 11, 217-234.

Perez-Martin, E., Rovira, A., Calsamiglia, M., Mankertz, A., Rodriguez, F., Segales, J., 2007. A new method to identify cell types that support porcine circovirus type 2 replication in formalin-fixed, paraffin-embedded swine tissues. J Virol Methods 146, 86-95.

Perez, L.J., de Arce, H.D., Cortey, M., Dominguez, P., Percedo, M.I., Perera, C.L., Tarradas, J., Frias, M.T., Segales, J., Ganges, L., Nunez, J.I., 2011. Phylogenetic networks to study the origin and evolution of porcine circovirus type 2 (PCV2) in Cuba. Vet Microbiol 151, 245-254.

Petroski, M.D., 2008. The ubiquitin system, disease, and drug discovery. BMC biochemistry 9 Suppl 1, S7.

Pfeffer, L.M., Kim, J.G., Pfeffer, S.R., Carrigan, D.J., Baker, D.P., Wei, L., Homayouni, R., 2004. Role of nuclear factor-kappaB in the antiviral action of interferon and interferon-regulated gene expression. J Biol Chem 279, 31304-31311.

Philippidis, P., Mason, J.C., Evans, B.J., Nadra, I., Taylor, K.M., Haskard, D.O., Landis, R.C., 2004. Hemoglobin scavenger receptor CD163 mediates interleukin-10 release and heme oxygenase-1 synthesis: antiinflammatory monocyte-macrophage responses in vitro, in resolving skin blisters in vivo, and after cardiopulmonary bypass surgery. Circulation research 94, 119-126.

Pogranichnyy, R.M., Yoon, K.J., Harms, P.A., Swenson, S.L., Zimmerman, J.J., Sorden, S.D., 2000. Characterization of immune response of young pigs to porcine circovirus type 2 infection. Viral immunology 13, 143-153.

Pollack, J.R., Perou, C.M., Alizadeh, A.A., Eisen, M.B., Pergamenschikov, A., Williams, C.F., Jeffrey, S.S., Botstein, D., Brown, P.O., 1999. Genome-wide analysis of DNA copy-number changes using cDNA microarrays. Nat Genet 23, 41-46.

Provencal, M., Michaud, M., Beaulieu, E., Ratel, D., Rivard, G.E., Gingras, D., Beliveau, R., 2008. Tissue factor pathway inhibitor (TFPI) interferes with endothelial cell migration by inhibition of both the Erk pathway and focal adhesion proteins. Thrombosis and haemostasis 99, 576-585.

Quintana, J., Segales, J., Rosell, C., Calsamiglia, M., Rodriguez-Arrioja, G.M., Chianini, F., Folch, J.M., Maldonado, J., Canal, M., Plana-Duran, J., Domingo, M., 2001. Clinical and pathological observations on pigs with postweaning multisystemic wasting syndrome. Vet Rec 149, 357-361.

Ramírez-Boo, M., 2009. Genómica y proteómica de la infección por Circovirus Porcino Tipo 2 (PCV2). University of Córdoba, Córdoba.

Ramirez-Boo, M., Nunez, E., Jorge, I., Navarro, P., Fernandes, L.T., Segales, J., Garrido, J.J., Vazquez, J., Moreno, A., 2011. Quantitative proteomics by 2-DE, 16O/18O labelling and linear ion trap mass spectrometry analysis of lymph nodes from piglets inoculated by porcine circovirus type 2. Proteomics 11, 3452-3469.

Ramirez-Mendoza, H., Castillo-Juarez, H., Hernandez, J., Correa, P., Segales, J., 2009. Retrospective serological survey of Porcine circovirus-2 infection in Mexico. Can J Vet Res 73, 21-24.

Raychaudhuri, S., Sutphin, P.D., Chang, J.T., Altman, R.B., 2001. Basic microarray analysis: grouping and feature reduction. Trends Biotechnol 19, 189-193.

Ren, S., Yu, H., Zhang, H., Liu, Y., Huang, Y., Ma, L., Wei, L., Wu, H., Chen, X., 2011. Polymorphisms of interferon-inducible genes OAS associated with interferon-alpha treatment response in chronic HBV infection. Antiviral Res 89, 232-237.

Resendes, A., Segales, J., Balasch, M., Calsamiglia, M., Sibila, M., Ellerbrok, H., Mateu, E., Plana-Duran, J., Mankertz, A., Domingo, M., 2004a. Lack of an effect of a commercial vaccine adjuvant on the development of postweaning multisystemic wasting syndrome (PMWS) in porcine circovirus type 2 (PCV2) experimentally infected conventional pigs. Veterinary research 35, 83-90.

Resendes, A.R., Majo, N., Segales, J., Mateu, E., Calsamiglia, M., Domingo, M., 2004b. Apoptosis in lymphoid organs of pigs naturally infected by porcine circovirus type 2. J Gen Virol 85, 2837-2844.

Ricklin, D., Hajishengallis, G., Yang, K., Lambris, J.D., 2011. Complement: a key system for immune surveillance and homeostasis. Nat Immunol 11, 785-797.

Rioux, J.D., Xavier, R.J., Taylor, K.D., Silverberg, M.S., Goyette, P., Huett, A., Green, T., Kuballa, P., Barmada, M.M., Datta, L.W., Shugart, Y.Y., Griffiths, A.M., Targan, S.R., Ippoliti, A.F., Bernard, E.J., Mei, L., Nicolae, D.L., Regueiro, M., Schumm, L.P., Steinhart, A.H., Rotter, J.I., Duerr, R.H., Cho, J.H., Daly, M.J., Brant, S.R., 2007. Genome-wide association study identifies new susceptibility loci for Crohn disease and implicates autophagy in disease pathogenesis. Nat Genet 39, 596-604.

Ripoll, V.M., Irvine, K.M., Ravasi, T., Sweet, M.J., Hume, D.A., 2007. Gpnmb is induced in macrophages by IFN-gamma and lipopolysaccharide and acts as a feedback regulator of proinflammatory responses. Journal of immunology 178, 6557-6566.

Rockett, J.C., Hellmann, G.M., 2004. Confirming microarray data--is it really necessary? Genomics 83, 541-549.

Rodriguez-Arrioja, G.M., Segales, J., Balasch, M., Rosell, C., Quintant, J., Folch, J.M., Plana-Duran, J., Mankertz, A., Domingo, M., 2000. Serum antibodies to porcine circovirus type 1 and type 2 in pigs with and without PMWS. Vet Rec 146, 762-764.

Rodriguez-Arrioja, G.M., Segales, J., Calsamiglia, M., Resendes, A.R., Balasch, M., Plana-Duran, J., Casal, J., Domingo, M., 2002. Dynamics of porcine circovirus type 2 infection in a herd of pigs with postweaning multisystemic wasting syndrome. Am J Vet Res 63, 354-357.

Rodriguez-Carino, C., Duffy, C., Sanchez-Chardi, A., McNeilly, F., Allan, G.M., Segales, J., 2011. Porcine circovirus type 2 morphogenesis in a clone derived from the l35 lymphoblastoid cell line. Journal of comparative pathology 144, 91-102.

Rodriguez-Carino, C., Sanchez-Chardi, A., Segales, J., 2010. Subcellular immunolocalization of porcine circovirus type 2 (PCV2) in lymph nodes from pigs with post-weaning multisystemic wasting syndrome (PMWS). Journal of comparative pathology 142, 291-299.

Rose, N., Abhervé-Guéguen, A., Le Diguerher, G., Eveno, E., Jolly, J.P., Blanchard, P., Oger, A., Jestin, A., Madec, F., 2005. Effect of the Pietrain breed used as terminal boar on post-weaning multisystemic wasting syndrome (PMWS) in the offspring in four PMWS-affected farms. Livest. Prod. Sci. 95 177-186.

Rose, N., Eveno, E., Grasland, B., Nignol, A.C., Oger, A., Jestin, A., Madec, F., 2009. Individual risk factors for Post-weaning Multisystemic Wasting Syndrome (PMWS) in pigs: a hierarchical Bayesian survival analysis. Preventive veterinary medicine 90, 168-179.

Rosell, C., Segales, J., Plana-Duran, J., Balasch, M., Rodriguez-Arrioja, G.M., Kennedy, S., Allan, G.M., McNeilly, F., Latimer, K.S., Domingo, M., 1999. Pathological, immunohistochemical, and in-situ hybridization studies of natural cases of postweaning multisystemic wasting syndrome (PMWS) in pigs. Journal of comparative pathology 120, 59-78.

Rovira, A., Balasch, M., Segales, J., Garcia, L., Plana-Duran, J., Rosell, C., Ellerbrok, H., Mankertz, A., Domingo, M., 2002. Experimental inoculation of conventional pigs with porcine reproductive and respiratory syndrome virus and porcine circovirus 2. J Virol 76, 3232-3239.

Sadler, A.J., Williams, B.R., 2008. Interferon-inducible antiviral effectors. Nature reviews. Immunology 8, 559-568.

Sallusto, F., Cella, M., Danieli, C., Lanzavecchia, A., 1995. Dendritic cells use macropinocytosis and the mannose receptor to concentrate macromolecules in the major histocompatibility complex class II compartment: downregulation by cytokines and bacterial products. The Journal of experimental medicine 182, 389-400.

Sambrook, J., Russel, D.W., 2001. Molecular Cloning: A Laboratory Manual, 3rd ed. Edition.

Sanchez, R.E., Jr., Meerts, P., Nauwynck, H.J., Pensaert, M.B., 2003. Change of porcine circovirus 2 target cells in pigs during development from fetal to early postnatal life. Vet Microbiol 95, 15-25.

Sanchez, R.E., Jr., Nauwynck, H.J., McNeilly, F., Allan, G.M., Pensaert, M.B., 2001. Porcine circovirus 2 infection in swine foetuses inoculated at different stages of gestation. Vet Microbiol 83, 169-176.

Sarli, G., Mandrioli, L., Laurenti, M., Sidoli, L., Cerati, C., Rolla, G., Marcato, P.S., 2001. Immunohistochemical characterisation of the lymph node reaction in pig post-weaning multisystemic wasting syndrome (PMWS). Veterinary immunology and immunopathology 83, 53-67.

Sauvage, V., Cheval, J., Foulongne, V., Gouilh, M.A., Pariente, K., Manuguerra, J.C., Richardson, J., Dereure, O., Lecuit, M., Burguiere, A., Caro, V., Eloit, M., 2011. Identification of the first human gyrovirus, a virus related to chicken anemia virus. J Virol 85, 7948-7950.

Schacker, T.W., Nguyen, P.L., Beilman, G.J., Wolinsky, S., Larson, M., Reilly, C., Haase, A.T., 2002. Collagen deposition in HIV-1 infected lymphatic tissues and T cell homeostasis. The Journal of clinical investigation 110, 1133-1139.

Schena, M., Heller, R.A., Theriault, T.P., Konrad, K., Lachenmeier, E., Davis, R.W., 1998. Microarrays: biotechnology's discovery platform for functional genomics. Trends Biotechnol 16, 301-306.

Schena, M., Shalon, D., Davis, R.W., Brown, P.O., 1995. Quantitative monitoring of gene expression patterns with a complementary DNA microarray. Science 270, 467-470.

Schlaepfer, E., Audige, A., Joller, H., Speck, R.F., 2006. TLR7/8 triggering exerts opposing effects in acute versus latent HIV infection. Journal of immunology 176, 2888-2895.

Schroeder, A., Mueller, O., Stocker, S., Salowsky, R., Leiber, M., Gassmann, M., Lightfoot, S., Menzel, W., Granzow, M., Ragg, T., 2006. The RIN: an RNA integrity number for assigning integrity values to RNA measurements. BMC Mol Biol 7, 3.

Schwarzbich, M.A., Gutknecht, M., Salih, J., Salih, H.R., Brossart, P., Rittig, S.M., Grunebach, F., 2012. The immune inhibitory receptor osteoactivin is upregulated in monocyte-derived dendritic cells by BCR-ABL tyrosine kinase inhibitors. Cancer immunology, immunotherapy : CII 61, 193-202.

Segales, J., 2012. Porcine circovirus type 2 (PCV2) infections: clinical signs, pathology and laboratory diagnosis. Virus Res 164, 10-19.
Segales, J., Allan, G.M., Domingo, M., 2005. Porcine circovirus diseases. Animal health research reviews / Conference of Research Workers in Animal Diseases 6, 119-142.
Segales, J., Domingo, M., 2002. Postweaning multisystemic wasting syndrome (PMWS) in pigs. A review. Vet Q 24, 109-124.
Segales, J., Mateu, E., 2006. Immunosuppression as a feature of postweaning multisystemic wasting syndrome. Veterinary journal 171, 396-397.
Segales, J., Olvera, A., Grau-Roma, L., Charreyre, C., Nauwynck, H., Larsen, L., Dupont, K., McCullough, K., Ellis, J., Krakowka, S., Mankertz, A., Fredholm, M., Fossum, C., Timmusk, S., Stockhofe-Zurwieden, N., Beattie, V., Armstrong, D., Grassland, B., Baekbo, P., Allan, G., 2008. PCV-2 genotype definition and nomenclature. Vet Rec 162, 867-868.
Segales, J., Pineiro, C., Lampreave, F., Nofrarias, M., Mateu, E., Calsamiglia, M., Andres, M., Morales, J., Pineiro, M., Domingo, M., 2004a. Haptoglobin and pig-major acute protein are increased in pigs with postweaning multisystemic wasting syndrome (PMWS). Veterinary research 35, 275-282.
Segales, J., Rosell, C., Domingo, M., 2004b. Pathological findings associated with naturally acquired porcine circovirus type 2 associated disease. Vet Microbiol 98, 137-149.
Segales, J., Urniza, A., Alegre, A., Bru, T., Crisci, E., Nofrarias, M., Lopez-Soria, S., Balasch, M., Sibila, M., Xu, Z., Chu, H.J., Fraile, L., Plana-Duran, J., 2009. A genetically engineered chimeric vaccine against porcine circovirus type 2 (PCV2) improves clinical, pathological and virological outcomes in postweaning multisystemic wasting syndrome affected farms. Vaccine 27, 7313-7321.
Shang, S.B., Jin, Y.L., Jiang, X.T., Zhou, J.Y., Zhang, X., Xing, G., He, J.L., Yan, Y., 2009. Fine mapping of antigenic epitopes on capsid proteins of porcine circovirus, and antigenic phenotype of porcine circovirus type 2. Molecular immunology 46, 327-334.
Shen, H.G., Zhou, J.Y., Zhang, X., Huang, Z.Y., He, J.L., Yan, Y., 2009. Interference of porcine circovirus type 2 ORF2 immunogenicity by ORF1 and ORF3 mixed DNA immunizations in mice. Virology 393, 104-111.
Shi, L., Reid, L.H., Jones, W.D., Shippy, R., Warrington, J.A., Baker, S.C., Collins, P.J., de Longueville, F., et al., 2006. The MicroArray Quality Control (MAQC) project shows inter- and intraplatform reproducibility of gene expression measurements. Nat Biotechnol 24, 1151-1161.
Shibahara, T., Sato, K., Ishikawa, Y., Kadota, K., 2000. Porcine circovirus induces B lymphocyte depletion in pigs with wasting disease syndrome. J Vet Med Sci 62, 1125-1131.
Singh-Gasson, S., Green, R.D., Yue, Y., Nelson, C., Blattner, F., Sussman, M.R., Cerrina, F., 1999. Maskless fabrication of light-directed oligonucleotide microarrays using a digital micromirror array. Nat Biotechnol 17, 974-978.
Sipos, W., Duvigneau, J.C., Willheim, M., Schilcher, F., Hartl, R.T., Hofbauer, G., Exel, B., Pietschmann, P., Schmoll, F., 2004. Systemic cytokine profile in feeder pigs suffering from natural postweaning multisystemic wasting syndrome (PMWS) as determined by semiquantitative RT-PCR and flow cytometric intracellular cytokine detection. Veterinary immunology and immunopathology 99, 63-71.
Smyth, G., Ritchie, M., Thorne, N., Wettenhall, J., Shi, W., 2012. limma: Linear Models for Microarray Data. http://www.bioconductor.org/packages/release/bioc/vignettes/limma/inst/doc/usersguide.pdf.
Smyth, G.K., 2004. Linear models and empirical bayes methods for assessing differential expression in microarray experiments. Stat Appl Genet Mol Biol 3, Article3.
Sohn, I., Kim, S., Hwang, C., Lee, J.W., Shim, J., 2008. Support vector machine quantile regression for detecting differentially expressed genes in microarray analysis. Methods Inf Med 47, 459-467.
Southern, E.M., 1975. Detection of Specific Sequences Among DNA Fragments Separated by Gel Electrophoresis. J. Mol. Biol. 98, 503-517.
Southern, E.M., Maskos, U., Elder, J.K., 1992. Analyzing and comparing nucleic acid sequences by hybridization to arrays of oligonucleotides: evaluation using experimental models. Genomics 13, 1008-1017.
Steiner, E., Balmelli, C., Herrmann, B., Summerfield, A., McCullough, K., 2008. Porcine circovirus type 2 displays pluripotency in cell targeting. Virology.
Stevenson, L.S., McCullough, K., Vincent, I., Gilpin, D.F., Summerfield, A., Nielsen, J., McNeilly, F., Adair, B.M., Allan, G.M., 2006. Cytokine and C-reactive protein profiles induced by porcine circovirus type 2 experimental infection in 3-week-old piglets. Viral immunology 19, 189-195.
Suzuki, F., Arase, Y., Suzuki, Y., Tsubota, A., Akuta, N., Hosaka, T., Someya, T., Kobayashi, M., Saitoh, S., Ikeda, K., Kobayashi, M., Matsuda, M., Takagi, K., Satoh, J., Kumada, H., 2004. Single

nucleotide polymorphism of the MxA gene promoter influences the response to interferon monotherapy in patients with hepatitis C viral infection. J Viral Hepat 11, 271-276.
Takahagi, Y., Toki, S., Nishiyama, Y., Morimatsu, F., Murakami, H., 2010. Differential effects of porcine circovirus type 2 (PCV2) vaccination on PCV2 genotypes at Japanese pig farms. J Vet Med Sci 72, 35-41.
Takaoka, A., Yanai, H., 2006. Interferon signalling network in innate defence. Cell Microbiol 8, 907-922.
Takeda, K., Kaisho, T., Akira, S., 2003. Toll-like receptors. Annu Rev Immunol 21, 335-376.
Timmusk, S., Fossum, C., Berg, M., 2006. Porcine circovirus type 2 replicase binds the capsid protein and an intermediate filament-like protein. J Gen Virol 87, 3215-3223.
Timmusk, S., Merlot, E., Lovgren, T., Jarvekulg, L., Berg, M., Fossum, C., 2009. Regulator of G protein signalling 16 (RGS16) is a target for a porcine circovirus type-2 protein. J Gen Virol.
Timmusk, S., Wallgren, P., Brunborg, I.M., Wikstrom, F.H., Allan, G., Meehan, B., McMenamy, M., McNeilly, F., Fuxler, L., Belak, K., Podersoo, D., Saar, T., Berg, M., Fossum, C., 2008. Phylogenetic analysis of porcine circovirus type 2 (PCV2) pre- and post-epizootic postweaning multisystemic wasting syndrome (PMWS). Virus Genes 36, 509-520.
Timpl, R., Sasaki, T., Kostka, G., Chu, M.L., 2003. Fibulins: a versatile family of extracellular matrix proteins. Nature reviews. Molecular cell biology 4, 479-489.
Tischer, I., Gelderblom, H., Vettermann, W., Koch, M.A., 1982. A very small porcine virus with circular single-stranded DNA. Nature 295, 64-66.
Tischer, I., Mields, W., Wolff, D., Vagt, M., Griem, W., 1986. Studies on epidemiology and pathogenicity of porcine circovirus. Arch Virol 91, 271-276.
Tischer, I., Rasch, R., Tochtermann, G., 1974. Characterization of papovavirus-and picornavirus-like particles in permanent pig kidney cell lines. Zentralbl Bakteriol Orig A 226, 153-167.
Todd, D., 2004. Avian circovirus diseases: lessons for the study of PMWS. Vet Microbiol 98, 169-174.
Tomas, A., Fernandes, L.T., Valero, O., Segales, J., 2008. A meta-analysis on experimental infections with porcine circovirus type 2 (PCV2). Vet Microbiol.
Trible, B.R., Kerrigan, M., Crossland, N., Potter, M., Faaberg, K., Hesse, R., Rowland, R.R., 2011. Antibody recognition of porcine circovirus type 2 capsid protein epitopes after vaccination, infection, and disease. Clinical and vaccine immunology : CVI 18, 749-757.
Troyanskaya, O.G., Garber, M.E., Brown, P.O., Botstein, D., Altman, R.B., 2002. Nonparametric methods for identifying differentially expressed genes in microarray data. Bioinformatics 18, 1454-1461.
Truong, C., Mahe, D., Blanchard, P., Le Dimna, M., Madec, F., Jestin, A., Albina, E., 2001. Identification of an immunorelevant ORF2 epitope from porcine circovirus type 2 as a serological marker for experimental and natural infection. Arch Virol 146, 1197-1211.
Tsai, S., Cassady, J.P., Freking, B.A., Nonneman, D.J., Rohrer, G.A., Piedrahita, J.A., 2006a. Annotation of the Affymetrix porcine genome microarray. Animal genetics 37, 423-424.
Tsai, S., Mir, B., Martin, A.C., Estrada, J.L., Bischoff, S.R., Hsieh, W.P., Cassady, J.P., Freking, B.A., Nonneman, D.J., Rohrer, G.A., Piedrahita, J.A., 2006b. Detection of transcriptional difference of porcine imprinted genes using different microarray platforms. BMC genomics 7, 328.
Tsai, Y.C., Jeng, C.R., Hsiao, S.H., Chang, H.W., Liu, J.J., Chang, C.C., Lin, C.M., Chia, M.Y., Pang, V.F., 2010. Porcine circovirus type 2 (PCV2) induces cell proliferation, fusion, and chemokine expression in swine monocytic cells in vitro. Veterinary research 41, 60.
Tuggle, C.K., Wang, Y., Couture, O., 2007. Advances in swine transcriptomics. Int J Biol Sci 3, 132-152.
Tusher, V.G., Tibshirani, R., Chu, G., 2001. Significance analysis of microarrays applied to the ionizing radiation response. Proc Natl Acad Sci U S A 98, 5116-5121.
van den Berg, B.H., Thanthiriwatte, C., Manda, P., Bridges, S.M., 2009. Comparing gene annotation enrichment tools for functional modeling of agricultural microarray data. BMC Bioinformatics 10 Suppl 11, S9.
Van Gelder, R.N., von Zastrow, M.E., Yool, A., Dement, W.C., Barchas, J.D., Eberwine, J.H., 1990. Amplified RNA synthesized from limited quantities of heterogeneous cDNA. Proc Natl Acad Sci U S A 87, 1663-1667.
VanGuilder, H.D., Vrana, K.E., Freeman, W.M., 2008. Twenty-five years of quantitative PCR for gene expression analysis. Biotechniques 44, 619-626.
Vincent, I.E., Balmelli, C., Meehan, B., Allan, G., Summerfield, A., McCullough, K.C., 2007. Silencing of natural interferon producing cell activation by porcine circovirus type 2 DNA. Immunology 120, 47-56.
Vincent, I.E., Carrasco, C.P., Guzylack-Piriou, L., Herrmann, B., McNeilly, F., Allan, G.M., Summerfield, A., McCullough, K.C., 2005. Subset-dependent modulation of dendritic cell activity by circovirus type 2. Immunology 115, 388-398.

Vincent, I.E., Carrasco, C.P., Herrmann, B., Meehan, B.M., Allan, G.M., Summerfield, A., McCullough, K.C., 2003. Dendritic cells harbor infectious porcine circovirus type 2 in the absence of apparent cell modulation or replication of the virus. J Virol 77, 13288-13300.

Vivier, E., Tomasello, E., Paul, P., 2002. Lymphocyte activation via NKG2D: towards a new paradigm in immune recognition? Curr Opin Immunol 14, 306-311.

Vogt, L., Schmitz, N., Kurrer, M.O., Bauer, M., Hinton, H.I., Behnke, S., Gatto, D., Sebbel, P., Beerli, R.R., Sonderegger, I., Kopf, M., Saudan, P., Bachmann, M.F., 2006. VSIG4, a B7 family-related protein, is a negative regulator of T cell activation. The Journal of clinical investigation 116, 2817-2826.

Wallace, R.B., Shaffer, J., Murphy, R.F., Bonner, J., Hirose, T., Itakura, K., 1979. Hybridization of synthetic oligodeoxyribonucleotides to phi chi 174 DNA: the effect of single base pair mismatch. Nucleic Acids Res 6, 3543-3557.

Wallgren, P., Brunborg, I.M., Blomqvist, G., Bergstrom, G., Wikstrom, F., Allan, G., Fossum, C., Jonassen, C.M., 2009. The index herd with PMWS in Sweden: presence of serum amyloid A, circovirus 2 viral load and antibody levels in healthy and PMWS-affected pigs. Acta veterinaria Scandinavica 51, 13.

Wang, D., Coscoy, L., Zylberberg, M., Avila, P.C., Boushey, H.A., Ganem, D., DeRisi, J.L., 2002. Microarray-based detection and genotyping of viral pathogens. Proc Natl Acad Sci U S A 99, 15687-15692.

Wang, F., Guo, X., Ge, X., Wang, Z., Chen, Y., Cha, Z., Yang, H., 2009. Genetic variation analysis of Chinese strains of porcine circovirus type 2. Virus Res.

Wang, X., Jiang, P., Li, Y., Jiang, W., Dong, X., 2007. Protection of pigs against post-weaning multisystemic wasting syndrome by a recombinant adenovirus expressing the capsid protein of porcine circovirus type 2. Vet Microbiol 121, 215-224.

Wang, Y., Couture, O.P., Qu, L., Uthe, J.J., Bearson, S.M., Kuhar, D., Lunney, J.K., Nettleton, D., Dekkers, J.C., Tuggle, C.K., 2008. Analysis of porcine transcriptional response to Salmonella enterica serovar Choleraesuis suggests novel targets of NFkappaB are activated in the mesenteric lymph node. BMC genomics 9, 437.

Wei, H., Lenz, S.D., Van Alstine, W.G., Stevenson, G.W., Langohr, I.M., Pogranichniy, R.M., 2010. Infection of cesarean-derived colostrum-deprived pigs with porcine circovirus type 2 and Swine influenza virus. Comp Med 60, 45-50.

Wei, L., Kwang, J., Wang, J., Shi, L., Yang, B., Li, Y., Liu, J., 2008. Porcine circovirus type 2 induces the activation of nuclear factor kappa B by IkappaBalpha degradation. Virology 378, 177-184.

Wei, L., Liu, J., 2009. Porcine circovirus type 2 replication is impaired by inhibition of the extracellular signal-regulated kinase (ERK) signaling pathway. Virology 386, 203-209.

Wei, L., Zhu, S., Wang, J., Liu, J., 2012. Activation of the phosphatidylinositol 3-kinase/Akt signaling pathway during porcine circovirus type 2 infection facilitates cell survival and viral replication. J Virol 86, 13589-13597.

Wei, L., Zhu, Z., Wang, J., Liu, J., 2009. JNK and p38 mitogen-activated protein kinase pathways contribute to porcine circovirus type 2 infection. J Virol 83, 6039-6047.

West, M.A., Wallin, R.P., Matthews, S.P., Svensson, H.G., Zaru, R., Ljunggren, H.G., Prescott, A.R., Watts, C., 2004. Enhanced dendritic cell antigen capture via toll-like receptor-induced actin remodeling. Science 305, 1153-1157.

Wiederkehr, D.D., Sydler, T., Buergi, E., Haessig, M., Zimmermann, D., Pospischil, A., Brugnera, E., Sidler, X., 2009. A new emerging genotype subgroup within PCV-2b dominates the PMWS epizooty in Switzerland. Vet Microbiol 136, 27-35.

Wilson, C.L., Miller, C.J., 2005. Simpleaffy: a BioConductor package for Affymetrix Quality Control and data analysis. Bioinformatics 21, 3683-3685.

Wu, Z.J., Irizarry, R.A., Gentleman, R., Martinez-Murillo, F., Spencer, F., 2004. A model-based background adjustment for oligonucleotide expression arrays. Journal of the American Statistical Association 99, 909-917.

Xiao, C.T., Halbur, P.G., Opriessnig, T., 2012. Complete genome sequence of a novel porcine circovirus type 2b variant present in cases of vaccine failures in the United States. J Virol 86, 12469.

Yang, X., Schadt, E.E., Wang, S., Wang, H., Arnold, A.P., Ingram-Drake, L., Drake, T.A., Lusis, A.J., 2006. Tissue-specific expression and regulation of sexually dimorphic genes in mice. Genome research 16, 995-1004.

Yauk, C.L., Berndt, M.L., 2007. Review of the literature examining the correlation among DNA microarray technologies. Environ Mol Mutagen 48, 380-394.

Yin, J.Q., Zhao, R.C., Morris, K.V., 2008. Profiling microRNA expression with microarrays. Trends Biotechnol 26, 70-76.

Yoon, S., Lee, G., Han, D., Song, J.Y., Kang, K.S., Lee, Y.S., 2010. Neutralization of infectivity of porcine circovirus type 2 (PCV2) by capsid-binding 2'F-RNA aptamers. Antiviral Res 88, 19-24.

Young, M.G., Cunningham, G.L., Sanford, S.E., Path, D., 2011. Circovirus vaccination in pigs with subclinical porcine circovirus type 2 infection complicated by ileitis. J. Swine Health Prod 19 6.

Yu, S., Opriessnig, T., Kitikoon, P., Nilubol, D., Halbur, P.G., Thacker, E., 2007a. Porcine circovirus type 2 (PCV2) distribution and replication in tissues and immune cells in early infected pigs. Veterinary immunology and immunopathology 115, 261-272.

Yu, S., Vincent, A., Opriessnig, T., Carpenter, S., Kitikoon, P., Halbur, P.G., Thacker, E., 2007b. Quantification of PCV2 capsid transcript in peripheral blood mononuclear cells (PBMCs) in vitro. Vet Microbiol 123, 34-42.

Zhang, H., Lunney, J.K., Baker, R.B., Opriessnig, T., 2011. Cytokine and chemokine mRNA expression profiles in tracheobronchial lymph nodes from pigs singularly infected or coinfected with porcine circovirus type 2 (PCV2) and Mycoplasma hyopneumoniae (MHYO). Veterinary immunology and immunopathology 140, 152-158.

Zhang, X., Zhou, J., Wu, Y., Zheng, X., Ma, G., Wang, Z., Jin, Y., He, J., Yan, Y., 2009. Differential proteome analysis of host cells infected with porcine circovirus type 2. Journal of proteome research 8, 5111-5119.

Zhao, S.H., Kuhar, D., Lunney, J.K., Dawson, H., Guidry, C., Uthe, J.J., Bearson, S.M., Recknor, J., Nettleton, D., Tuggle, C.K., 2006. Gene expression profiling in Salmonella Choleraesuis-infected porcine lung using a long oligonucleotide microarray. Mamm Genome 17, 777-789.

Zhong, S., Li, C., Wong, W.H., 2003. ChipInfo: Software for extracting gene annotation and gene ontology information for microarray analysis. Nucleic Acids Res 31, 3483-3486.

Zhu, B., Xu, F., Li, J., Shuai, J., Li, X., Fang, W., 2012. Porcine circovirus type 2 explores the autophagic machinery for replication in PK-15 cells. Virus Res 163, 476-485.